4-1-1984

PWM motor control: Model and servo analysis

Rick J. Sandor

PWM MOTOR CONTROL:

MODEL AND SERVO ANALYSIS

BY

RICK J. SANDOR

A THESIS SUBMITTED
IN
PARTIAL FULFILLMENT
OF THE
REQUIREMENTS FOR THE DEGREE OF

MASTER OF SCIENCE

IN

ELECTRICAL ENGINEERING

APPROVED BY:

PROF. R. Unnikrishnan
(THESIS ADVISOR)

PROF. James E. Palmer

PROF. [Illegible]

PROF. [Illegible]

PROF. Harry E. Rhody 5/4/84
(DEPARTMENT HEAD)

DEPARTMENT OF ELECTRICAL ENGINEERING
COLLEGE OF ENGINEERING
ROCHESTER INSTITUTE OF TECHNOLOGY
ROCHESTER, NEW YORK
APRIL, 1984

1.0 Abstract

In recent years, the performance requirements of high power servo motor systems utilizing pulse width modulated (PWM) switching amplifiers have steadily increased.

These PWM motor amplifiers perform an important function in the d.c. servo system by boosting the low level command signal to the high voltage and current levels required by the motor. Ideally, this power gain is to be constant over all input frequencies but, in reality, gain is frequency dependent which affects system dynamics. The amplifier gain and phase versus frequency relationships and amplifier noise and d.c. offsets which may affect system response must be known to the servo designer to properly design the motor control system.

The switching effects of the PWM amplifier may result in making the overall system unstable if the system bandwidth is kept high with respect to the PWM switching frequency. Since the standard servo design techniques utilize linear system modeling, analysis, and compensation, it would be very advantageous to the design engineer to have a linear model which best approximates the true nonlinear PWM amplifier. This work will look at the output response of the PWM amplifier with respect to stability and output ripple. A linear model will be developed which simulates

these stability and ripple effects in a position control servo system and which is valid as system bandwidth reaches one-third the PWM switching frequency. This work extends the application of the "Principle of Equivalent Areas" [14] to the bipolar PWM amplifier. It is then combined with a detailed analysis of the PWM waveform by Double Fourier Transform to yield the unique PWM switching effects in a position control servo system. Theoretical results of the newly derived sampling plus harmonic linear model are verified by computer simulation.

Acknowledgements

The author wishes to express his gratitude to Professor R. Unnikrishnan for his guidance and patience during this work. The author also recognizes that this educational opportunity was made possible through the permission and resource of the Eastman Kodak Company and the encouragement of the author's immediate supervision.

Table of Contents

List of Figures

List of Symbols

f_s	- PWM switching frequency
T	- PWM switching period
$V_{in}(t)$	- PWM amplifier input voltage
t_1	- Time at which the PWM output changes state within a single cycle
$V_a(t)$	- PWM amplifier output voltage applied to the motor
V_s	- PWM amplifier peak voltage
$I_a(t)$	- Servo motor armature current
$\alpha(t)$	- Duty cycle of the PWM output waveform
V_{max}	- Maximum value of $V_{in}(t)$ before saturation or 1/2 the input voltage range
L	- Motor inductance
R	- Motor resistance
$\omega(t)$	- Motor angular velocity
K_B	- Motor back emf
Δi	- Motor current variation from average due to PWM switching
I_{av}	- Average motor current
s	- Complex variable
t	- Time
$H(s)$	- Laplace transform of a hold network
J	- Total inertia of servo system load
T_f	- Coulomb friction torque
F	- Motor windage
$T_1(t), T_1(s)$	- Tortional tension in the coupling between the motor and the load
J_m	- Motor inertia

$\theta_m(t)$	- Angular position of the motor
J_L	- Load inertia
B_c	- Tortional coupling elastic damping between motor and load
K_c	- Tortional coupling spring constant between the motor and load
P_1	- Mechanical time constant pole of the servo system
$G(\omega), g(t), G(s)$	- Control system plant transfer function (frequency, time, and complex variable)
ω	- Angular frequency of a sinusoidal signal
ω_s	- Angular frequency equal to the PWM switching frequency
$\theta(t)$	- Tooling position and output of the servo control system
$\tau(t), \tau(s)$	- Motor torque as a function of time and complex variable
K_T	- Motor torque constant
$e_1(t)$	- Error signal between the command and tooling position
k_p	- Position sensor conversion constant
$e_2(t)$	- Output of position compensation network
$e_3(t)$	- Error signal between the command and motor velocity
k_{TACH}	- Tachometer conversion constant
$d(t)$	- PWM amplifier dither signal
$e(t)$	- PWM sum of $V_{in}(t)$ and the dither signal
$V_{in}^*(t)$	- Sampled PWM input signal
E_i	- Magnitude of sinusoidal input voltage
a_o	- Constant Fourier coefficient
a_n	- Fourier coefficient
b_n	- Fourier coefficient

$N(E_i, \omega)$	- Describing function
$R(j\omega)$, $r(t)$, $R(s)$	- Control system input signal as a function of frequency, time, and complex variable
$C(j\omega)$, $c(t)$, $C(s)$	- Control system output signal as a function of frequency, time, and complex variable
$K(\omega)$	- Control system feedback transfer function
k_1	- Feedback gain on the tachometer signal
k_2	- Feedback gain on the potentiometer signal
$\theta_d(s)$	- Desired position of the position servo system
β	- Feedback zero angle to desired poles

2.0 Introduction

This section will define the PWM motor amplilfier and summarize its advantages. The many types of PWM will be discussed and the bipolar PWM amplifier will be presented in detail as the subject of this work.

Linear amplifiers are the simplest motor drives and are constructed using linear gain elements to drive a power stage. The mathematical relationship between the output and input voltage can be described by a first order differential equation with very high d.c. gains. With the proper choice of voltage or current feedback, the amplifier can be made to have a constant gain up to very high frequency. The amplifier has a high performance and its effects on servo system response are easy to predict. In general, linear motor amplifiers are preferred in wide-bandwidth, low-power systems. There is, however, a significant disadvantage in high power applications.

Linear amplifiers control motor voltage or current by controlling the voltage applied to the motor. The amplifier must drop a voltage equal to the difference between the supply voltage and the voltage applied to the motor while delivering the proper current. Thus, linear amplifiers have the problem of high power dissipation in the output transistor stage. The motor and amplifier are

connected in series across the power supply and share the supply voltage among them. If the supply voltage is 100V, the motor voltage is 20V, and the motor current is 10A, the power delivered to the motor is 200W. This compares to 800W dissipation in the amplifier which is undesirable and requires special care in providing for heat transfer.

Switching motor amplifiers offer a solution to this problem. The switching amplifier avoids high power dissipation in the power transistor output stage by cycling the output transistors from saturation to an off state. When the output stage is turned on, the saturation voltage across it is negligible and when it is turned off, the current is zero. In either case, the power dissipation in the transistors is small. Amplifiers operating in this way, acquire the term switching amplifiers. Advantages of PWM amplifiers are adequately discussed in the existing literature [1, 2, 3, 4, 6, 11, 26, 28].

One form of switching amplifiers varies both its switching frequency and pulse width as a function of the input signal as well as the parameters of the system. This pulse frequency modulated amplifier is not often encountered and will not be addressed in this report.

Other switching amplifiers utilize a separate fixed frequency oscillator and thus a fixed pulse rate. Only the pulse width varies with the input signal and these amplifiers are called pulse-width modulated (PWM) amplifiers. Control of the pulse width is most often performed by controlling the sequencing of power transistors arranged in an H-bridge configuration as shown in Figure 1. Discussion of the many PWM variations and their circuit implementations can be found in the literature [1, 2, 3, 4, 6, 11, 28].

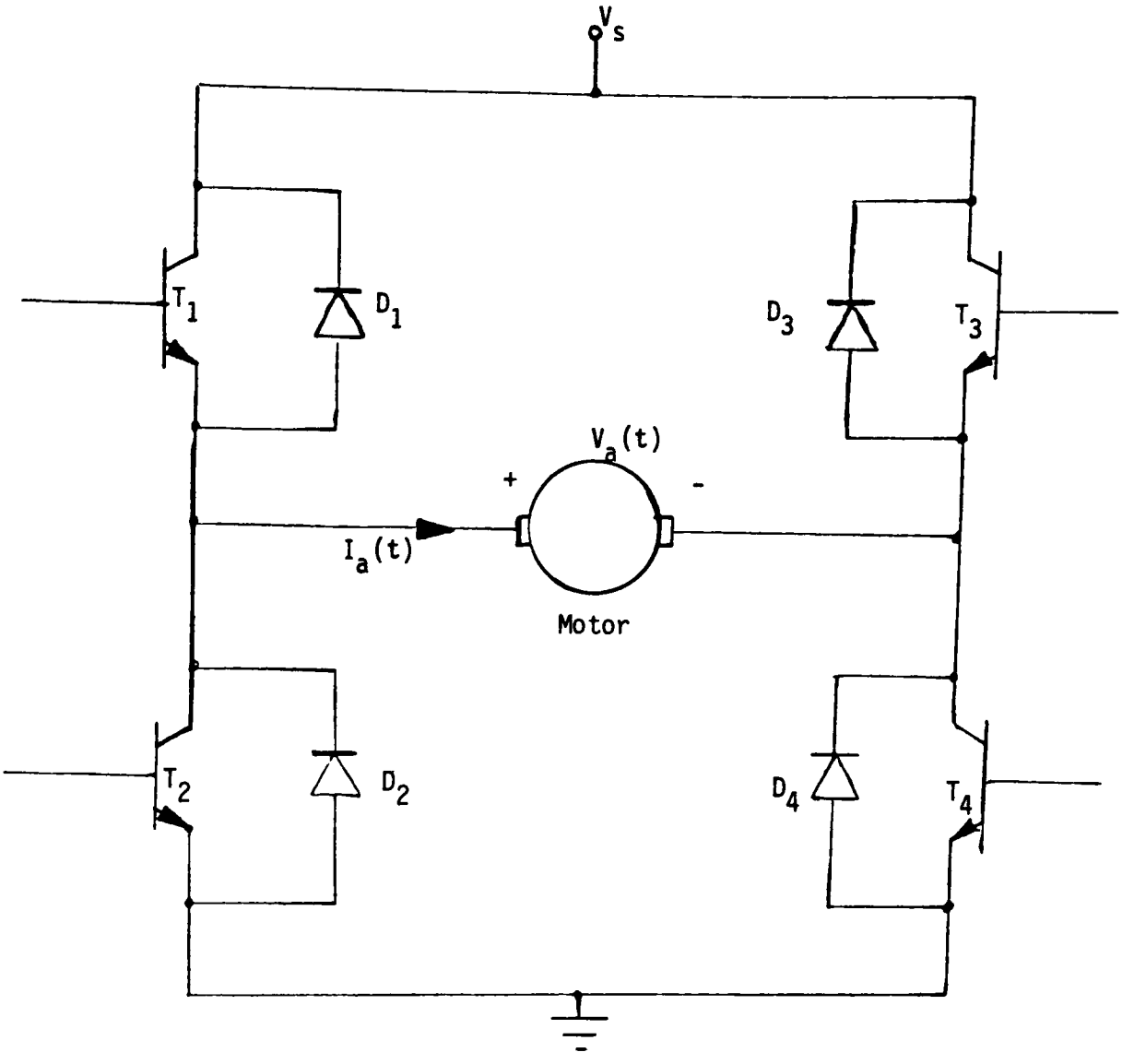

Figure 1

H-Bridge Transistor Configuration of a Typical PWM Output Stage

Of the many types of PWM, there are two main operating modes found in servo application. For the unipolar mode of PWM operation, the switching sequence depends on the sign of the amplifier input command V_{in}. Let the switching frequency be f_s and the switching period be T. Also, assume that the "on" phase is during the first part of the period. It lasts between t=0 and $t=t_1$, and is followed by the "off" phase which lasts through the rest of the switching period. The switching sequence depends on the sign of the input V_{in}. When V_{in} is positive, T_4 is turned on continuously. Transistor T_1 is turned on during the "on" phase and T_2 is turned on during the "off" phase. The resulting amplifier output, $V_a(t)$, applied to the motor becomes

$$V_a(t) = \begin{cases} V_s & 0 \leq t < t_1 \\ 0 & t_1 \leq t < T \end{cases} \qquad (2.1)$$

where V_s is the peak amplifier output voltage. When V_{in} is negative, T_3 is turned on continuously. Transistor T_2 is turned on during the "on" phase and T_1 is turned on during the "off" phase. The resulting amplifier output becomes

$$V_a(t) = \begin{cases} -V_s & 0 \leq t < t_1 \\ 0 & t_1 \leq t < T \end{cases} \qquad (2.2)$$

The output waveform as a function of a sinusoidal input is shown in Figure 2(a).

A second mode of PWM operation, called the bipolar mode, switches positive and negative supply voltage to the motor every cycle. Transistors T_1 and T_4 are turned on during the "on" phase and transistors T_2 and T_3 are turned on during the "off" phase. The resulting amplifier output to the motor becomes

$$V_a(t) = \begin{cases} V_s & 0 \leq t < t_1 \\ -V_s & t_1 \leq t < T \end{cases} \qquad (2.3)$$

and is shown in Figure 2(b).

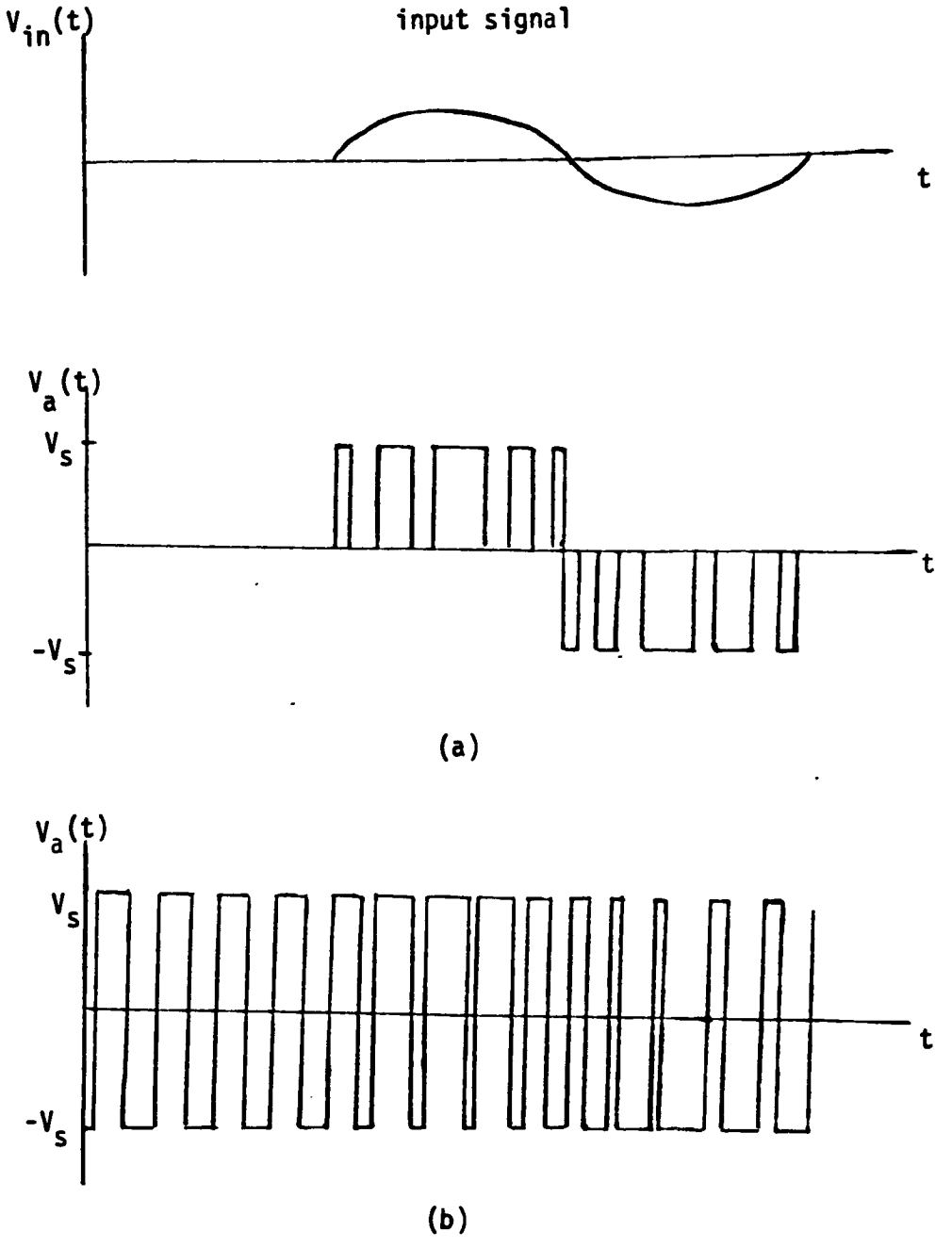

Figure 2

(a) Output Waveform of Unipolar a PWM Amplifier in Response to a Sinusoidal Input
(b) Output Waveform of a Bipolar PWM Amplifier in Response to a Sinusoidal Input

The bipolar mode described above has the disadvantage that at time t_1 one transistor pair must be turned off and the other must be turned on. Since there is a discharge time in the transistors, care must be taken that two transistors do not conduct simultaneously and form a short circuit across the power supply. To avoid this, a delay interval must be introduced between one transistor pair turning off and the other turning on. The delay interval has to be longer than the discharge time. Also, the power transistors have a finite turn on rise time in which they are in their linear, high power dissipation region. Time in this region must be minimized. The two disadvantages described above tend to limit the switching frequency. Amplifier manufacturers recognize this problem and tend to keep switching frequencies low enough such that the time taken up by the dead band delay interval and the transistor rise time is a small percentage of the total cycle time.

The bipolar PWM motor amplifier is the amplifier that, from the author's experience, is most commonly used in industry. Thus, the bipolar PWM amplifier will be the focus of the remainder of this paper. To avoid unnecessary complexity, this analysis will assume that the PWM amplifier has perfect switching, meaning that the previously discussed deadband and transistor rise time are both zero. This assumption is consistent with the analysis attempted in the references.

3.0 Background

This section summarizes the work found in the references concerning the desciption and analysis of pulse width modulation and its effects on system performance. Although each study offers some interesting insight into some aspect of PWM operation, this section will also explain why these studies were deficient in meeting the goals of this work. The references can roughly be divided into three categories:

(a) Simplified d.c. model, average currents and current variations

(b) Sampling models and stability studies

(c) Fourier transform and first harmonic models

Principles which will be used later in this paper are also detailed.

In order to properly design a machine control servo system, one must understand how the bipolar PWM amplifier will affect system performance. The first attempts to analyze motor response to the switching PWM output utilized circuit analysis techniques to determine motor voltage and current. The duty cycle $\alpha(t)$ of the output

PWM waveform is dependent on $V_{in}(t)$ and is defined as:

$$\alpha(t) = \frac{V_{in}(t)}{V_{max}} \tag{3.1}$$

where V_{max} is the maximum of V_{in} or 1/2 the maximum input voltage range. It follows that $-1 \leq \alpha \leq 1$. For the PWM output waveform as shown in Figure 3 with the assumption that the input is relatively constant over the switching period, the average or dc value of the output voltage is given by:

$$V_{av} = 1/T \int_0^T V_a(t)\, dt = \alpha V_s = \frac{V_s}{V_{max}} V_{in} \tag{3.2}$$

Thus, a simplified d.c. gain model of the PWM system is given as:

$$V_{av}(t)/V_{in}(t) = V_s/V_{max} \tag{3.3}$$

with the stipulation that the model is valid as long as the system bandwidth remains significantly below the switching frequency and the input is relatively constant over the switching period. This model and stipulation were presented by Kuo [1], Electro-Craft Corporation [2], Geiger [3], Tal [4], and Taft, Banister, and State [28].

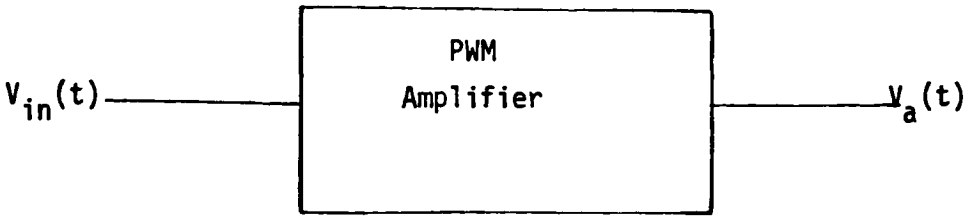

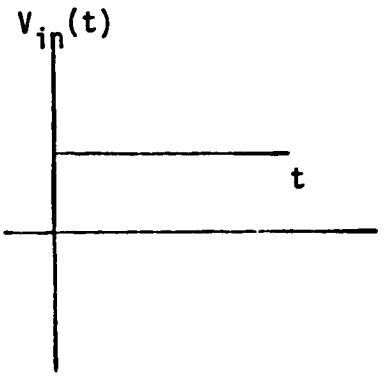

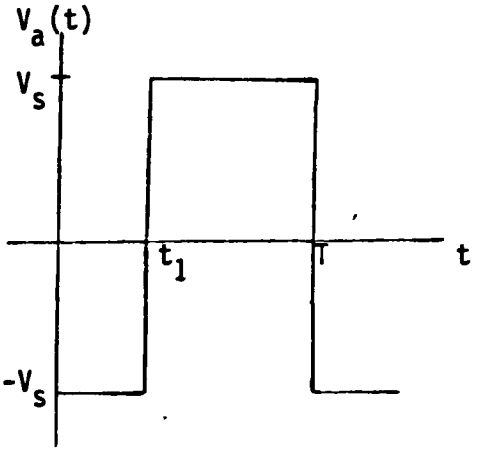

$$\alpha = \frac{V_{in}}{V_{max}}$$

$$t_1 = \frac{1-\alpha}{V_{max}}$$

$$V_a(t) = \begin{cases} -V_s & 0 \le t < t_1 \\ V_s & t_1 \le t < T \end{cases}$$

Figure 3

Typical PWM Output Cycle

Although the model is linear and can be used in many low response applications, it does not give warning of unknown destabilizing effects as the bandwidth is pushed higher. Also lacking is the ripple switching effects which are suspected to be present. Depending on the reference used, "significantly below the switching frequency" is defined between 1/3 to 1/10 the switching frequency f_s.

The effect of switching was analyzed in these same references by circuit analysis over each portion of the output voltage given in equation (2-3). When applied to a dc permanent magnet servo motor, the differential equation of the motor is given as

$$L\, dI_a(t)/dt + R\, I_a(t) + K_B\, \omega(t) = V_a(t) \qquad (3$$

where:

$I_a(t)$ = motor armature current

$\omega(t)$ = motor velocity

L = motor inductance

R = motor resistance

K_B = motor back emf

The solution of this differential equation results in a falling and rising exponential motor current as shown in Figure 4. Over a switching cycle, the motor current has some dc value with a maximum current variation (Δi) whose magnitude is a nonlinear function of duty cycle. This relationship, which can accurately predict current variations in steady state, is inappropriate for linear systems modeling and analysis necessary for accurate servo design.

Circuit analysis techniques are also used by Kuo [1]; Tal [4]; Damle and Dubey [5]; Okamoto, Ichida, Fujinami, and Imura [15]; Verma [11]; and Verma, Baird, and Aatre [26].

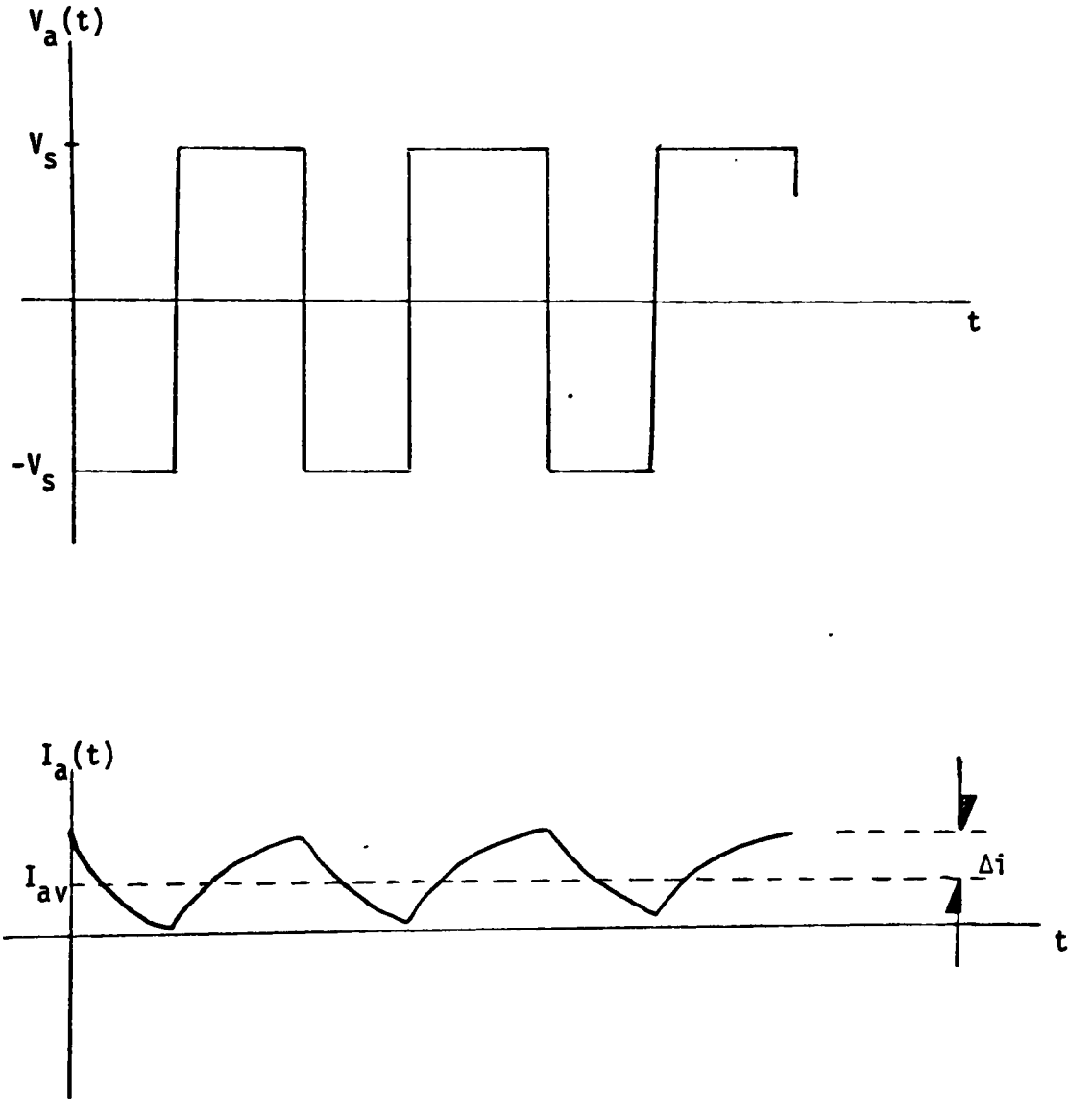

Figure 4

Motor Current in Response to A Typical PWM Amplifier Output

Verma [11], and Verma, Baird, and Aatre [26] use both a circuit analysis approach and a lattice function approach to look at current ripple and speed variation of a unipolar PWM controlled dc motor.

In the circuit analysis approach, the system is considered as a simple circuit having a battery, a switch, and a motor in series. The switch is assumed to be a time modulated power switch with conduction periods adjusted according to the drive requirements. Interrelations between various parameters, such as the pulse width, pulse period, current ripple factor, and the motor time constant, are established under stalled motor conditions. The speed analysis of PWM controlled dc motors by the second approach involves the use of the lattice function and the discrete Laplace transform concepts. These techniques yielded good results in predicting the current ripple factor and speed variation factor; however, they do not lend themselves to linear systems analysis and compensation.

Andeen, [14], recognized the nonlinear nature of PWM control and the lack of mathematical means of analysis. Mathematical means have been well developed, however, for pulse amplitude modulation or sample data control which is a linear process. Andeen applied the "principle of equivalent areas" to transform a unipolar PWM process into a

sample data process and then applied z-transform compensation techniques to counter the destabilizing effects of PWM as system bandwidth rises toward the switching frequency. This equivalent model was shown to be quite successful by experiment in predicting the early destabilizing effects of PWM as bandwidth is increased. This model is valid, at best, up to a bandwidth 1/2 the switching frequency which is adequate for application to motor control systems. The sample data model, which is shown in Figure 5, along with input and output waveforms, does not show the output ripple associated with the first harmonic of the unipolar PWM switching. This effect should be even stronger for bipolar PWM. The "principle of equivalent areas" will be analyzed in greater detail for the bipolar PWM along with study of the first harmonic ripple.

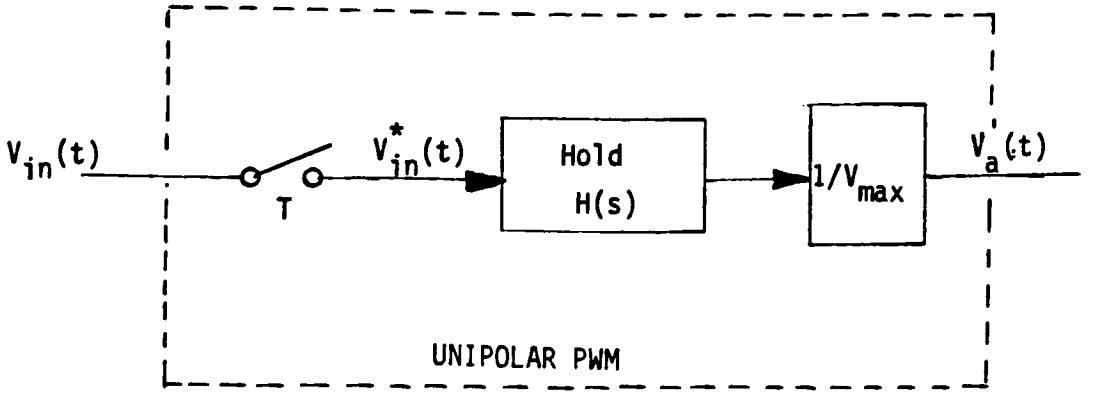

(a)

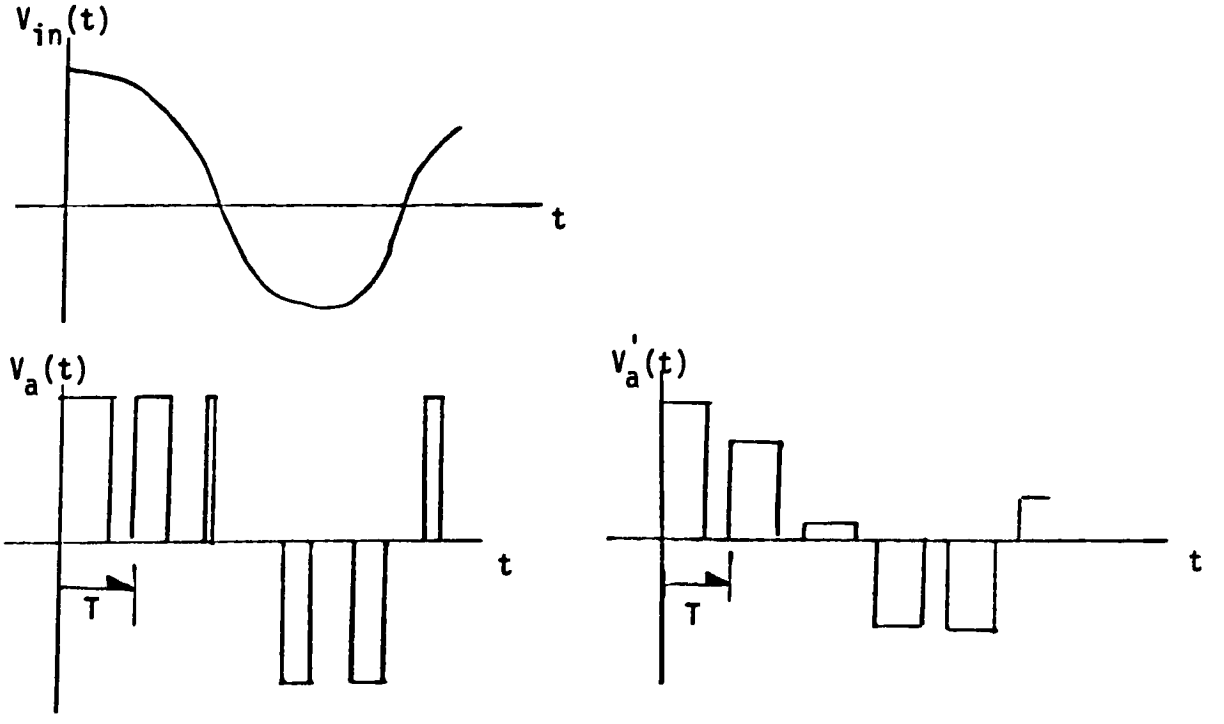

(b)

Figure 5

(a) Sample Data Model of a Normalized Unipolar PWM by Andeen
(b) Input Waveform and Unipolar Output and Equivalent Sample Data Output Waveforms

Parrish and McVey [10] and Serebryakov [12] lend support to the sample data model of the PWM. These references use sample data to take into account the sampling nature of thyristor drive systems and single-phase silicon-controlled rectifier systems.

Kravitz [22] also uses a sample and hold model to represent the closed loop switching regulator system.

Stability of pulse width controlled dc voltage stabilizers is examined by Kitayev and Stoyanov [23] through a sample and hold model. This paper also demonstrated that z-transform theory could be used to analyze the system.

One method of linearizing a nonlinear system is by the method of describing functions which is found in several of the References [18, 17, 28, 29]. In this technique, the input is sinusoidal.

$$V_{in}(t) = E_i \sin \omega t \tag{3.5}$$

If the nonlinear system is assumed to be symmetric, there is no DC term in the output. In general, the output of the nonlinear system $V_a(t)$ is also periodic having the same fundamental periods as that of the input signal. Fourier Series can be used to express the output of the nonlinear device.

$$V_a(t) = A_0/2 + \sum_{n=1}^{\infty} A_n \cos n\omega t + \sum_{n=1}^{\infty} B_n \sin n\omega t \qquad (3.6)$$

where:

$$A_n = 2/\pi \int_0^{\pi} V_a(t) \cos n\omega t \; d(\omega t) \qquad (3.7)$$

and:

$$B_n = 2/\pi \int_0^{\pi} V_a(t) \sin n\omega t \; d(\omega t) \qquad (3.8)$$

By definition, the describing function, N, is an equation expressing the ratio of the amplitudes and the phase angle between the fundamental of the output and the input sinusoids.

$$N(E_i,\omega) = [(A_1^2 + B_1^2)^{\frac{1}{2}}/E_i] \; e^{j \, \mathrm{Tan}^{-1}(A_1/B_1)} \qquad (3.9)$$

Higher order harmonics are neglected since the harmonic terms are generally small compared to the fundamental term and the dynamics of the servo control system inherently act as a low pass filter. The gain and phase terms of the describing function $N(E_i,\omega)$ can be used in a standard block diagram or transfer function as shown in Figure 6 to predict stability and response.

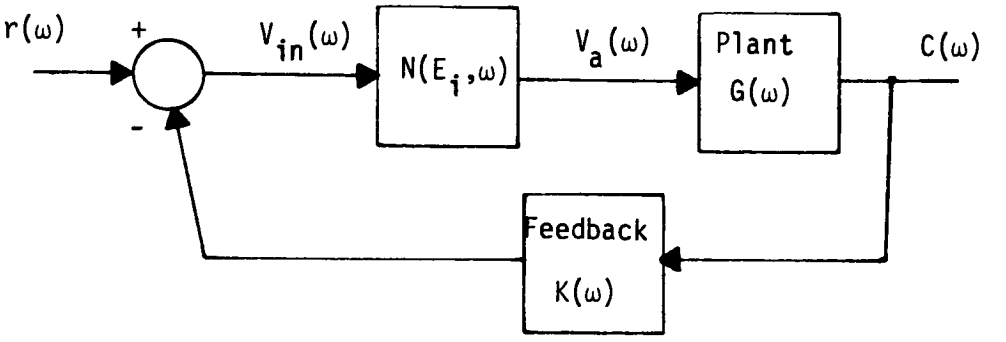

$$\frac{C(\omega)}{r(\omega)} = \frac{G(\omega)N(E_i,\omega)}{1+G(\omega)N(E_i,\omega)K(\omega)}$$

Figure 6

Block Diagram of A PWM System Utilizing A Describing Function As A Model

The' and Furmage [18] use describing functions to predict subharmonic oscillations and to measure the relative degree of stability of bipolar PWM control systems. Their technique utilizes an envelope created by a set of describing functions for the PWM which is then used to test system stability from a Nyquist criterion. From the transfer function in Figure 6, the characteristic equation on which the Nyquist plot is based is:

$$1 + G(j\omega)\ N(E_i,\omega)\ K(j\omega) \qquad (3.10)$$

The normal linear procedure is to obtain a polar plot of:

$$|G(j\omega)\ N(E_i,\omega)\ K(j\omega)| \qquad (3.11)$$

which makes the point -1 + j0 the critical point for stability analysis. By re-arranging the characteristic equation as:

$$G(j\omega)\ K(j\omega) = \frac{-1}{N\ (Ei,\omega)} \qquad (3.12)$$

the linear system function factors are separated from the describing function factor. Thus, $|G(j\omega)\ K(j\omega)|$ may be plotted as a polar transfer function curve. The term $|-1/N(E_i,\omega)|$ may also be plotted on the same sheet to the same scale, however, it is a function of both signal

amplitude E_i and frequency ω. Thus, plotting $|-1/N(E_i, \omega)|$ results in a family of curves. System stability can be investigated by inspecting the relative location of points of the $|G(j\omega)\ K(j\omega)|$ curve with respect to the corresponding $|-1/N(E_i,\omega)|$ curves. The system is stable if for all frequencies the points on the $|G(j\omega)K(j\omega)|$ curve lie outside the corresponding $|-1/N(E_i, \omega)|$ curves.

This system yielded very good results in predicting stability when compared to simulations on the analog computer. Further, if a system is found unstable, series compensators can be analyzed to determine which would bring the system $|G(j\omega)K(j\omega)|$ curve outside the $|-1/N(E_i, \omega)|$ curves.

Although very good stability predictions were obtained, plotting all the Nyquist curves is time consuming and they cannot be used in a standard linear systems model and analysis. Also, the first harmonic ripple cannot be predicted in stable systems.

Taft, Banister, and Slate [28] discuss several different driver configurations for bipolar PWM amplifiers controlling d.c. motors. The input/output relationships for both the d.c. gain term and the first harmonic term of the square wave output are presented for each configuration. Although the d.c. gain is essentially linear up to

saturation for most configurations, the first harmonic term is shown to be a very nonlinear function of the input. Describing function analysis was used to study the limit cycle PWM oscillator. A pulse width modulated signal is obtained by closing a feedback loop around a switching element to cause the system to have a high frequency limit cycle. This approach requires no external dither source. Dither sources, which are used in most motor amplifiers encountered by the author, will be further discussed in the analysis section. Limit cycle PWM oscillators will not be discussed in this paper. Further work is required to linearize the nonlinear relationships generated [28].

Kolk [29] derives describing functions for a wide variety of unipolar PWM situations which include saturated and unsaturated trailing edge modulation and saturated and unsaturated leading edge modulation. Assymptotic approximation for rapid PWM sampling compared to the input is also analyzed. The result is a family of curves showing the variation of describing function magnitude and phase. Experimental investigation verified conclusions drawn about stability and limit cycle behavior.

Some interesting studies have been done on electrohydraulic servo systems utilizing bipolar PWM valve drives [33, 24]. Because of close tolerances and fluid contaminants,

electrohydraulic servovalves are subject a number of nonlinearities at zero velocity. When an electrohydraulic servo mechanism is driven by a PWM control, the high frequency switching of the PWM output, and the resulting dither in the valve spool, greatly reduces the sensitivity to fluid contamination and the effects of such nonlinearities as hysteresis, threshold, stiction, dead zone, and null shift. Thus, the PWM switching effects improve system performance.

Tsai and Ukrainetz [33] attempt to model and analyze a closed loop hydraulic servo system using PWM control and predict its output response including the valve spool dither. Thus an appropriate transfer function of the pulse width modulator had to be developed. This transfer function was derived from a double Fourier series analysis of the modulated waveform. A double Fourier series analysis of pulse width modulation was earlier presented by Black [35] along with a description of leading edge and trailing edge modulation and uniform sampling and natural sampling PWM. Uniform and natural sampling will be further described in Section 4. A double Fourier analysis was used by Black [4] to determine the spectra of the PWM signal with its infinite number of harmonics and sidebands. The resultant pulse-width modulator model by Tsai and Ukrainetz is shown in Figure 7. Note that, in addition to the linear d.c. gain element corresponding to

the average value of the output, a second system input corresponding to the first harmonic has been added. This first harmonic input may provide the PWM switching effects in the output that one suspects is present. Since the PWM switching was found to have negligible effect on the electrohydraulic transient response, the extent of output ripple was omitted from experimental verification. Thus, it is not known whether the constant amplitude given for the harmonic input is correct. Also, there is no means in this model of predicting instability or de-stabilizing effects as system bandwidth approaches switching frequency. Good agreement was shown in this paper between actual and predicted frequency response for the overall closed loop hydraulic system.

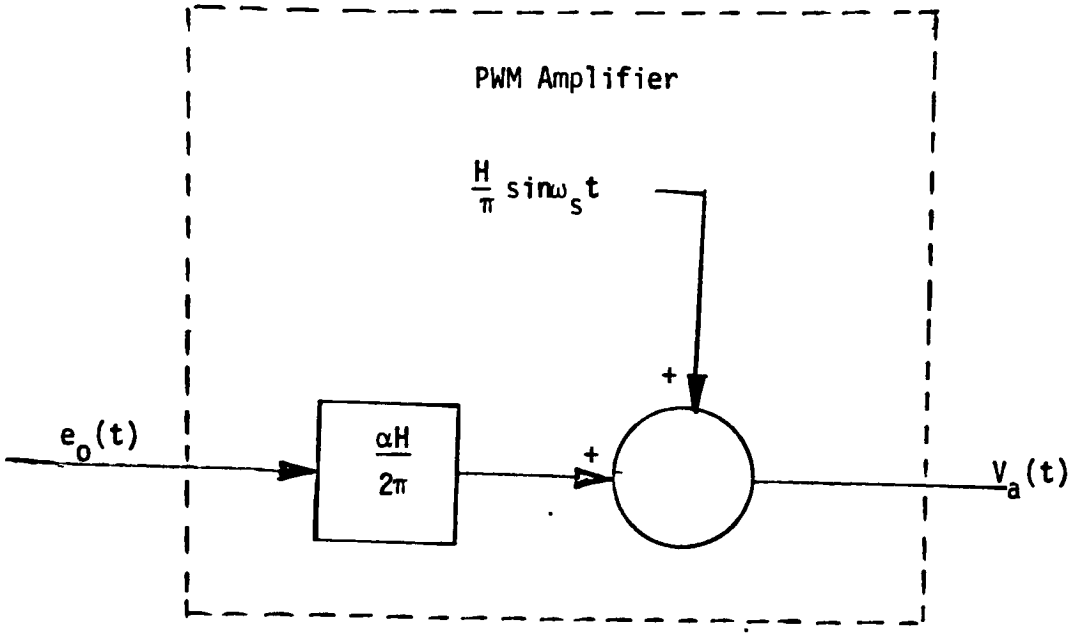

H = peak-to-peak amplitude of the modulated output wave form,

α = modulation index

Figure 7

Pulse Width Modulator Model Derived from Double Fourier Transform Analysis by Tsai and Ukrainetz [33]

This paper will study very closely the double Fourier series analysis technique applied to the bipolar PWM motor amplifier.

Ghonaimy and Aly [19] discuss a phase plane technique for PWM modeling. This method has the disadvantage, however, of being applicable only for second order systems. Phase plane is also utilized by Karetnyi and Sheryaev [21].

Many papers on PWM discuss stability through Liapunov's second method. It is not clear, however, how this method could be used in linear systems analysis and compensation.

4.0 PWM Servo Control System Analysis and Model

This section presents the analysis done on the PWM signal and its effect within a motor control servo system. A linear model is developed which provides the same effects within a motor control servo system as the true non-linear PWM amplifier. Figure 8 traces the development which will be presented in this section. The electro-mechanical position control servo problem consisting of a piece of tooling driven by a permanent magnet d.c. motor is introduced. The model development uses ordinary linear differential equations to describe the system components and ultimately the system transfer function.

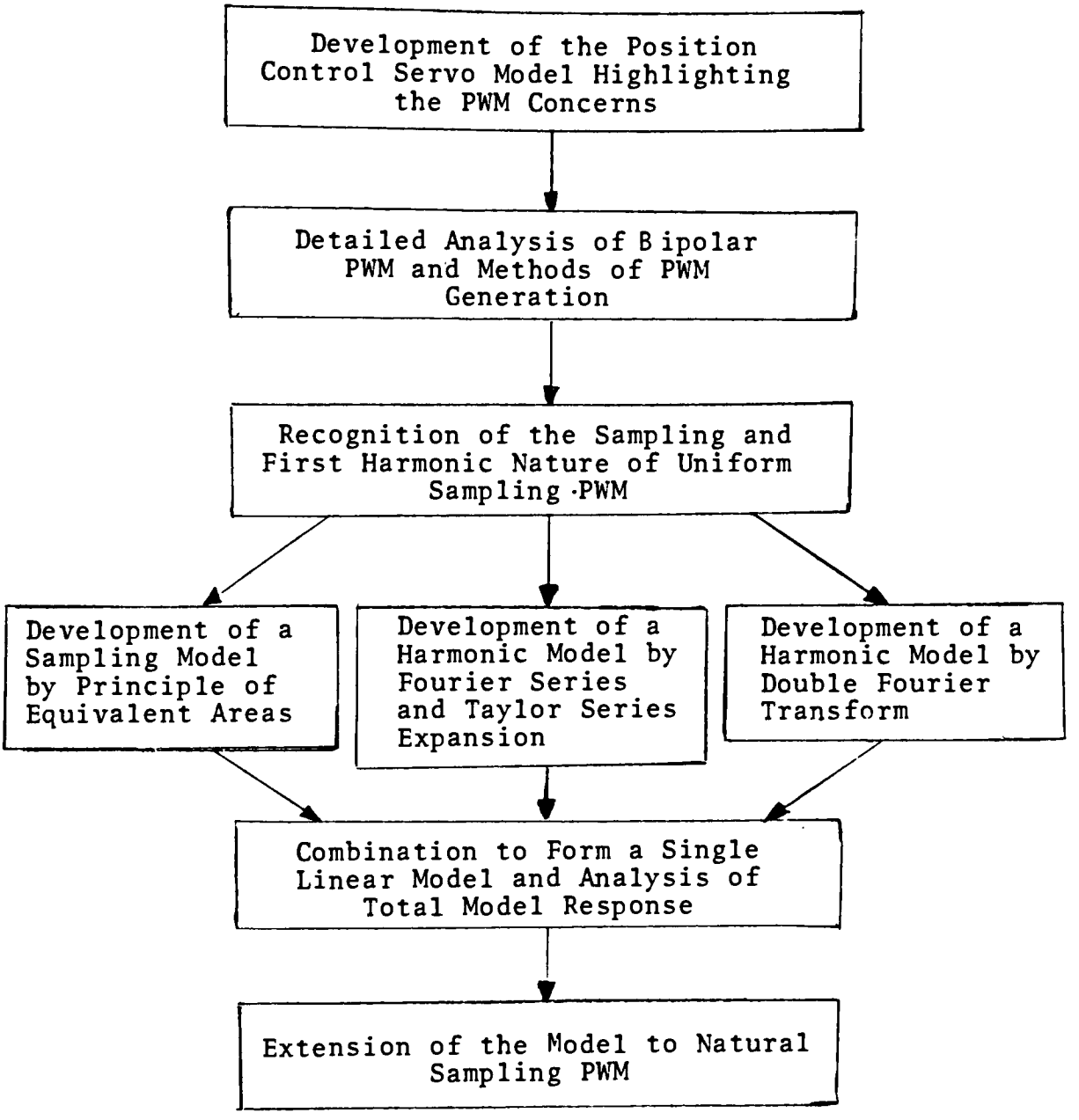

Figure 8

Development Block Diagram of the PWM Amplifier Linear Model

Obviously missing in this development is a linear description of the PWM motor amplifier. One is tempted to use a simple d.c. gain as the transfer function which would be acceptable in a low response application; however, the servo designer is often asked to extend response and accuracy into regions which make the use of this transfer function uncomfortable. One wishes to have a mathematical description which would show output ripple and the onset of instability, if applicable. To accomplish this, the stability and first harmonic ripple analysis are attacked separately. The sampling nature of PWM is explored as a clue toward stability and the "Principle of Equivalent Areas" is used to develop a model for uniform sampling PWM. In parallel, the switching ripple effect is analyzed first by Fourier series and Taylor series expansion and second by double Fourier transform. Both techniques yield linearized models. The sampling and first harmonic models are then combined and the results of this combination studied. Finally, the model is modified and presented as a linearized description of natural sampling PWM.

4.1 Position Control Servo Model

A typical control problem encountered in machine design for industry is the position control of a piece of tooling. The position could be linear or angular displacement depending on the application. A typical

schematic diagram of an angular position control system is shown in Figure 9. The load is a piece of tooling which performs some operation such as cutting, punching, sealing, etc. The tooling is driven by a permanent magnet d.c. motor powered by a PWM motor amplifier. Tooling position is measured by a sensor such as a potentiometer or encoder and velocity is measured by the tachometer on the motor. Velocity and position compensation are added as required to obtain the desired response.

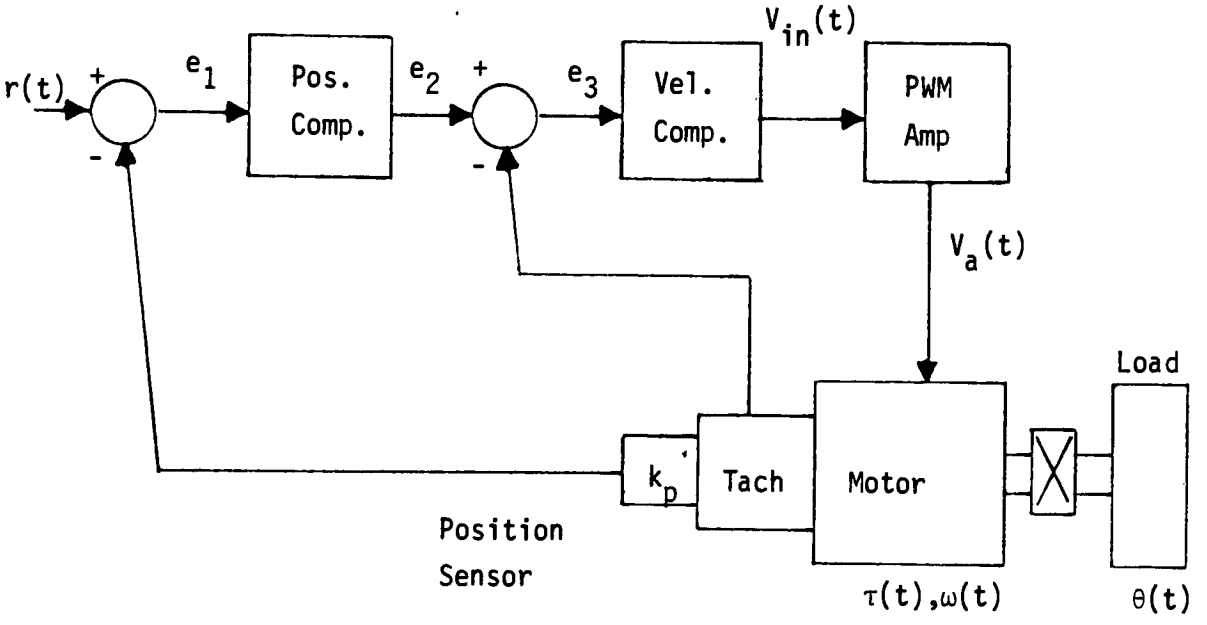

Figure 9

Schematic Diagram of An Angular Position Control System

The standard tools used by the servo system designer to achieve the desired system performance are linear systems analysis and compensation. Although no system is completely linear, mechanical nonlinearities such as friction, dead zones, and cogging, and electrical nonlinearities such as saturation and hysteresis are minimized or eliminated in a good design. Thus, linear differential equations are used to describe the remainder of the system and are described as follows:

a) Permanent Magnet d.c. Motor

The equivalent electrical circuit of the dc motor consists of a series resistor, inductor, and voltage source. Motor windings create the resistance and inductance. The action of the armature windings cutting the lines of magnetic flux generates the back electromotive force (EMF) proportional to motor speed $\omega(t)$. Torque generated by the motor $\tau(t)$ is proportional to armature current $I_a(t)$. The resulting differential equation is given by Eq (3.4). The motor transfer function becomes:

$$\tau(s)/V_a(s) = \frac{K_T/L}{s + R/L} \qquad (4.1)$$

b) Motor/Load Relationships

The load elements of a typical motor system consist of inertia J, Coulomb friction T_f, and a windage term which produces a torque proportional to load velocity. If the motor and load are assumed to be rigidly coupled, which is valid for many low response servo applications, the differential equations and transfer function are:

$$\tau(t) = J\, d\omega(t)/dt + F\, \omega(t) + T_f \qquad (4.2)$$

$$\omega(t) = d\theta(t)/dt \qquad (4.3)$$

$$\frac{\theta(s)}{\tau(s) - T_f(s)} = \frac{1/J}{s(s + F/J)} \qquad (4.4)$$

As one begins to look at the motor/load response at higher frequencies, the coupling between the motor and load begins to show tortional flexibility, the magnitude and frequency of which may effect precision systems. The tortional coupling can be effectively modeled by a second order spring differential equation where $T_1(t)$ is the instantaneous tension in the coupling. The resulting equations and transfer functions are:

$$\tau(t) = J_m \, d^2\theta_m(t)/dt^2 + F \, d\theta_m(t)/dt + T_1(t) + T_f \qquad (4.5)$$

$$T_1(t) = J_L \, d^2\theta(t)/dt^2 \qquad \text{assuming no windage} \qquad (4.6)$$

$$T_1(t) = K_c[\theta_m(t) - \theta(t)] + B_c[d\theta_m(t)/dt - d\theta(t)/dt] \qquad (4.7)$$

$$\frac{\theta(s)}{\tau(s) - T_f(s)} = \frac{B_c s + K_c}{(J_m s^2 + Fs)(J_L s^2 + B_c s + K_c) + J_L s^2 (B_c s + K_c)} \qquad (4.8)$$

$$\frac{\omega(s)}{\tau(s) - T_f(s)} = \frac{J_L s^2 + B_c s + K_c}{(J_m s^2 + Fs)(J_L s^2 + B_c s + K_c) + J_L s^2 (B_c s + K_c)} \qquad (4.9)$$

The tortional coupling is very underdamped and is very susceptable to external excitation as might happen from a switching motor power supply. Excluding the pole at the origin, there are three poles in the characteristic equation of the preceeding transfer function. It can be assumed that one pole is the mechanical pole at a very low frequency and that the spring constant K_c is large [1]. This assumption is true for solid shafts and stiff couplings. At low frequencies,

$$K_c >> sB_c \quad \text{and} \qquad (4.10)$$

$$K_c >> s^2 J_L \qquad (4.11)$$

Thus, the characteristic equation of the system described by Eq. (4.8) and (4.9) reduces to:

$$(sJ_m + F)K_c + J_L K_c s = 0 \tag{4.12}$$

$$p1 = -F/(J_m + J_L) = -F/J \tag{4.13}$$

The other two resonant poles are largely determined by the tortional coupling [1]. At high frequency,

$$J_m s >> F \tag{4.14}$$

The resultant characteristic equation at high frequency is:

$$s^2 J_L J_m + sB_c(J_L + J_m) + K_c(J_L + J_m) = 0 \quad \text{or,} \tag{4.15}$$

$$s^2 J_e + sB_c + K_c = 0 \tag{4.16}$$

where:

$$J_e = J_L J_m/(J_L + J_m) \tag{4.17}$$

The remaining two poles are the roots of the quadratic equation (Eq. 4.16). The motor/load transfer functions can be approximated by

$$\frac{\theta_L(s)}{\tau(s) - T_f(s)} = \frac{1/J\ (B_c s + K_c)}{(s + F/J)(s^2 + B_c/J_e\ s + K_c/J_e)} \qquad (4.18)$$

$$\frac{\omega_m(s)}{\tau(s) - T_f(s)} = \frac{1/J\ (J_L s^2 + B_c s + K_c)}{(s + F/J)(s^2 + B_c/J_e\ s + K_c/J_e)} \qquad (4.19)$$

Equations (4.18) and (4.19) contain lightly damped resonant poles which can be easily excited by PWM harmonics.

c. Position Compensation

The position compensation network is typically a proportional plus integral plus derivative (PID) compensation or lag/lead network as required to achieve the desired system performance. The compensator acts on the error signal between the command and tooling position measured by the feedback

element. The transfer function is of the form,

$$\frac{E_2(s)}{E_1(s)} = \frac{a_1 s^2 + a_2 s + a_3}{s^2 + b_1 s + b_2} = A(s) \qquad (4.20)$$

$$E_1(s) = r(s) - k_p \theta(s) \qquad (4.21)$$

d. Velocity Compensation

The velocity compensation network is of the same form as the position compensation and is added as required to achieve desired performance. The velocity compensator acts on the error signal between the output of the position compensator and the motor velocity as measured by the motor tachometer. The transfer function is of the form,

$$\frac{V_{in}(s)}{E_3(s)} = \frac{c_1 s^2 + c_2 s + c_3}{s^2 + f_1 s + f_2} \qquad (4.22)$$

$$E_3(s) = E_2(s) - K_{tach}\omega(s) \qquad (4.23)$$

The output of the velocity compensation is the input to the PWM motor amplifier.

The resulting system block diagram is shown in Figure 10. Except for the PWM motor amplifier transfer function, the system has been fully described by Eqs. (4.1), (4.4), (4.20), and (4.21) and awaits the entry of system parameters. It is here that the servo designer encounters the problem of modeling his bipolar PWM amplifier. The simplest solution is to use the d.c. gain model of Eq. (3.3) and ignore PWM effects. This solution is inadequate if, in his zeal for higher response and greater accuracy, the designer has pushed system bandwidth into the "vicinity" of the PWM switching frequency. The "vicinity" of the PWM switching frequency is yet to be defined. The remainder of this paper will attempt to model the true nature of the PWM amplifier as applied to the servo system of Figure 10. Deviation of the true system response from a system with a simple d.c. gain model will be analyzed and tested by computer simulation. Specifically, the next section will take a close look at the bipolar PWM signal and the various methods for bipolar PWM generation.

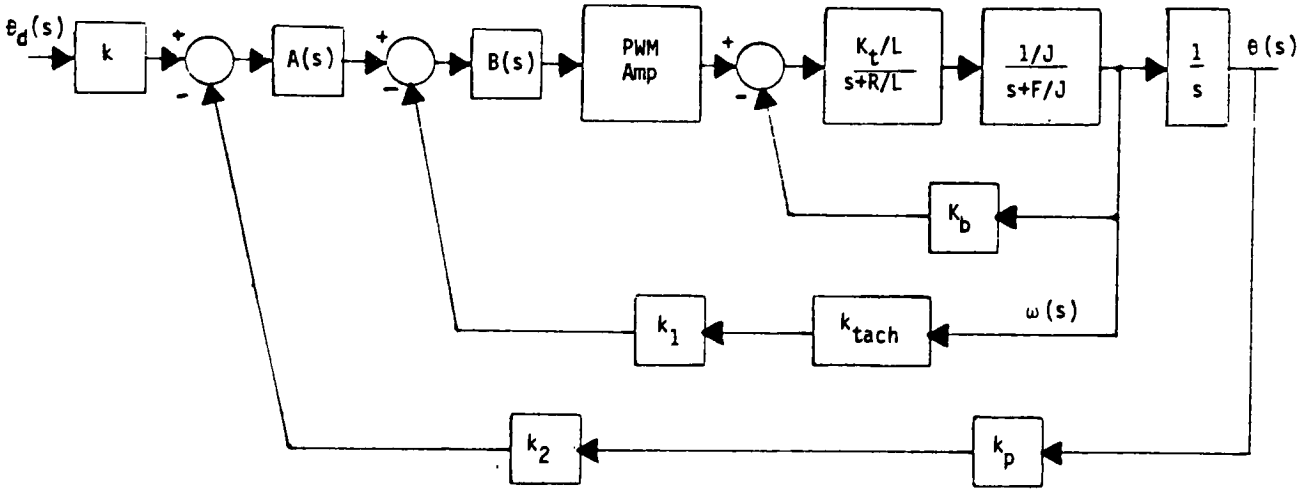

ASSUMING RIGID COUPLING BETWEEN

THE MOTOR AND LOAD ($K_c = \infty$)

Figure 10

System Block Diagram of an Angular

Position Control Servo System

4.2 Detailed Analysis of Bipolar PWM and Methods of Generation

In bipolar pulse width modulation, constant amplitude rectangular pulses are generated whose width are directly proportional to the modulating voltage. This modulation process is most often performed by comparing the input signal $V_{in}(t)$ with a high frequency reference dither signal. The two signals are added together and then fed to a comparator or relay element [3,6,28]. The relay element coverts the resulting sum into a two level signal $V_a(t)$ as shown in Figure 11. The sawtooth dither signal shown makes the trailing edge of the pulse indicative of the input dc level. This is sometimes called trailing edge modulation.

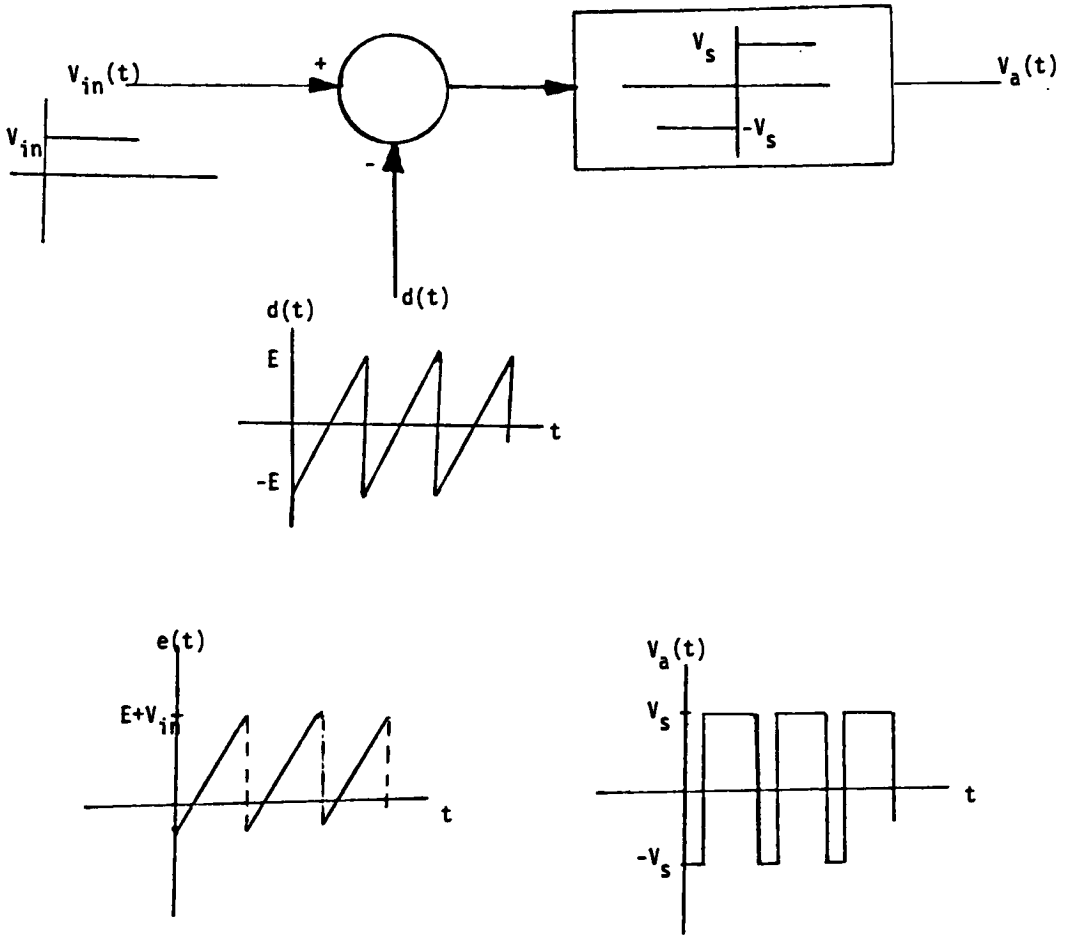

Figure 11

PWM Generation Using a Dither Signal and Relay Element

There are three types of dither signals which may be used in the PWM generation [6] [35]:

1. Sawtooth waveform with leading edge modulation.

2. Sawtooth waveform with trailing edge modulation.

3. Triangular waveform with both leading and trailing edge modulation.

The three dither signals are shown in Figure 12. Other types of dither signals can be used such as sine waves; however, these add further nonlinearities to the system [28].

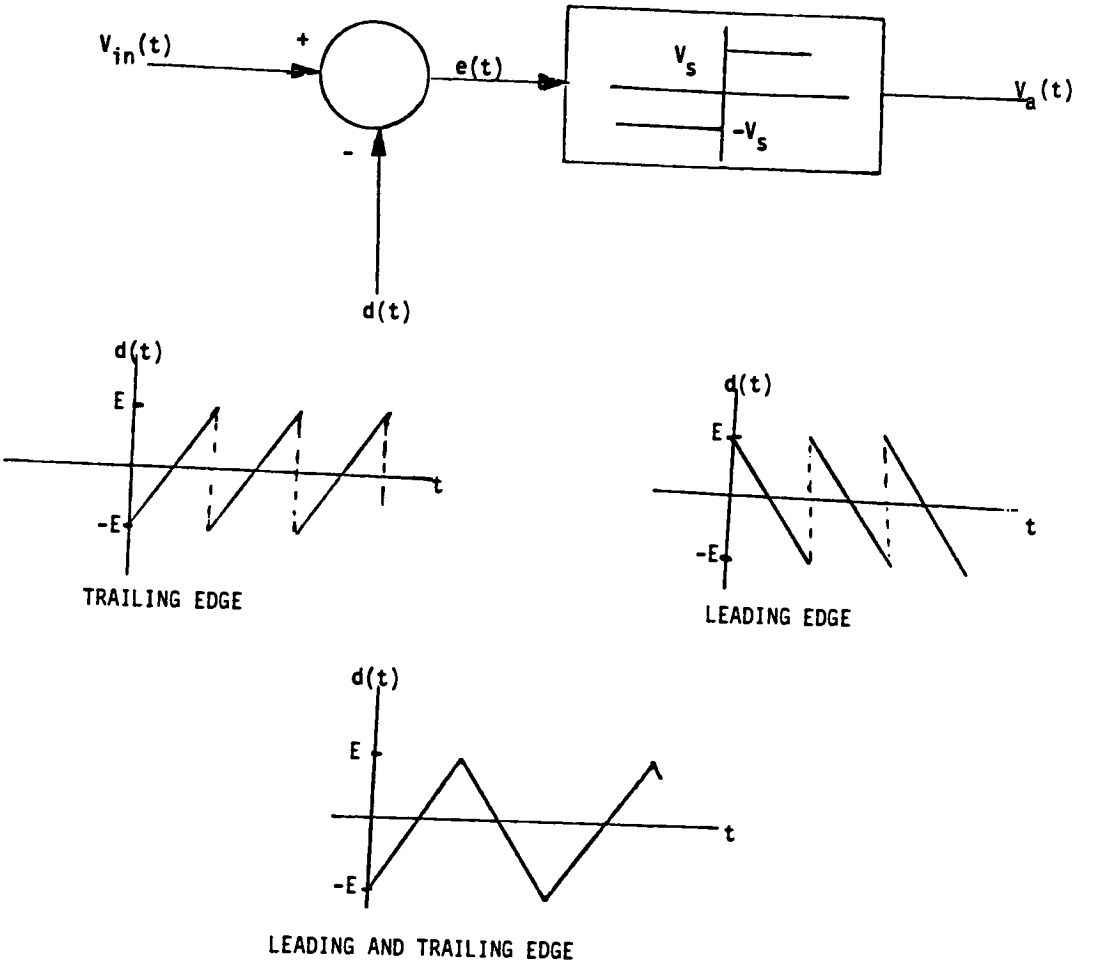

Figure 12

Dither Signals Used in PWM Modulation

The dither signal is a high frequency signal which determines the switching frequency f_s and time period T of the PWM amplifier. The input signal $V_{in}(t)$ is varying much more slowly than the dither signal in normal application. This is true since the motor servo control system acts as a low pass filter severely attenuating high frequency signals in the system. If the system input r(t) is slowly varying, $V_{in}(t)$ will not have a high frequency content.

The input signal $V_{in}(t)$ can perform the modulation process by two methods. In the first, the input signal is sampled at a constant rate as determined by the frequency of the dither signal (f_s). The value of $V_{in}(t)$ at the sampling instant $V_{in}^*(t)$ determines the width of the output pulse. This form of modulation is known as uniform sampling PWM [35].

In the second method, the input signal is simply compared to the dither signal and allowed to switch the output whenever the sum changes sign. The polarity of the output depends on the polarity of the sum of the input plus dither signal. This form of modulation is known as natural sampling PWM [35]. The two modulation methods are shown in Figure 13 (a) and (b).

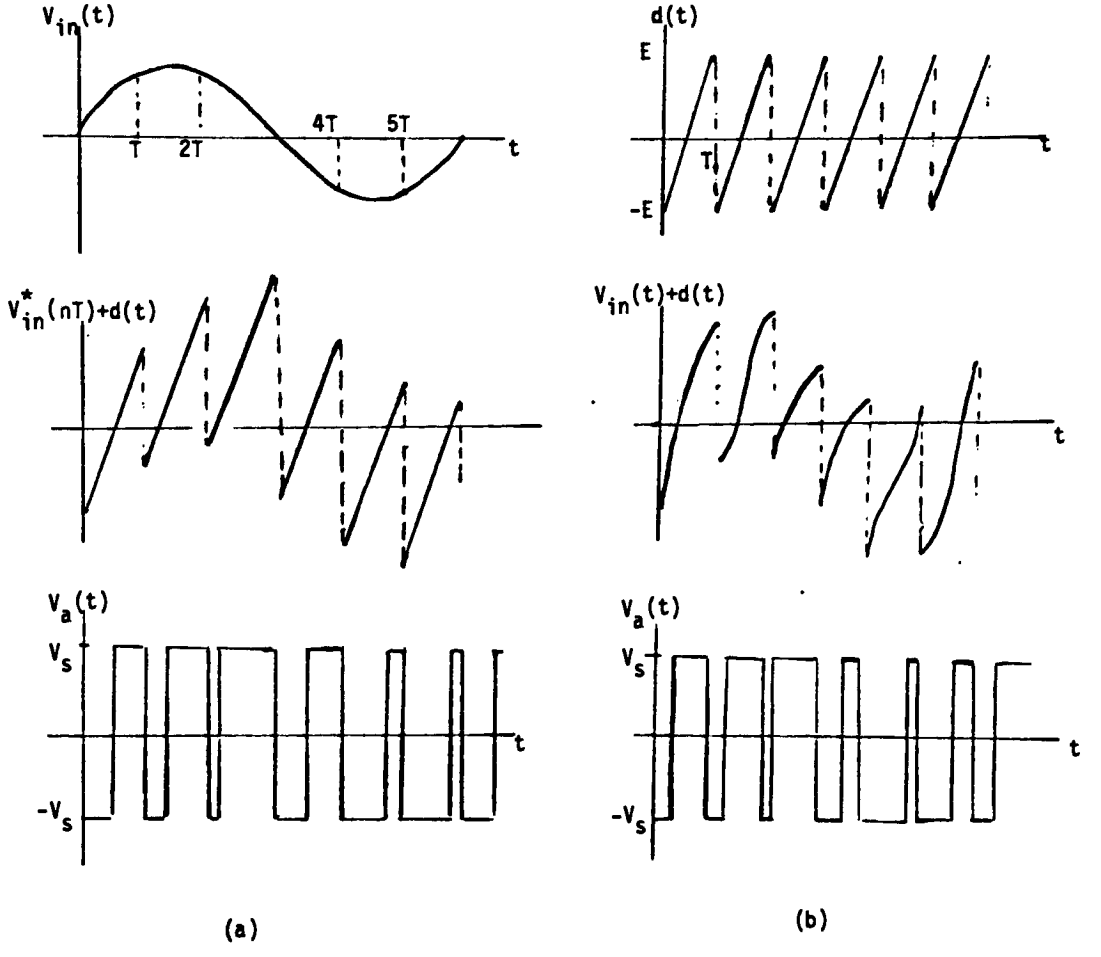

Figure 13

(a) Uniform Sampling PWM
(b) Natural Sampling PWM

If the input $V_{in}(t)$ is constant or varing slowly with respect to the PWM switching frequency, the value of the input is essentially constant over the switching period T and the two methods of modulation yield equivalent results. Both modulation schemes are, in effect, sampling schemes. For uniform sampling, the value of the input at the beginning of the switching period determines the pulse width for that period. For natural sampling, the sampling point is more difficult to determine as the pulse width is determined instantaneously at the point where the sum of the input plus the dither changes sign. Thus, the sampling point is dependent on the instantaneous magnitude of the input $V_{in}(t)$. If the input is constant or slowly varying, the input changes little over a switching period and the time between switching points is essentially constant and equal to the period of the dither signal. For inputs other than saturation the sampling point will be out of phase with the start of the switching period and occur more towards the center of the cycle. As the frequency content of the input approaches the switching frequency, the period of the natural sampling PWM method becomes more and more nonuniform adding to the nonlinearity of the system.

This analysis will start with the study of uniform sampling PWM modulation and the derivation of a model. It is hoped that natural sampling can then be looked at again

with the intent of modifying the uniform sampling model to account for natural sampling peculiarities. For low frequency inputs, this would seem quite promising.

There are potentially two areas to be explored in the analysis of pulse width modulation which may effect the servo system response. One area is the stability problem which arises as the system bandwidth and thus input signal spectral content approach the PWM switching frequency. The sampling nature of the pulse width modulation would seem to provide a lot of insight into the onset of instability. The second area is the system output ripple due to the switching PWM waveform. A Fourier series description of the switching signal which is linearized would seem to represent the ripple effects. The inherent low pass filter nature of the servo system will attenuate the higher frequency components of the Fourier description. Thus, these two areas will be looked at separately and the resultant linearized models combined to form the total PWM model.

4.3 Sample and Hold Model for Uniform Sampling PWM Systems by the Principle of Equivalent Areas

Although the pulse width modulator has been described as a sampling system, one can readily see that the PWM sampling process is a nonlinear method of representing the input

data. The input and output fail the important superposition principle which states that the response produced by the simultaneous application of two different forcing functions is the sum of the two individual responses. It is this principle which makes possible the transfer function analysis technique. Because of this nonlinear nature, mathematical means of handling PWM devices have been hard to develop.

Mathematical means have been well developed, however, for pulse amplitude modulation processes which are linear. These sampled data systems have outputs which are a sequence of equally spaced, equal duration pulses whose amplitudes are proportional to the input at the sampling instant. Due to the abundance and thorough development of linear analysis techniques for pulse amplitude modulation systems, it would be advantageous to transform the bipolar PWM signal with its equally spaced, constant amplitude output pulses to an equivalent pulse amplitude modulation system. It appears that this can be done by the Principle of Equivalent Areas [14].

According to the Principle of Equivalent Areas [14], two input signals are dynamically equivalent if their integrals evaluated over corresponding sampling intervals are equal, and the sampling frequency determined by this interval is at least twice the highest significant

frequency in the frequency spectrum of the dynamic system. Mathematically,

$$\int_{(n-1)T}^{nT} v(t)\,dt = \int_{(n-1)T}^{nT} v'(t)\,dt \qquad (4.24)$$

where v(t) is the nonlinear signal and v'(t) is the equivalent pulse amplitude modulation signal. Rather than use narrow pulses, the pulse amplitude or sample data system utilizes a hold circuit after sampling to smooth out the energy transferred to the system during the sampling period. The hold circuit in a sense averages or filters the pulsed signal over the sampling period. The servo system elements themselves perform additional filtering to smooth out the effects of the pulsed nature. For the sample and hold model to be valid, it must be assumed that the pulse width modulation works in combination with system elements which include low pass elements having a largest time constant less than 1/2 the sampling period [14]. This assumption is valid for the motor control servo system under study [1, 2, 3, 4] as it is the intent of this analysis to explore system response as bandwidth approaches switching frequency.

A typical PWM input signal and response is shown in Figure 14. The input signal is allowed to vary from $\pm V_{max}$ which is the maximum voltage level of the dither signal or is the voltage at which output saturation occurs. At

saturation, the sum of the input plus the dither signal does not change sign and the output becomes a pure dc level. This analysis will not attempt to model any saturation effects as this is another nonlinearity. Thus, the input is subject to the following limitation,

$$-V_{max} \leq V_{in}(t) \leq V_{max} \tag{4.25}$$

Also note in Figure 14 that the output has been normalized to the input and the output switches between $\pm V_{max}$. The PWM amplifier gain will be determined in the Fourier analysis. The object of this application of the "Principle of Equivalent Areas" is to solve for a pulse amplitude modulation signal $V_a^*(t)$ which is an equivalent input to the rest of the system as the nonlinear signal $V_a(t)$.

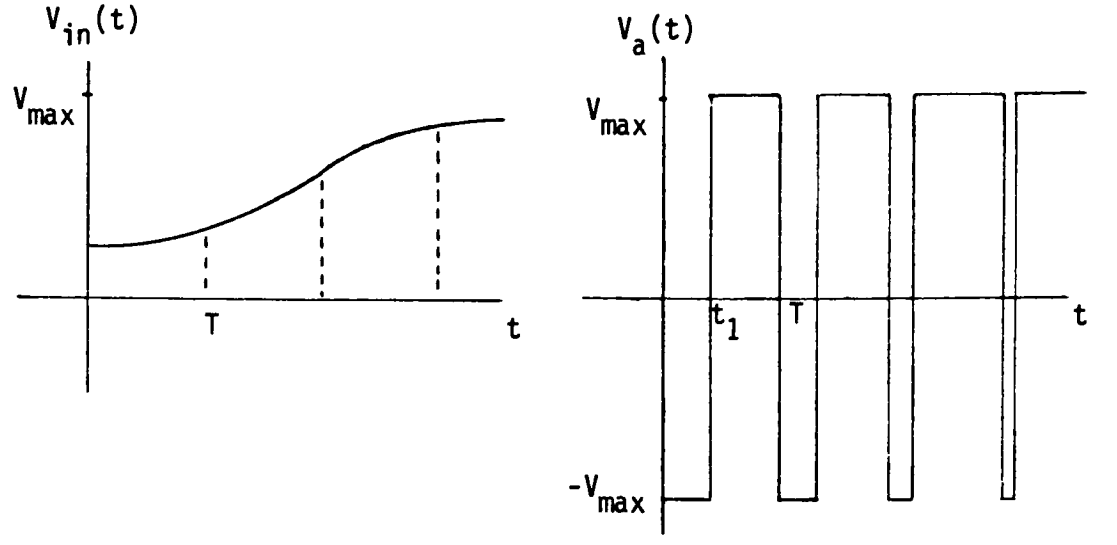

(a)

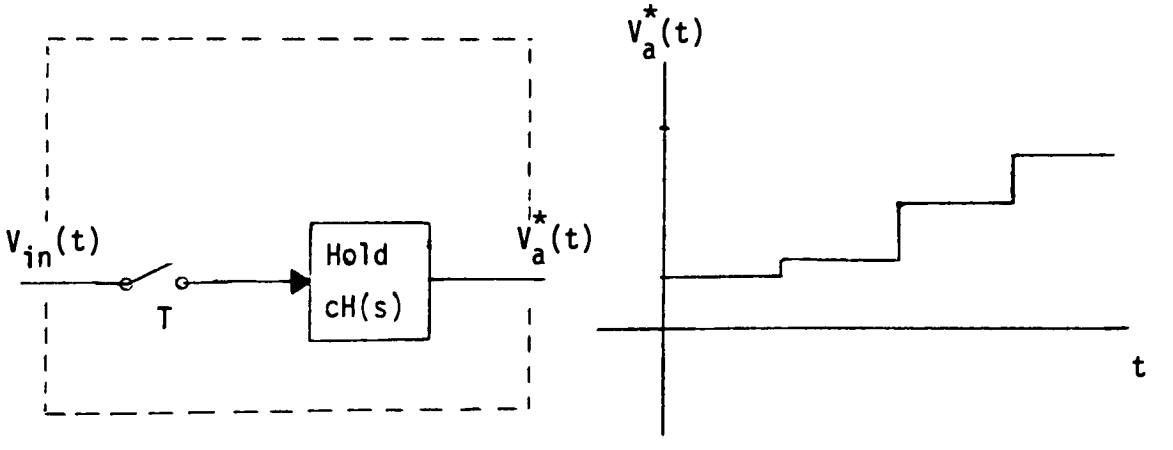

(b)

Figure 14

(a) Typical PWM Input Signal and Normalized Response
(b) Equivalent Sample Data Model

To determine the area of the output PWM waveform for the interval $0 \leq t < T$, the switching time t_1 must be determined as shown in Figure 14. Time t_1 is the time at which the sum of the input plus the dither signal cross zero. If the term $V_{in}(0)/V_{max}$ is defined as the duty cycle $\alpha(0)$, time t_1 is given as:

$$t_1 = \tfrac{1}{2}(1 - \alpha(0))T \tag{4.26}$$

By definition, $1 \leq \alpha(t) \leq 1$. The area under the output signal $V_a(t)$ can be calculated as:

$$\text{Area} = t_1(-V_{max}) + (1 - t_1)\, V_{max} = \alpha(0)TV_{max} = V_{in}(0)T \tag{4.27}$$

In general, the area under the nth cycle is given as:

$$\text{Area} = V_{in}[(n-1)T]T \tag{4.28}$$

For the sample and hold model to be equivalent to the PWM signal by the Principle of Equivalent Areas, the area under the nth sample and hold cycle must also be given by Eq. (4.28).

Note that this is true if the input signal is sampled directly and held over the duration of the switching period. Thus, the sample and hold shown in Figure 15 effectively represents the sampling nature of the PWM

amplifier and is an equivalent input to the rest of the system if the plant bandwidth is less than 1/2 the PWM switching frequency 1/T. System stability can now be analyzed by the standard sampling criteria associated with sampled systems. This indicates that z transform techniques can be used to analyze and compensate for instabilities caused by the switching nature of the PWM system. The next section will explore the switching effects.

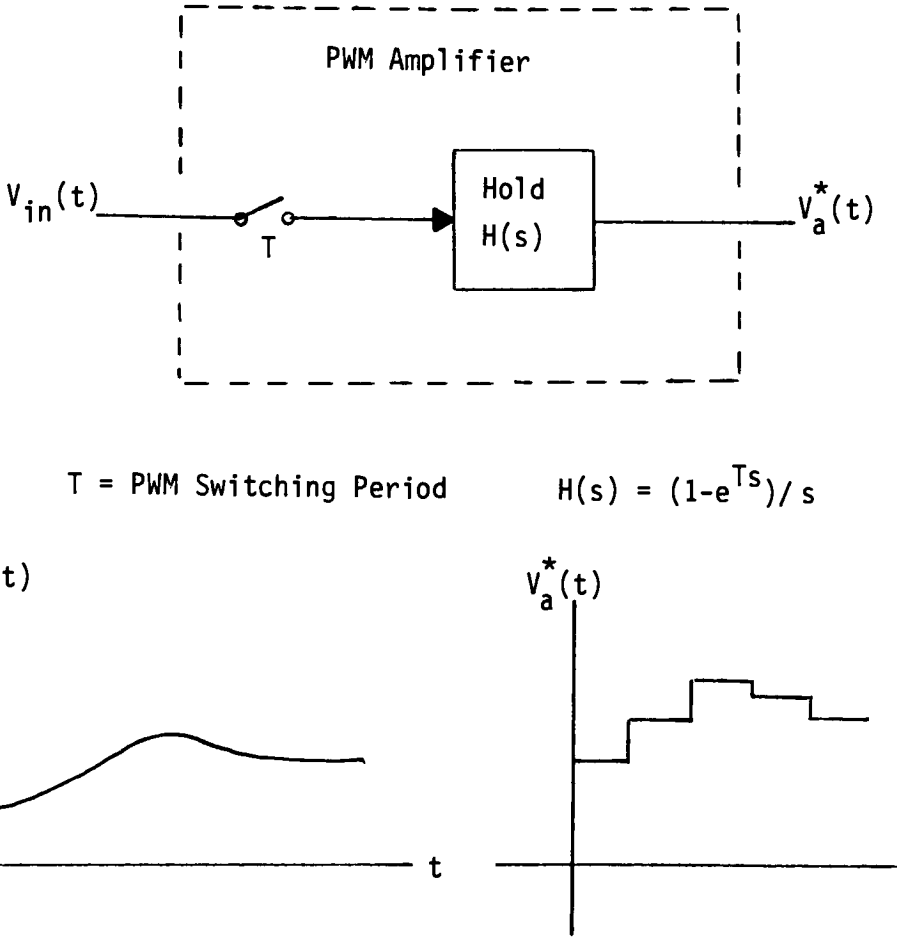

Figure 15

Equivalent Sample and Hold Model Developed by the Principle of Equivalent Areas

4.4 PWM Amplifier Switching Harmonic Model by Fourier Series and Taylor Series Expansion

As shown in the preceding section, the sampling nature of the PWM amplifier can be represented by a sample and hold equivalent model as long as system bandwidth remains low enough. Such a model will provide some insight into system stability; however, it is not clear how this model can predict the torque and the output ripple due to amplifier switching. To model this effect, a detailed look at the output waveform utilizing Fourier Series will be undertaken.

Figures 11 and 14 show the PWM block diagram and resulting waveforms. The output $V_a(t)$ is a rectangular waveform with the time in the positive and negative region dependent on the input. If the input were constant over all time, the time t_1 of the positive transition as given by Eq. (4.26) would be constant and the output $V_a(t)$ would be periodic and describeable by a Fourier series.

In reality, however, $V_{in}(t)$ is not constant and α and t_1 vary from cycle to cycle with the input. From the preceding sample and hold analysis, the most that can be assumed is that the sampled input $V_{in}^*(nT)$, and thus α and t_1 are constant only during a single switching cycle and then updated. This section will add the assumption that a

Fourier Series of a single switching cycle, which requires infinite periodicity, is an accurate mathematical approximation of the single cycle. Since the input is slowly varying with respect to the switching period in practical systems, this approximation appears valid.

The assumption that the input is constant over a single cycle is certainly true for uniform sampling PWM; however, this assumption may break down for natural sampling PWM, if variations in the input approach the PWM switching frequency. In this case, the rapidly changing input distorts the dither signal when the two are added together. Although the sampling nature remains, the sampling rate is varying with the sum crossover. Computer simulation will determine the inaccuracy caused by the assumption that the input is constant over the switching cycle for the natural sampling PWM amplifier. For bandwidths well below the switching frequency, this assumption should be valid for both cases.

The Fourier Series to be used to describe the switching cycle is defined as:

$$V_a(t) = a_0/2 + \sum_{n=1}^{\infty} \left(a_n \cos\frac{2\pi n}{T}t + b_n \sin\frac{2\pi n}{T}t\right) \qquad (4.29)$$

where

$$a_n = 2/T \int_0^T V_a(t)\cos\frac{2\pi n}{T}t \, dt \tag{4.30}$$

$$b_n = 2/T \int_0^T V_a(t)\sin\frac{2\pi n}{T}t \, dt \tag{4.31}$$

$$a_0 = 2/T \int_0^T V_a(t) \, dt \tag{4.32}$$

For each cycle, the output is given by Eq. (2.3) where for the nth cycle,

$$t_1 = \tfrac{1}{2}(1 - \alpha(nT))T \tag{4.33}$$

and

$$\alpha(nT) = V_{in}^*(nT)/V_{max} \tag{4.34}$$

Solving for the DC term and first harmonic:

$$a_0 = 2/T[\int_0^{t_1} -V_s \, dt + \int_{t_1}^T V_s \, dt] = 2\alpha(nT)V_s \tag{4.35}$$

$$a_1 = 2/T[\int_0^{t_1} -V_s\cos(\tfrac{2\pi}{T}t)\,dt + \int_{t_1}^{T} V_s\cos(\tfrac{2\pi}{T}t)\,dt]$$

$$= -2V_s/\pi \sin[\pi(1 - \alpha(nT))] \qquad (4.36)$$

$$b_1 = 2/T[\int_0^{t_1} -V_s\sin(\tfrac{2\pi}{T}t)\,dt + \int_{t_1}^{T} V_s\sin(\tfrac{2\pi}{T}t)\,dt]$$

$$= 2V_s/\pi(\cos[\pi(1 - \alpha(nT))] - 1) \qquad (4.37)$$

Due to the inherent low pass nature of the motor servo system, higher order series terms will be attenuated and it will be assumed that they have no significant effect and will be neglected.

Thus:

$$V_a(t) \cong \alpha V_s - 2V_s/\pi \sin[\pi(1 - \alpha)]\cos\tfrac{2\pi}{T}t + 2V_s/\pi(\cos[\pi(1 - \alpha)] - 1)\sin\tfrac{2\pi}{T}t \qquad (4.38)$$

By the trig identify:

$$\sin(x - y) = \sin x \cos y - \cos x \sin y \qquad (4.39)$$

$$V_a(t) = \alpha(nT)V_s - 2V_s/\pi \sin\tfrac{2\pi}{T}t + 2V_s/\pi \sin(\tfrac{2\pi}{T}t - \pi[1 - \alpha(nT)]) \qquad (4.40)$$

where $\alpha(nT)$ is the input

It can be seen that the amplifier output is made up of three terms, the last of which is clearly non-linear with respect to the duty cycle input α . Before a linear model can be developed, this equation must be linearized. The technique used will be a Taylor Series expansion.

If the PWM amplifier output is applied to a permanent magnet d.c. motor, the resultant differential equation describing the system is given by Eq. (3.4). Since the motor is a linear system, this analysis will consider the total response to be the superposition of the response to the three terms of Eq. (4.40). This is a nonlinear system equation due to the last term.

$$\text{Term 1 ------ } V_{a1}(t) = \alpha(nT)V_s \tag{4.41}$$

$$\alpha(nT)V_s = L\, dI_a(t)/dt + RI_a(t) + K_b\omega(t) \tag{4.42}$$

The transfer function becomes:

$$I_{a1}(s) = \frac{1/L[V_s\alpha(s) - K_b\omega(s)]}{s + R/L} \tag{4.43}$$

$$\text{Term 2 -------- } V_{a2}(t) = -2V_s/\pi \sin \frac{2\pi}{T}t \tag{4.44}$$

$$V_{a2}(t) = L\, dI_a(t)/dt + R\, I_a(t) + K_b\omega(t) \tag{4.45}$$

The transfer function becomes:

$$I_{a2}(s) = \frac{1/L[V_{a2}(s) - K_b\omega(s)]}{s + R/L} \tag{4.46}$$

$$\text{Term 3 ---------- } V_{a3}(t) = 2V_s/\pi \sin[\frac{2\pi}{T}t - \pi(1 - \alpha(nT))] \tag{4.47}$$

$$V_{a3}(t) = L\, dI_a(t)/dt + R\, I_a(t) + K_b\omega(t) \tag{4.48}$$

Eq. (4.48) is a nonlinear system equation in terms of the input $\alpha(nT)$ which is constant over each cycle. One method of linearizing this nonlinear equation is to do a Taylor

series expansion about an equilibrium point. Rearranging the previous equation:

$$dI_{a3}(t)/dt = -R/L\ I_{a3}(t) - K_b/L\ \omega(t) + 2V_s/L\pi\ \sin[\frac{2\pi}{T}t - \pi(1 - \alpha(nT))]$$

$$= f(I_{a3}(t),\alpha(t),\omega(t),t) \qquad (4.48)$$

By the definition of the equilibrium point, the change in current at equilibrium is zero or:

$$dI_{a3}(t)/dt|_{equil} = 0 \qquad (4.49)$$

Thus,

$$0 = -R/L\ I_{a3e} - K_b/L\ \omega_e + 2V_s/L\pi\ \sin[\frac{2\pi}{T}t - \pi(1 - \alpha_e)] \qquad (4.50)$$

where I_{a3} , ω_e, and α_e are the equilibrium current, motor speed, and PWM duty cycle, respectively. If we choose the system at rest as the equilibrium point, $\alpha_e = 0$. If the torque ripple caused by the PWM switching is high frequency and the motor/load gain and mechanical time constant are small, the equilibrium motor speed will be responding with very low amplitude and will be essentially zero ($\omega_e = 0$). The validity of this assumption may break down for a responsive motor system which will show a lot

of ripple which is one of the effects this work is trying to study. Also, zero duty cycle is the point of maximum ripple [11]. In this case, the oscillating velocity must be calculated and used as the equilibrium velocity ω_e. Computer simulation will help verify the assumption of $\omega_e = 0$.

Substituting $\omega_e = \alpha_e = 0$ into Eq. (4.50), the equilibrium current is found as:

$$I_{a3e} = -2V_s/R\pi \sin(\frac{2\pi}{T}t) \qquad (4.51)$$

If the system is perturbed about the equilibrium point, the instantaneous current $I_{a3}(t)$ is equal to the equilibrium current plus a perturbation term $\Delta i_{a3}(t)$. The terms $\Delta\alpha(t)$ and $\Delta\omega(t)$ are the duty cycle and motor speed perturbation terms.

$$I_{a3}(t) = I_{a3e}(t) + \Delta i_{a3}(t) \qquad (4.52)$$

Differentiating the motor current and using Eq. (4.49):

$$d\Delta i_{a3}(t)/dt = f(I_{a3e}(t) + \Delta i_{a3}(t), \alpha_e + \Delta\alpha(nT), \omega_e + \Delta\omega(t), t) \qquad (4.53)$$

Performing a Taylor series expansion about the equilibrium point:

$$d\Delta i_{a3}(t)/dt = f(I_{a3e}(t),\alpha_e,\omega_e,t) + \partial f/\partial I_{a3}|_{I_{a3e},\omega_e,\alpha_e} \Delta i_{a3}(t)$$

$$+ \partial f/\partial \alpha|_{I_{a3e},\alpha_e,\omega_e} \Delta\alpha(nT) + \partial f/\partial \omega|_{I_{a3e},\omega_e,\alpha_\varepsilon} \Delta\omega(t)$$

$$+ \text{higher order nonlinear terms}$$

Neglecting the higher order terms and differentiating,

$$d\Delta i_{a3}(t)/dt = -R/L\ \Delta i_{a3}(t) - 2V_s/L\ \cos(\tfrac{2\pi}{T}t)\Delta\alpha(t) - K_b/L\ \Delta\omega(t) \quad (4.54)$$

Since the equilibrium point was chosen to be the system at rest,

$$\Delta\alpha(nT) = \alpha(nT) - \alpha_e = \alpha(nT) \quad (4.55)$$

$$\Delta\omega(t) = \omega(t) - \omega_e = \omega(t) \quad (4.56)$$

substituting (4.55) and (4.56) into Eq. (4.54),

$$d\Delta i_{a3}(t)/dt = -R/L\ \Delta i_{a3}(t) - 2V_s/L\ \cos(\tfrac{2\pi}{T}t)\alpha(nT) - K_b/L\ \omega(t) \quad (4.57)$$

The total motor current generated by the third term $V_{a3}(t)$ is the sum of the equilibrium and purterbation currents as given by Eq. (4.52).

Figure 16 shows the resultant block diagram of the third motor term. Note that the nonlinear system equation has been reduced to a linear equation in terms the input α; however, the model now includes a time varying coefficient which is periodic with the switching frequency. This time varying coefficient adds great complexity to the simple linear systems analysis techniques which are used in system design.

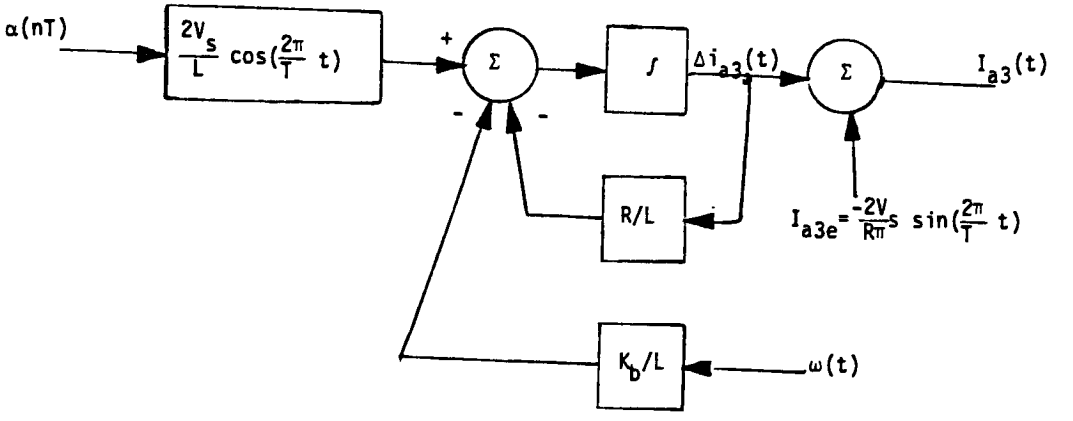

Linear system with time varying coefficient

Figure 16

Block Diagram of the Linearized PWM Output

Using Taylor Series Expansion

To remove the time varying coefficient from the PWM model, the Taylor Series expansion must be re-computed considering equilibrium to include an equilibrium point in time t_e. Instantaneous time t is now equal to the equilibrium time plus time puterbation Δt.

If t_e is chosen as T/4 and substituted into Eq. (4.51), the equilibrium current reduces to:

$$I_{a3e} = -2V_s/R\pi \tag{4.58}$$

Recomputing the Taylor Series Expansion results in:

$$d\Delta i_{a3}(t)/dt = -R/L\ \Delta i_{a3}(t) - K_b/L\ \Delta\omega(t) \tag{4.59}$$

This equation now shows the linearized PWM model to be time invariant and greatly simplified. The validity of the equilibrium point in time remains to be proven. As noted previously, the total motor response is the superposition of the response to the three terms in $V_a(t)$ or:

$$I_a(t) = I_{a1}(t) + I_{a2}(t) + I_{a3e} + \Delta i_{a3}(t) \tag{4.60}$$

Figure 17 shows the total PWM block diagram derived from the Fourier and Taylor series analysis. This model would replace the PWM block in the overall system block diagram. Note that the PWM switching effects are represented by the first harmonic input $(2/\pi)\sin(2\pi t/T)$. The magnitude of the output oscillation will be dependent on the plant attenuation between the amplifier and the position output at the switching frequency.

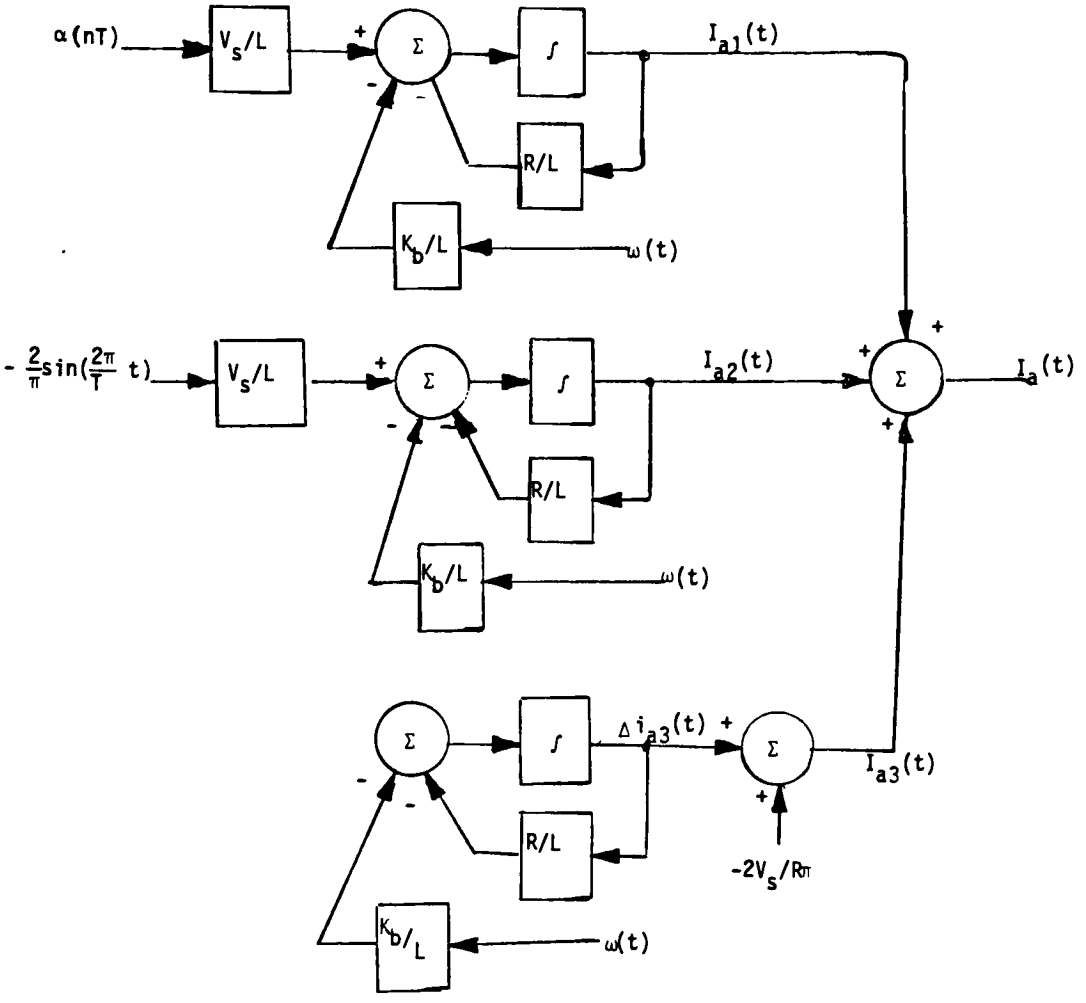

(a)

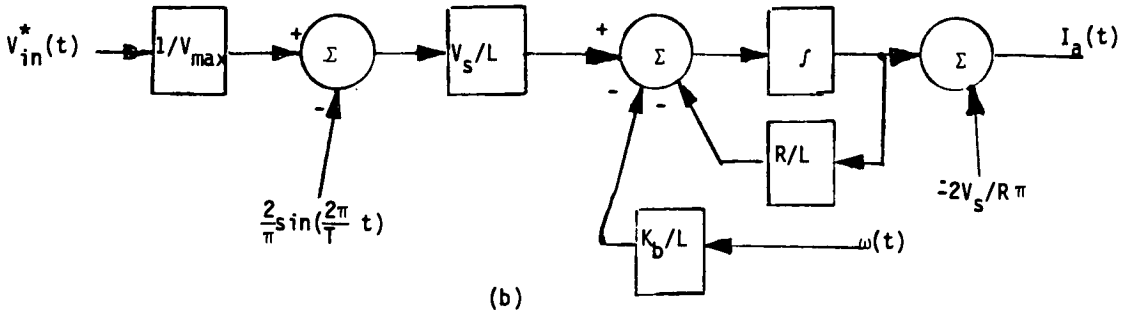

(b)

Figure 17

(a) PWM Block Diagram Derived from Fourier and Taylor Series Analysis

(b) Equivalent Block Diagram

Also, note that the plant now contains a dc offset or bias due to the equilibrium current term $-2V_s/R\pi$. Although this term will not affect the dynamic response, it will affect the final steady state value of the output. Thus, a steady state error will be introduced in addition to the ripple from the first harmonic. The validity of this term is dependent on the assumption that the equilibrium velocity is zero.

Computer simulations will be run to confirm the accuracy of the PWM amplifier model which includes the choice of the equilibrium point in time equal to T/4 and the equilibrium motor velocity equal to zero. To avoid these assumptions, a second linearization method by Double Fourier Analysis will be attempted in the next section.

4.5 Uniform Sampling PWM Amplifier Switching Harmonic Model by Double Fourier Transform Analysis

An alternate method of analyzing the PWM signal as suggested by Black [35] and Tsai and Ukrainetz [33] is the Double Fourier Transform Analysis. The PWM amplifier block diagram and resulting waveforms are again shown in Figure 11 and 14. As described previously, it is assumed that the input is constant over a switching period and the Fourier Series representation assuming infinite periodicity is an accurate approximation of the varying PWM

signal. The Fourier Series representation is given by Eqs. (4.29) to (4.32).

For this analysis, an input is applied to the PWM amplifier which is slowly varying with period $U = 2\pi/\nu$. If the input is varying with period U, it is assumed that the Fourier coefficients a_n and b_n are also varying at the same frequency. Thus, coefficients a_n and b_n can be represented by their own Fourier Series with time τ a more slowly varying time frame with respect to t and the switching period.

$$a_n(\tau) = c_{0n}/2 + \sum_{m=1}^{\infty} [c_{mn}\cos(m\nu\tau) + d_{mn}\sin(m\nu\tau)] \tag{4.61}$$

$$b_n(\tau) = f_{0n}/2 + \sum_{m=1}^{\infty} [f_{mn}\cos(m\nu\tau) + g_{mn}\sin(m\nu\tau)] \tag{4.62}$$

where

$$c_{mn} = 2/U \int_0^U a_n(\tau)\cos(m\nu\tau)\, d\tau \tag{4.63}$$

$$d_{mn} = 2/U \int_0^U a_n(\tau)\sin(m\nu\tau)\, d\tau \tag{4.64}$$

$$f_{mn} = 2/U \int_0^U b_n(\tau)\cos(m\nu\tau)\, d\tau \tag{4.65}$$

$$g_{mn} = 2/U \int_0^U b_n(\tau)\sin(m\nu\tau)\, d\tau \tag{4.66}$$

By substituting the varying coefficients of Eqs. (4.61) and (4.62) into the Fourier Series given by Eqs. (4.29) through (4.32):

$$V_a(t,\tau) = 1/2[c_{00}/2 + \sum_{m=1}^{\infty} c_{m0}\cos(m\nu\tau) + d_{m0}\sin(m\nu\tau)] + \sum_{n=1}^{\infty}([c_{0n}/2 + \sum_{m=1}^{\infty}(c_{mn}\cos(m\nu\tau) + d_{mn}\sin(m\nu\tau))]\cos(\frac{2\pi n}{T}t) + [f_{0n}/2 + \sum_{m=1}^{\infty}(f_{mn}\cos(m\nu\tau) + g_{mn}\sin(m\nu\tau))]\sin(\frac{2\pi n}{T}t)) \quad (4.67)$$

Rearranging terms:

$$V_a(t,\tau) = c_{00}/4 + 1/2 \sum_{m=1}^{\infty}[c_{m0}\cos(m\nu\tau) + d_{m0}\sin(m\nu\tau)] + 1/2 \sum_{n=1}^{\infty}[c_{0n}\cos(\frac{2\pi n}{T}t) + f_{0n}\sin(\frac{2\pi n}{T}t)] + \sum_{n=1}^{\infty}\sum_{m=1}^{\infty}[c_{mn}\cos(m\nu\tau)\cos(\frac{2\pi n}{T}t) + d_{mn}\sin(m\nu\tau)\cos(\frac{2\pi n}{T}t) + f_{mn}\cos(m\nu\tau)\sin(\frac{2\pi n}{T}t) + g_{mn}\sin(m\nu\tau)\sin(\frac{2\pi n}{T}t)] \quad (4.68)$$

Due to the low pass filter nature of the motor servo system, the high frequency terms will be severely attenuated. Also, it is assumed that low frequency sideband harmonics have a small coefficient. Only the terms C_{00}, C_{10}, d_{10}, C_{01}, and f_{01} which are the dc and first harmonic terms will be considered significant.

By substitution of Eqs. (4.30) and (4.31) into Eqs. (4.63) through (4.66):

$$c_{mn} = \frac{4}{UT} \int_0^U \int_0^T V_a(t,\tau)\cos(\frac{2\pi n}{T}t)\cos(m\nu\tau)\, dt\, d\tau \qquad (4.69)$$

$$d_{mn} = \frac{4}{UT} \int_0^U \int_0^T V_a(t,\tau)\cos(\frac{2\pi n}{T}t)\sin(m\nu\tau)\, dt\, d\tau \qquad (4.70)$$

$$f_{mn} = \frac{4}{UT} \int_0^U \int_0^T V_a(t,\tau)\sin(\frac{2\pi n}{T}t)\cos(m\nu\tau)\, dt\, d\tau . \qquad (4.71)$$

$$g_{mn} = \frac{4}{UT} \int_0^U \int_0^T V_a(t,\tau)\sin(\frac{2\pi n}{T}t)\sin(m\nu\tau)\, dt\, d\tau \qquad (4.72)$$

Let the PWM input be

$$\alpha(\tau) = a \sin(\nu\tau) \quad , \quad 0 \leq a \leq 1 \qquad (4.73)$$

The time of the PWM output transition t_1 is now given as:

$$t_1 = T/2 + (T/2)(a \sin(\nu\tau)) \qquad (4.74)$$

where the term (a sinνT) is considered a constant over a switching period T.

The input signal is assumed to be changing much more slowly than the PWM switching. In other words, the input and t_1 are assumed constant over a switching period T. The second time variable τ is a more slowly varying time frame than the switching time t. The amplifier output is now given as:

$$V_a(t,\tau) = \begin{cases} -V_s & 0 \le t < T/2 - (T/2)(a \sin(\nu\tau)) \\ V_s & T/2 - (T/2)(a \sin(\nu\tau)) \le t < T \end{cases} \qquad (4.75)$$

The double Fourier Series coefficients can now be solved as follows:

$$c_{00} = \frac{4}{UT}\left[\int_0^U \int_0^{T/2 - T/2 \text{ asin } \nu\tau} -V_s \, dt \, d\tau + \int_0^U \int_{T/2 - T/2 \text{ asin } \nu\tau}^{T} V_s \, dt \, d\tau \right]$$

$$= \frac{4}{UT}[-V_s T\pi/\nu + V_s T\pi/\nu] = 0 \qquad (4.76)$$

$$c_{01} = \frac{4}{UT}\left[\int_0^U \int_0^{T/2 - T/2 \text{ asin } \nu\tau} -V_s \cos\left(\frac{2\pi}{T}t\right) dt \, d\tau + \int_0^U \int_{T/2 - T/2 \text{ asin}\nu\tau}^{T} V_s \cos\left(\frac{2\pi}{T}t\right) dt \, d\tau \right]$$

$$= \frac{4}{UT}\left[\int_0^{2\pi/\nu} -2V_s\left(\frac{T}{2\pi}\right)\sin(\pi - \pi a \sin\nu\tau) \, d\tau \right]$$

$$= \frac{-\nu}{\pi^2} V_s \int_0^{2\pi/\nu} \sin(a\pi \sin(\nu\tau)) \, d\tau = 0 \qquad (4.77)$$

The last step of Eq. (4.77) can be proved as shown below:

$$\text{let} \quad \nu\tau = x \tag{4.78}$$

$$\int_0^{2\pi/\nu} \sin(a\pi \sin(\nu\tau))\, d\tau = \int_0^{2\pi} \sin(a\pi \sin x)\, 1/\nu\, dx \tag{4.79}$$

$$= 1/\nu j 2 \int_0^{2\pi} (e^{ja\pi \sin x} - e^{-ja\pi \sin x})\, dx$$

From FM communications theory, the integral of Eq. (4.79) is the difference of two Bessel functions of the first kind which are defined as:

$$J_n(\beta) = 1/2\pi \int_0^{2\pi} e^{j[\beta \sin x - nx]}\, dx \tag{4.80}$$

Thus, Eq. (4.79) reduces to:

$$\int_0^{2\pi/\nu} \sin(a\pi \sin \nu\tau)\, d\tau = \frac{\pi}{\nu j} [J_0(a\pi) - J_0(a\pi)] = 0 \tag{4.81}$$

Continuing,

$$c_{10} = \frac{4}{UT}\left[\int_0^U \int_0^{T/2 - T/2\,a\sin\nu\tau} -V_s\cos\nu\tau\, dt\, d\tau + \int_0^U \int_{T/2 - T/2\,a\sin\nu\tau}^{T} V_s\cos\nu\tau\, dt\, d\tau\right]$$

$$= 4V_s a/U \int_0^{2\pi/\nu} \cos\nu\tau \sin\nu\tau\, d\tau = 0 \qquad (4.82)$$

$$d_{10} = \frac{4}{UT}\left[\int_0^U \int_0^{T/2 - T/2\,a\sin\nu\tau} -V_s\sin\nu\tau\, dt\, d\tau + \int_0^U \int_{T/2 - T/2\,a\sin\nu\tau}^{T} V_s\sin\nu\tau\, dt\, d\tau\right]$$

$$= 4V_s a/U \int_0^{2\pi/\nu} \sin^2\nu\tau\, d\tau = 2V_s a \qquad (4.83)$$

$$f_{01} = \frac{4}{UT}\left[\int_0^U \int_0^{T/2 - T/2\,a\sin\nu\tau} -V_s\sin\left(\frac{2\pi}{T}t\right) dt\, d\tau + \int_0^U \int_{T/2 - T/2\,a\sin\nu\tau}^{T} V_s\sin\left(\frac{2\pi}{T}t\right) dt\, d\tau\right]$$

$$= \frac{4}{UT}\int_0^{2\pi/\nu} -V_s T/\pi\,[1 + \cos(\pi a \sin\nu\tau)]\, d\tau$$

$$= -4V_s/\pi + \left(\frac{-4V_s}{2\pi^2}\right)\int_0^{2\pi} \cos(\pi a \sin x)\, dx$$

$$= -4V_s/\pi - \frac{4V_s}{2\pi}\left[\frac{1}{2\pi}\int_0^{2\pi}\left(e^{j\pi a \sin x} + e^{-j\pi a \sin x}\right) dx\right]$$

$$= -4V_s/\pi - \frac{4V_s}{2\pi}(2J_0(\pi a)) \qquad (4.84)$$

The final step of Eq. (4.84) was derived from FM communications theory as the sum of two Bessell functions of the first kind which are of the form given by Eq. (4.80)

Also, by the properties of Bessel functions

$$J_n(\beta) = J_n(-\beta) \qquad n \text{ even} \tag{4.85}$$

$$\text{Thus, } f_{01} = -4V_s/\pi\,(1 + J_0(\pi a)) \tag{4.86}$$

The coefficient "a" in the above analysis is the magnitude of the duty cycle input and thus has a range between zero and one ($0 \leq a \leq 1$). The Bessel function varies as shown in Figure 18 and is shown to be a nonlinear function of the input magnitude.

$$J_0(\beta)=1/2\pi \int_0^{2\pi} e^{j\beta \sin x} dx \qquad 0 \leq a \leq 1$$

$$\beta=\pi a \qquad 0 \leq \beta \leq \pi$$

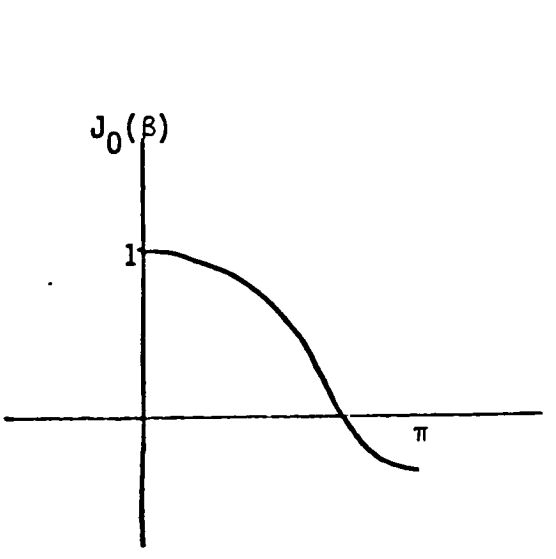

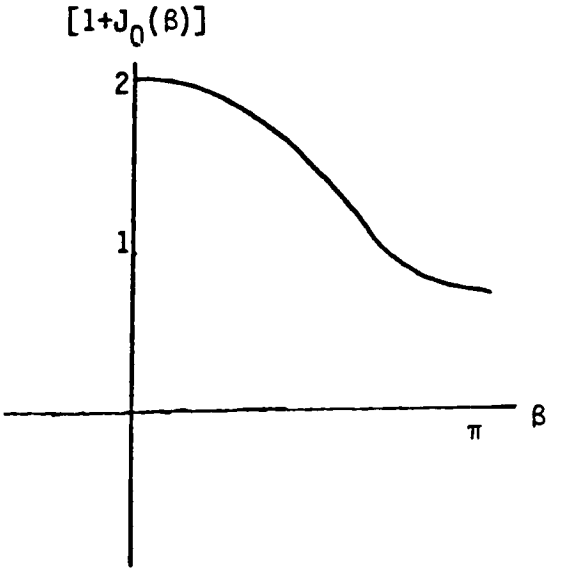

$$-.292 \leq J_0(\pi a) \leq 1$$

Figure 18

Variations of the Bessel Function in the Term f_{01}

Also shown in Figure 18 is the variation of the term (1 + $J_0(\beta)$). Variations in the magnitude of the Bessell function affect the magnitude of the Fourier coeficient f_{01} which has a range dependent on the magnitude of the input sinusoid of:

$$-8V_s/\pi \leq f_{01} \leq -2.83V_s/\pi \qquad (4.87)$$

This nonlinear situation with respect to the input can be linearized by the judicious choice of a nominal value of the Bessel function which will be assumed constant for all input magnitudes. Tsai and Ukrainetz [33] make no mention of the Bessel term and thus appear to be assuming a nominal value close to zero for the majority of typical system inputs. The term f_{01} is simply given as $-4V_s/\pi$.

If the designer is interested in the steady state response of the position control servo system to a constant input, the duty cycle term $\alpha(t)$ would be expected to reach a steady state value close to zero (a = 0) which is a symmetric PWM output signal. Thus, a more appropriate choice of $J_0(\pi a)$ for this type of study may be $J_0(\pi a)$

$= J_0(0) = 1$ which would result in $f_{01} = -8V_s/\pi$. Computer simulations will be studied to determine the proper choice of f_{01}.

In summary from Eqs. (4.76), (4.77), (4.82), (4.83), and (4.86):

$$C_{00} = 0$$
$$C_{01} = 0$$
$$C_{10} = 0$$
$$d_{10} = 2 V_s a$$

f_{01} varies between $-8V_s/\pi$ and $-2.83V_s/\pi$ dependent on the input magnitude.

Thus,

$$V_a(t,\tau) = \tfrac{1}{2}c_{00} + \tfrac{1}{2}c_{10}\cos \nu\tau + \tfrac{1}{2}d_{10}\sin \nu\tau + \tfrac{1}{2}c_{01}\cos(\tfrac{2\pi}{T}t) + \tfrac{1}{2}f_{01}\sin(\tfrac{2\pi}{T}t)$$
$$= V_s a \sin \nu\tau - \tfrac{1}{2}f_{01}\sin(\tfrac{2\pi}{T}t) \qquad (4.88)$$

Higher order terms were considered insignificant and neglected. Substituting Eq. (4.73) into Eq. (4.88),

$$V_a(t,\tau) = V_s[\alpha(\tau) - f \sin 2\pi t/T] \qquad (4.89)$$

where $1.42/\pi \leq f \leq 4/\pi$ depending on the analysis desired.

Note that the output equation is a linear combination of the input duty cycle and a first harmonic term whose amplitude will be finalized by computer simulation. The duty cycle $\alpha(\tau)$ is considered to be the sampled value of $V_{in}(t)/V_{max}$ as modeled previous by the principle of equivalent areas. More simply,

$$V_a(t) = V_s(\alpha^*(nT) - f \sin(2\pi t/T)) \qquad (4.89)$$

where $\alpha^*(nT)$ is the sampled duty cycle.

Figure 19 shows the resulting linear block diagram of the PWM system which would represent the switching effects.

Note that, as in the Fourier series and Taylor series expansion model, the PWM amplifier is represented by a d.c. gain and an externally input sinusoid.

Although the term f is a non-linear function of the input magnitude, its range is relatively small and it will be linearized by the choice of some nominal value. The

additional sinusoidal input represents the first harmonic content of the amplifier and will cause output ripple if the frequency response of the remainder of the system is high enough.

Two models have now been presented representing the strong harmonic content of the amplifier. The next section will construct and analyze the total PWM model including the sampling nature of the PWM representing system stability.

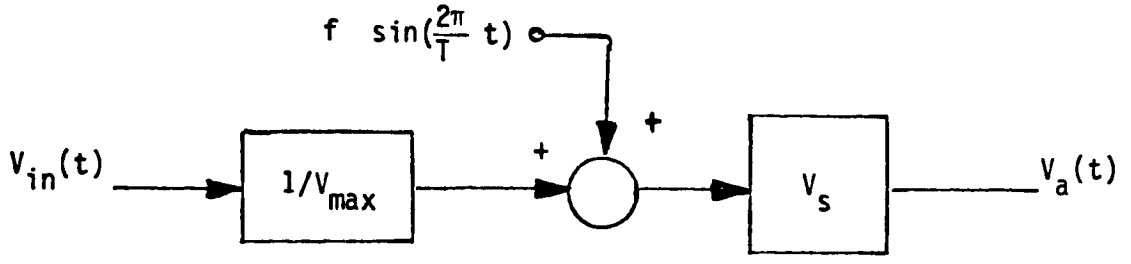

$$-1.42/\pi \leq f \leq -4/\pi$$

f is a nonlinear function of the input magnitude which will be linearized by choosing a nominal value.

Figure 19

Linear Block Diagram of the Double Fourier Series PWM Model

4.6 Construction and Analysis of the Total Uniform Sampling PWM Amplifier Model

As described in Section 4.2, the PWM amplifier is recognized to have both a sampling nature whose effect is on stability and a strong first harmonic content causing output ripple. This section proposes to construct a complete PWM model including both effects.

Section 4.3 developed a sample and hold model of the PWM's sampling nature. This model is shown in Figure 15. The switching harmonics were first analyzed by Fourier series and Taylor series expansion in Section 4.4 and a linear model representation is shown in Figure 17. An alternate analysis was conducted in Section 4.5 by double Fourier transform yielding the model of Figure 19.

The linear models created by Taylor Series expansion and double Fourier series are seen to be quite similar with the following exceptions:

1. The double Fourier transform model does not have a d.c. bias or offset term being summed to the motor current creating an offset in the system output.

2. The amplitude of the externally applied first harmonic input developed by double Fourier transform was found to have a range of possible values. The appropriate harmonic amplitude was found to be a nonlinear function of the PWM amplifier input. The range of values, however, is relatively small and, if it is assumed that the servo system is to reach steady state with amplifier input approximately zero, the appropriate constant for the harmonic amplitude appears to be $4/\pi$.

Both harmonic models assume that the input is essentially constant over a switching period for the application of the Fourier series. The stability analysis of Section 4.3 resulted in the development of a sample and hold model, the output of which is constant over a switching cycle. The sample and hold model thus interfaces nicely to and becomes an excellent leading stage for the Fourier transform models. Further, the sample and hold model of Section 4.3 was developed for a normalized system. The last stage, the PWM amplifier gain was to be determined by double Fourier transform technique. The resultant total PWM representation is shown in Figure 20 for both the Taylor series and double Fourier series applications.

Although the double Fourier transform model does not have a d.c. offset, a d.c. offset in the output position will be present in both models due to the interaction between

the first harmonic input and the sampler both running at the same frequency. Because the system is closed loop, the first harmonic will appear at the sampler attenuated and shifted in phase due to the action of the plant. The sampler will sample each time at the same point in first harmonic period and hold that value throughout the cycle. Since the first harmonic and plant dynamics are constant, this phenomenon will provide a steady state offset in the output which may add to or subtract from the steady state position depending on the phase shift in the first harmonic. This offset can also be predicted by z-transform analysis of the system for the first harmonic input. The magnitude of this d.c. offset will be dependent on the first harmonic attenuation. Thus, as the bandwidth is raised toward the switching frequency, this d.c. offset should grow. Computer simulation will verify this phenomenon. If the first harmonic amplitude is larger in the double Fourier series model, the d.c. offset will also be greater.

The double Fourier series model was developed for a sinusoidal input with the frequency unspecified. Since any input can be considered the infinite sum of sinusoids and the amplifier model is linear and does not depend on frequency, superposition applies, and the model is valid for any input $V_{in}(t)$.

Note that all the modeling done so far is for uniform sampling PWM. The next section will discuss natural sampling and a potential model.

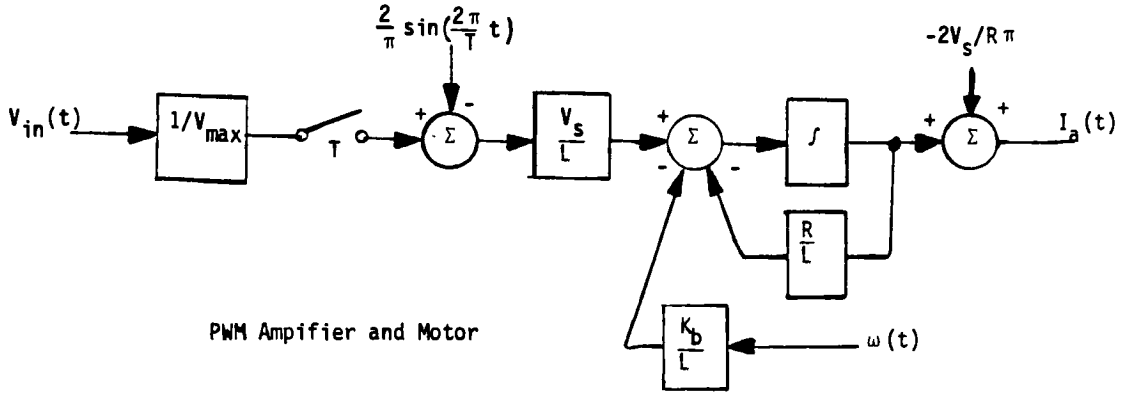

(a)

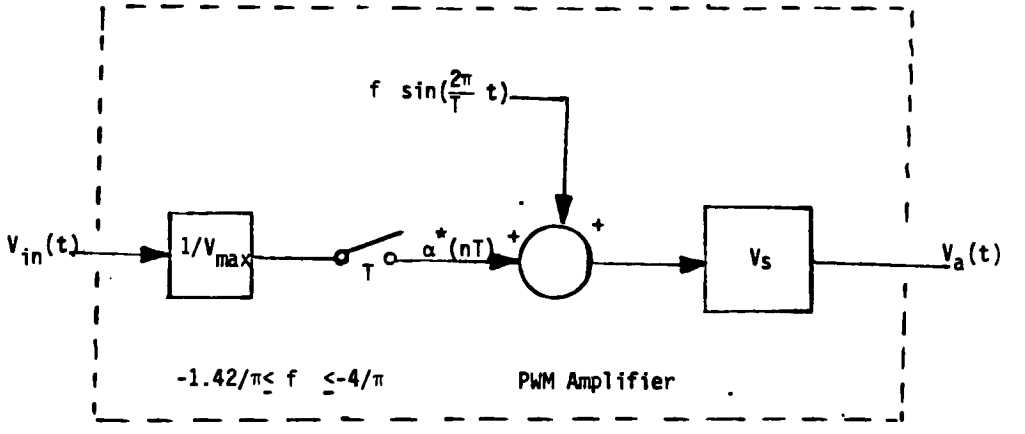

(b)

Figure 20

Block Diagrams for the Total Uniform Sampling PWM Models

(a) Taylor Series Expansion Model
(b) Double Fourier Series Model

4.7 Analysis and Model Alteration for Natural Sampling PWM

The models generated previously were uniform PWM sampling models where the input is sampled at the beginning of the PWM cycle. The sampled value is held constant and determines the pulse width for that cycle.

As discussed previously, the input to the natural sampling PWM is updated continuously and the point where the input compared to the dither signal changes sign determines the pulse width for that cycle. This form of PWM retains a sampling nature with the sampling point varying from the beginning of the cycle. For d.c. or slowly varying inputs which are at steady state, the sampling point would seem to be at or near the center of the cycle. In other words, the sampling is shifted 180° from the start of the switching period and the first harmonic phase. Thus, it may be possible to model natural sampling PWM with the same models developed previous with only a 180° phase shift added to the first harmonic input. The resultant system models are shown in Figure 21.

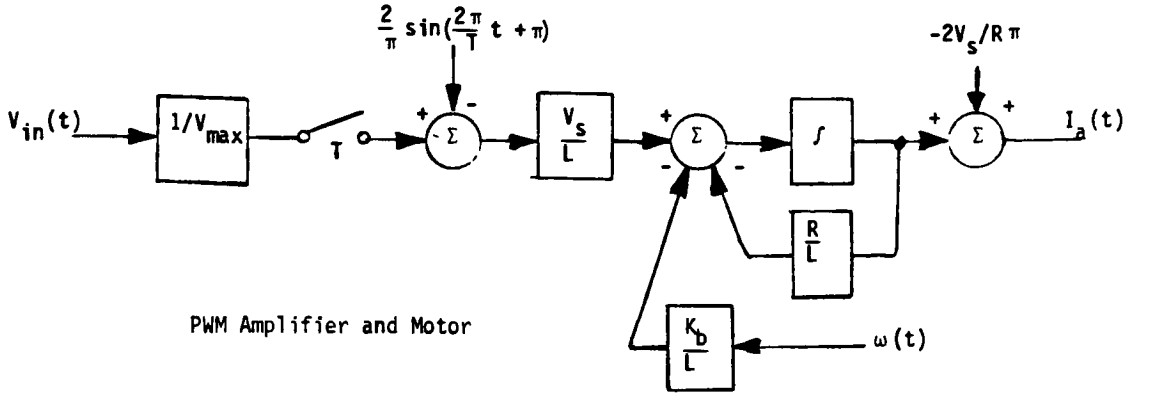

(a)

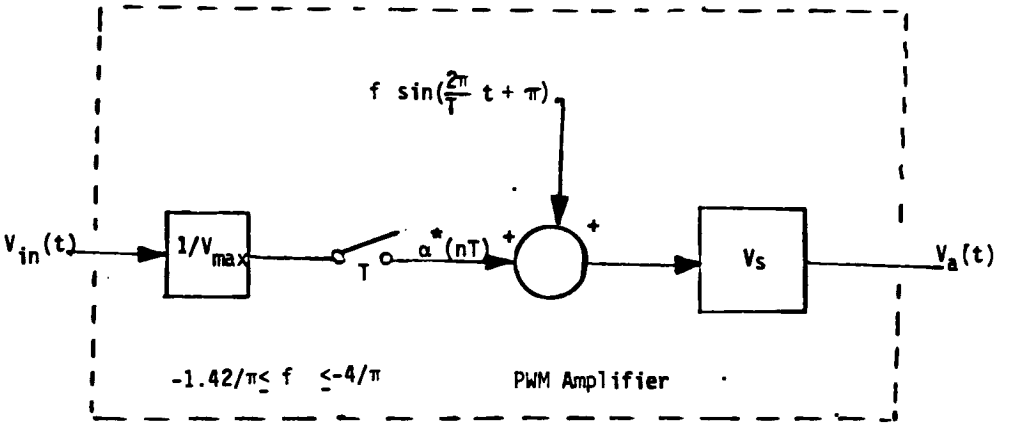

(b)

Figure 21

PWM Block Diagrams For a Natural Sampling PWM Model by:

(a) Taylor Series Expansion
(b) Double Fourier Series

One noticeable effect of the phase shift will be a change in the d.c. offset resulting from the interaction of the first harmonic and the sampler. The offset should be approximately the same magnitude but of opposite sign as encountered previously for Uniform sampling. As noted previously, the assumption that the input is constant for an entire switching cycle may break down for natural sampling PWM if variations in the input approach the switching frequency. The validity of this natural sampling PWM model will be checked by computer simulation in the next section.

5.0 Computer Simulation of Uniform and Natural Sampling PWM and Linearized Models

As seen in the preceeding analysis, two linear sample data models have been developed as an approximation for both uniform and natural sampling nonlinear PWM motor amplifiers. In both models, it is necessary that the input is changing more slowly than the switching PWM signal or that the switching frequency is more than twice the system bandwidth. This limitation is acceptable since practical motor servo systems are low frequency systems and it is the intent of this study to observe and predict the effects of PWM switching as system bandwidths are extended toward the switching frequencies.

The computer simulations to verify the linear models will be done using the "Easy 5 Dynamic Analysis System" which is a computer simulation package available through the Boeing Computer Services Company. Easy 5 can do the traditional linear control systems analysis with multiple inputs, outputs, and feedback loops. Easy 5 can also analyze discrete time systems and the combination of discrete and analog systems. Finally, Easy 5 can exactly simulate the time response of nonlinear or time varying parameter systems. This can be done by writing Fortran code to exactly duplicate a non-linear block and this block can be utilized within a control system.

Modeling on Easy 5 is accomplished by describing the control system by "Standard" or user defined component blocks which have the same mathematical relationship as the components in the control system. Thus, a true PWM amplifier can be created as shown in Figure 22. A sawtooth wave, whose frequency determines the PWM switching frequency, is generated in a Fortran block and is summed with the amplifier input. The amplifier input is sampled in the case of uniform sampling PWM or input continuously for natural sampling PWM. The sum is fed to a Fortran comparator block which determines the polarity of the output.

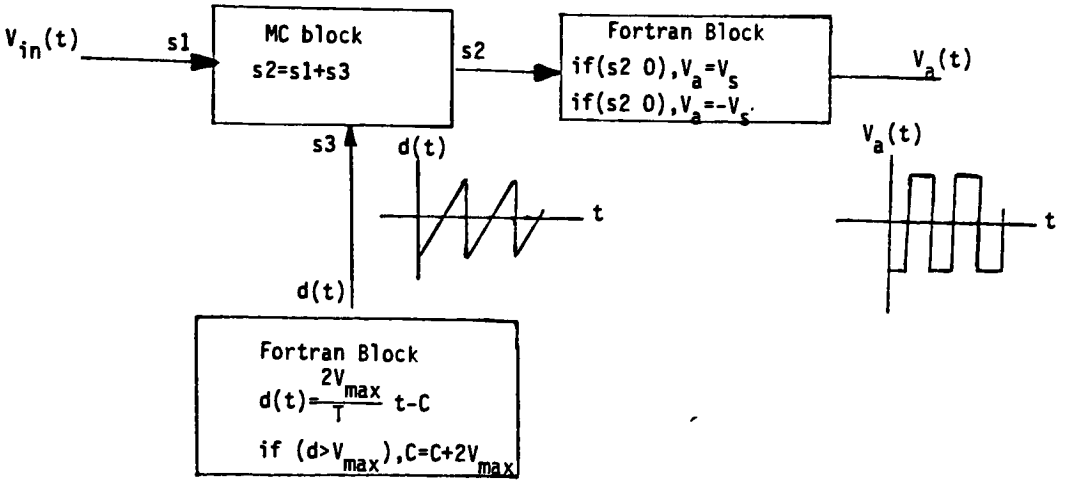

(a)

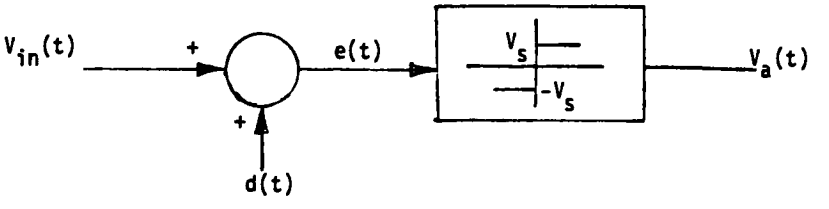

(b)

Figure 22

(a) PWM Amplifier Representation on Easy 5 Modeling and Simulation Analysis

(b) Equivalent PWM Block Diagram

The nonlinear PWM simulation will be used to generate the true response to a system containing a PWM amplifier. The simulation will start with a switching frequency ten times the closed loop system bandwidth calculated by assuming a d.c. gain for the amplifier. The transient and steady state response will be studied and compared with both the d.c. gain model simulation and simulations using the linearized models developed in this work. The ratio of switching frequency to system bandwidth will then be decreased to five, four, and three. In each case, for both uniform and natural sampling PWM, the nonlinear PWM response will be compared with the response generated by the d.c. gain and the linearized models.

5.1 Servo Control System With Typical Components

The position control servo system to be analyzed was shown previously in Figure 10. The simulation will be done using typical components as follows:

Motor - Torque Systems 3509-DF

$R = .8$ ohms

$L = .0012$ H

$K_T = 12.2$ oz. in./A

$K_B = .0862$ V-sec/rad

Tachometer Gain = .067 V-sec/rad

The tachometer gain will be electrically modified as required to meet desired performance.

Load - Typical

Motor Inertia = .011 oz. in sec^2

Load Inertia = .1 oz. in sec^2

Total J = .111 oz. in sec^2

F = .01 oz.-in-sec/rad

The position sensor will be a ten turn potentiometer attached to the load with a gain of 0.477 volts/radian. Static and coulomb friction will be ignored in the analysis. The analysis will also assume a rigid coupling between the motor and the load (K_c = infinity).

The resultant system block diagram with no compensation is shown in Figure 23 (a). It is assumed that the amplifier has an input signal range of $\pm$ 10 volts and has an output magnitude of $\pm$ 50 volts.

The gains k_1 and k_2 are feedback gains on the tachometer velocity feedback and the potentiometer position feedback, respectively. The feedback gains are part of the compensation and will be used to obtain the desired response.

Utilizing block algebra, the system can be reconfigured as shown in Figure 23 (b). The feedback configuration results in an adjustable feedback zero which will affect system dynamics.

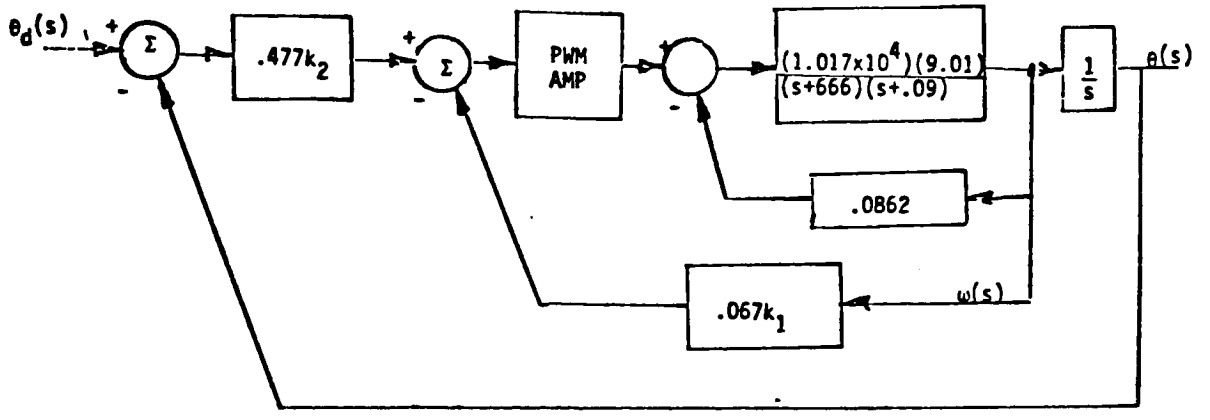

(a)

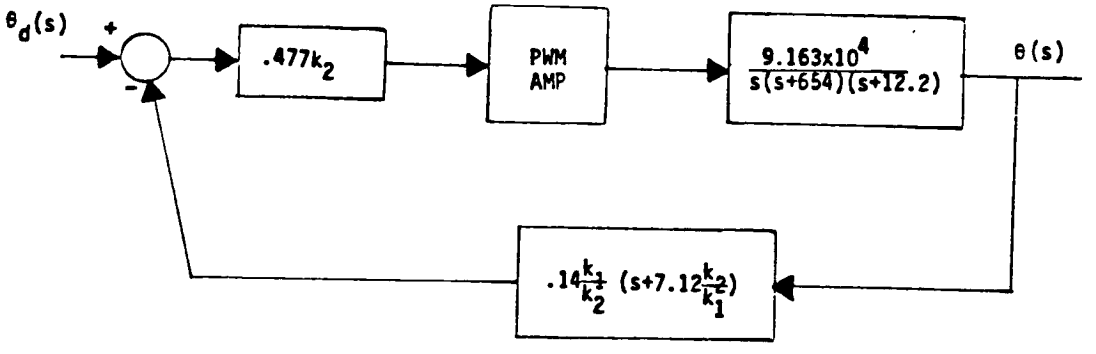

(b)

Figure 23

(a) Servo System Block Diagram With Typical Components
(b) Equivalent System Block Diagram

If the simple gain model V_s/V_{max} with no sampling or harmonic input is used for the PWM amplifier, the "PWM Amp" block in Figure 23 can be replaced by a block with a d.c. gain of five. This model would be valid for a very low bandwidth system with respect to the switching frequency.

It is desired for the purpose of this analysis to set up the servo system as a dominant second order system with a 10 Hz bandwidth. The equivalent transfer function is of the form:

$$C(s)/R(s) = \frac{\omega_n^2}{s^2 + 2\delta\omega_n s + \omega_n^2} \qquad (5.1)$$

If the damping ratio is 0.7, the natural frequency becomes 62.3 rad/sec. for 10 Hz bandwidth.

Substituting into Eq. (5.1)

$$C(s)/R(s) = \frac{3872}{(s + 44 + j44)(s + 44 - j44)} \qquad (5.2)$$

where the dominant second order poles are $s = -44 \pm j44$.

Figure 24 shows the system root locus with zero tachometer gain and the desired dominant second order closed loop poles. As can be seen, compensation is required to achieve

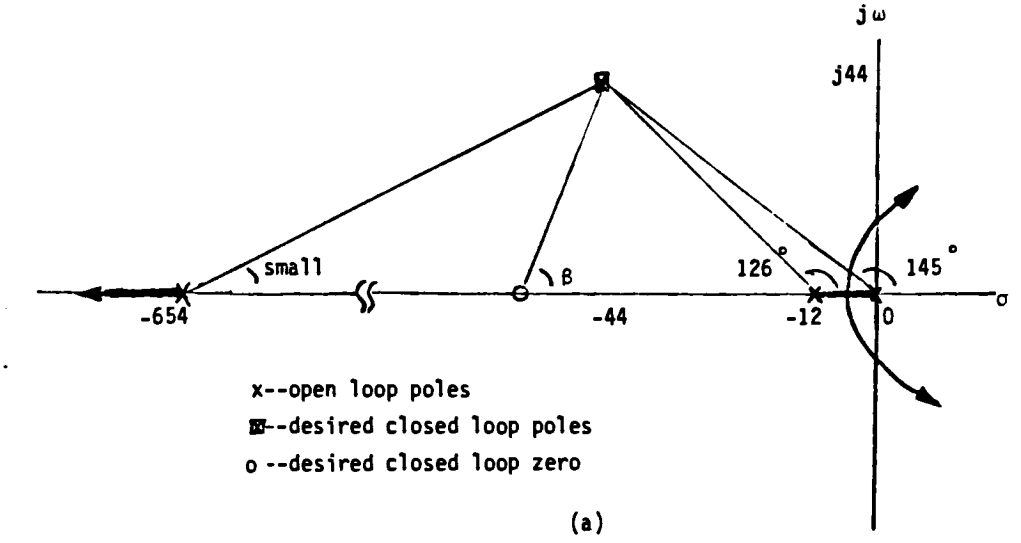

(a)

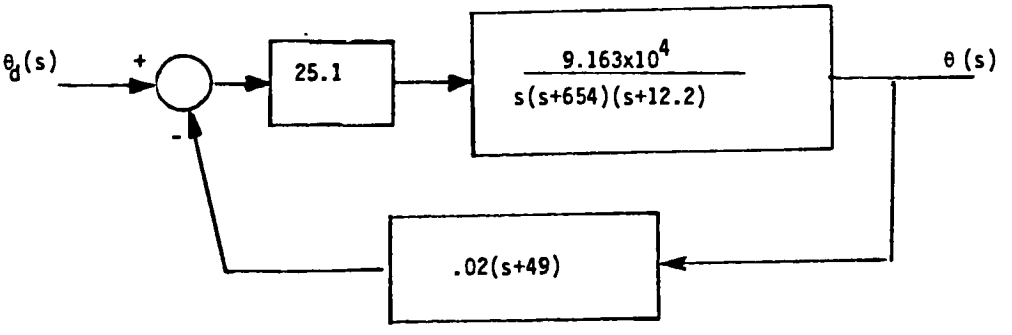

(b)

Figure 24

(a) Root Locus Plot of Uncompensated Zero Tachometer System
(b) Resultant Block Diagram After Feedback Compensation

the desired closed loop poles. The compensation will consist of the feedback zero resulting from the tachometer and potentiometer feedbacks as shown in Figure 24. the feedback zero, $s = -7.12\ K_2/K_1$ will be located by root locus angle criteria. Figure 25 (a) shows that the system is lacking 78° at the desired pole locations which can be corrected by a zero at $s = -50.5$ or $\beta = 78°$. Thus:

$$-7.12\ k_2/k_1 = -50.5 \tag{5.3}$$

The closed loop transfer function in terms of position and velocity feedback gain is:

$$\frac{\theta(s)}{\theta_d(s)} = \frac{2.185 \times 10^5\ K_2}{s^3 + 666s^2 + (7979 + 30590\ K_1)s + 217800\ K_2} \tag{5.4}$$

If the third closed loop system pole migrating in from $s = -654$ is assumed to be at $s = -600$ for the final gain, the characteristic equation of the above transfer function must satisfy Eq. (5.3) and the following:

$$s^3 + 666s^2 + (7979 + 30590\ k_1)s + 217800\ k_2 = (s + 600)(s + 44 + j44)(s + 44 - j44) \tag{5.5}$$

The gains $k_2 = 10.5$ and $k_1 = 1.55$ satisfy Eqs. (5.3) and (5.5) and represent the electrical position and velocity feedback gains required in the system. The resultant transfer becomes:

$$\frac{\theta(s)}{\theta_d(s)} = \frac{2.294 \times 10^6}{(s + 577)(s + 44.5 + j44.5)(s + 44.5 - j44.5)} \tag{5.6}$$

The 10 Hz bandwidth system block diagram which will be analyzed is shown in Figure 25 (b).

5.2 Step Response Using the Simple D.C. Gain Model

In the simplest PWM model, the PWM amplifier is replaced by a simple d.c. gain where:

$$\text{gain} = V_s/V_{max} = 50/10 = 5$$

Inserting a PWM gain of five into the model of Figure 23 and applying a two radian step command at t = 0 results in a computer transient response as shown in Figure 25. As can be seen, the system rise time and single overshoot are that of a 10 Hz bandwidth system with a damping of 0.7. If the PWM switching frequency is very large, this would be an accurate representation. Note the final value of the output which has settled at two radians and contains no ripple.

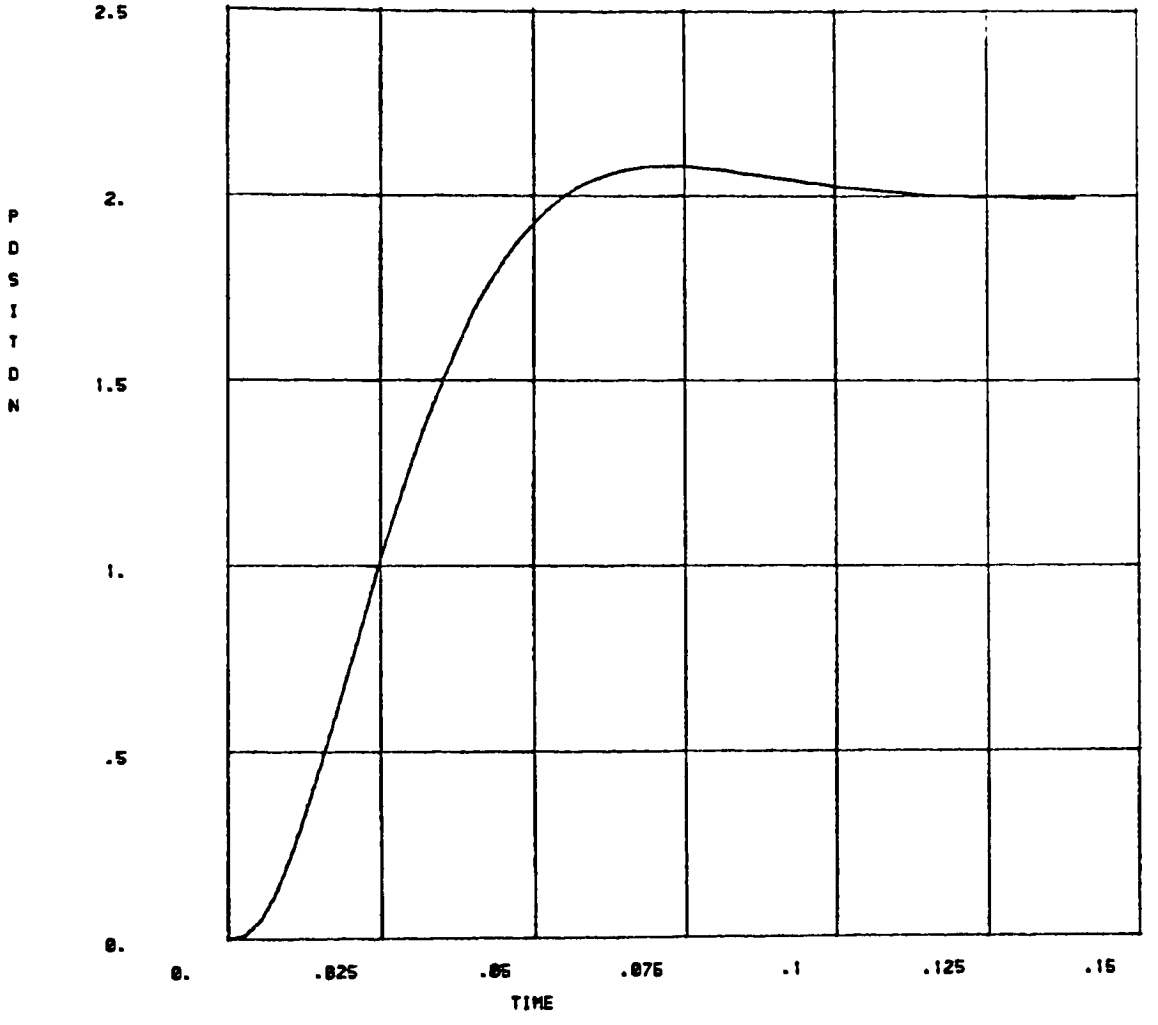

Figure 25

Transient Response of a Servo System

Utilizing the Simple PWM Model

5.3 Step Response Simulation Utilizing Nonlinear PWM

If the PWM amplifier block were replaced by the actual nonlinear PWM system as shown previously in Figure 22, the true position output would be obtained to the two radian step command.

A PWM switching frequency of 100 Hz will be initially used which is ten times the system bandwidth. This frequency is artifically low for the majority of PWM servo amplifiers found on the market; however, for analysis purposes, it is more convenient to tailor the switching frequency to the 10 Hz system bandwidth than vise versa. Further, the dynamics seen should be essentially equivalent to a 100 Hz bandwidth system operating with a 1000 Hz switching frequency. It is also realized that a realistic 100 Hz PWM amplifier would be accompanied by a specification by the vendor for more system inductance. The filtering action would only decrease but not eliminate the magnitude of the switching dynamics while increased compensation to maintain a 10 Hz bandwidth would partially negate the effect. Thus, for model verification purposes, a slightly unrealistic PWM amplifier will be utilized.

Figures 26 shows the transient response of the position control system utilizing uniform sampling and natural sampling PWM. Both amplifier systems show essentially the

same rise time and single overshoot characteristic of the system. A closer look at steady state in Figure 27, however, reveals the effects of the nonlinear switching waveform. The output is seen to be oscillating at the switching frequency with a magnitude of 0.016 radians. Surprisingly, the ripple is occurring not about the expected value but is offset from the desired position of two radians by -0.15 radians and 0.15 radians for uniform and natural sampling, respectively. In other words, the PWM amplifier is adding a d.c. bias to the output which is negative for uniform sampling and positive for natural sampling. These switching effects should be predicted by the equivalent linear model developed previously to be useful.

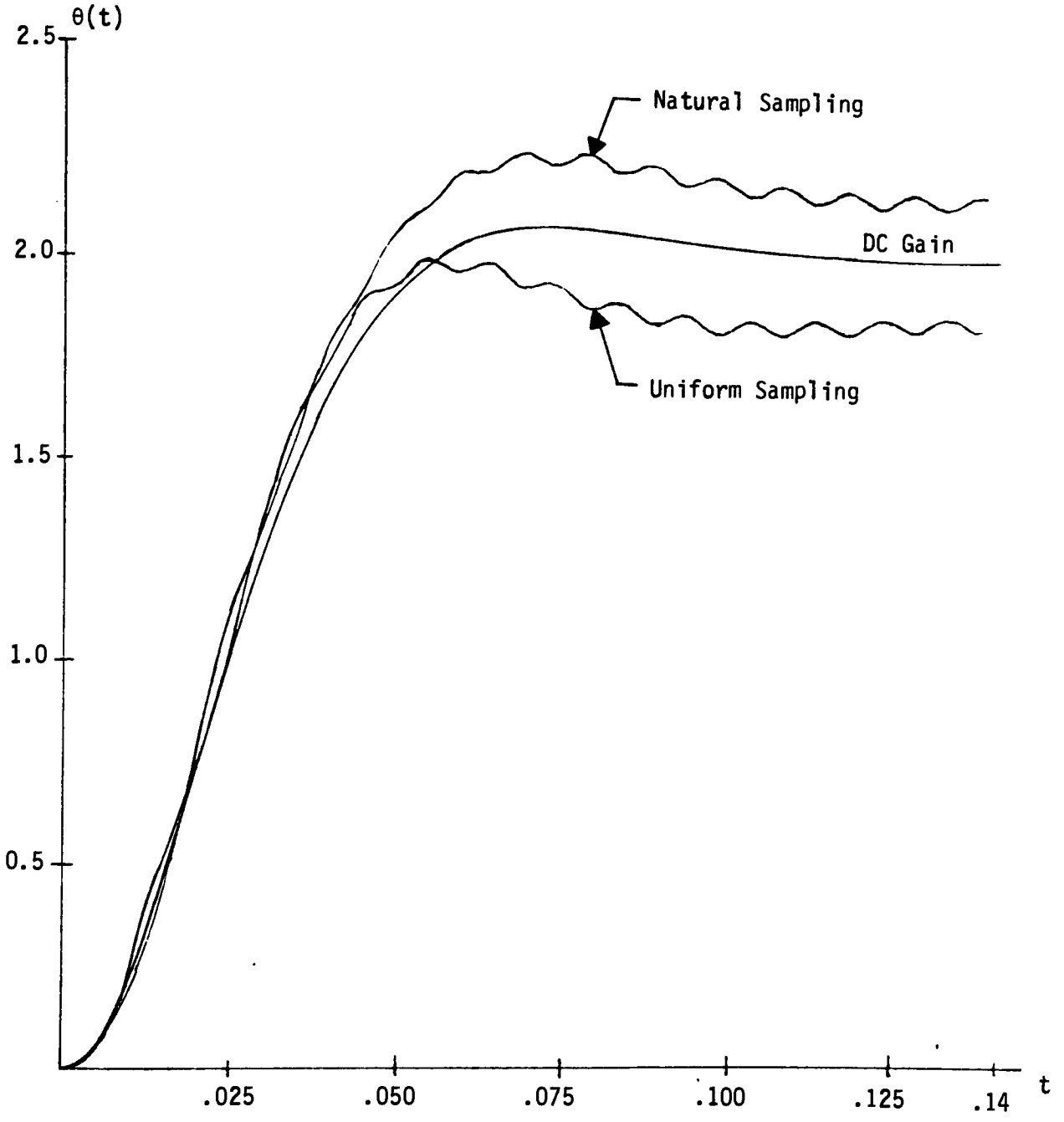

Figure 26

Transient Response of a System Utilizing a Uniform Sampling PWM Amplifier and Natural Sampling PWM Amplifier

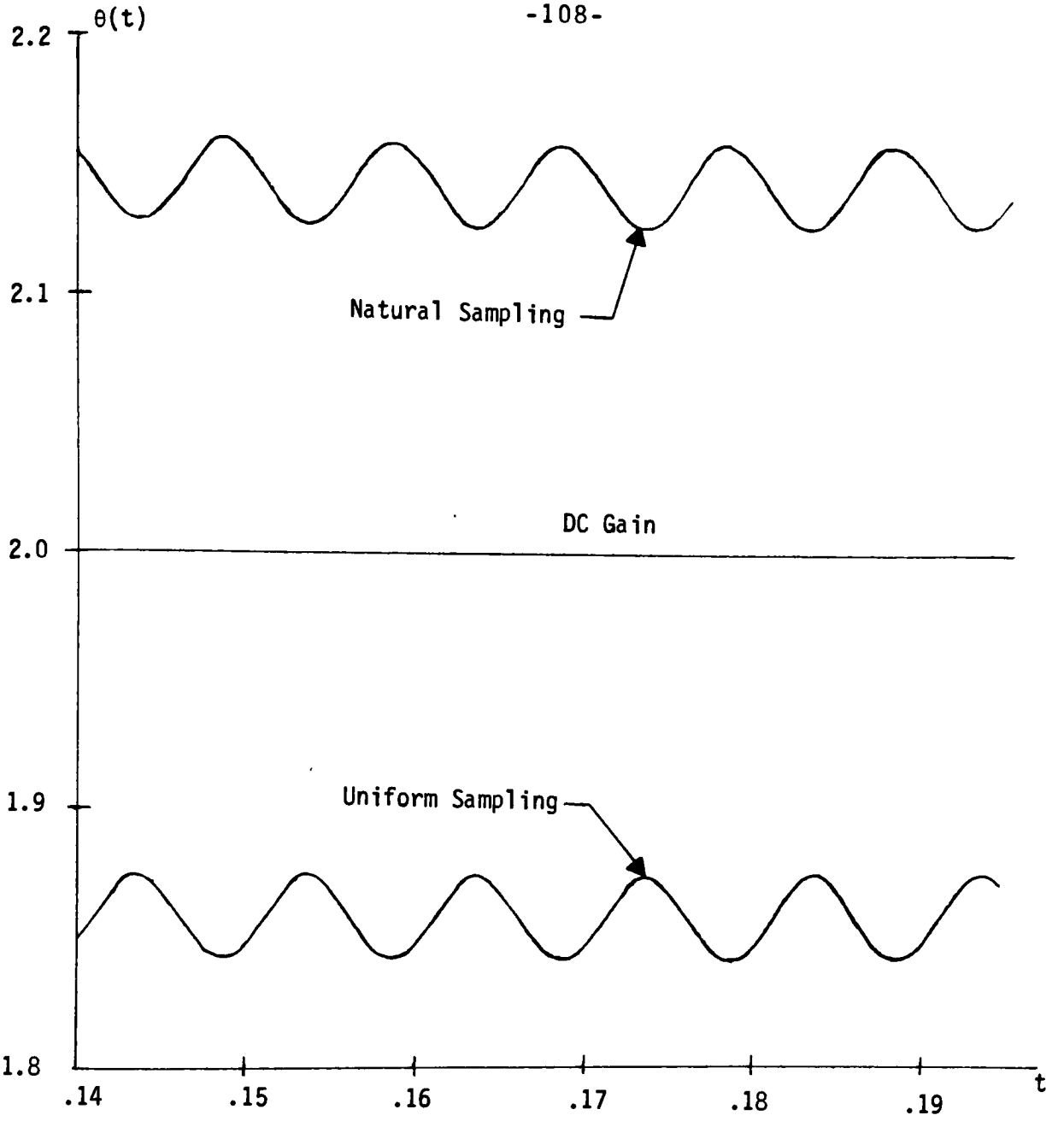

Figure 27

Steady State Response of a System Utilizing a Natural Sampling PWM Amplifier and a Uniform Sampling PWM Amplifier

Also of interest are the effects on system stability as the ratio between switching frequency and bandwidth deceases. Figures 28 and 29 show the position response to a two radian input as the switching frequency decreases to 50, 40, and 30 hertz. Figure 28 is for uniform sampling, and Figure 29 is for natural sampling. As can be seen from the rise times and overshoots, damping and system stability decrease significantly as the frequency decreases to the point that the system is unstable at 30 Hz for uniform sampling. Also note that the steady state ripple and d.c. bias or offset increase significantly as the frequency decreases. The offset increases in opposite directions from the desired output for uniform sampling versus natural sampling.

Natural sampling PWM is seen to be inherently more stable than uniform sampling PWM. Since the input is free running when being compared to the dither, the switch from negative to positive supply at the amplifier output is based on the most recent input information.

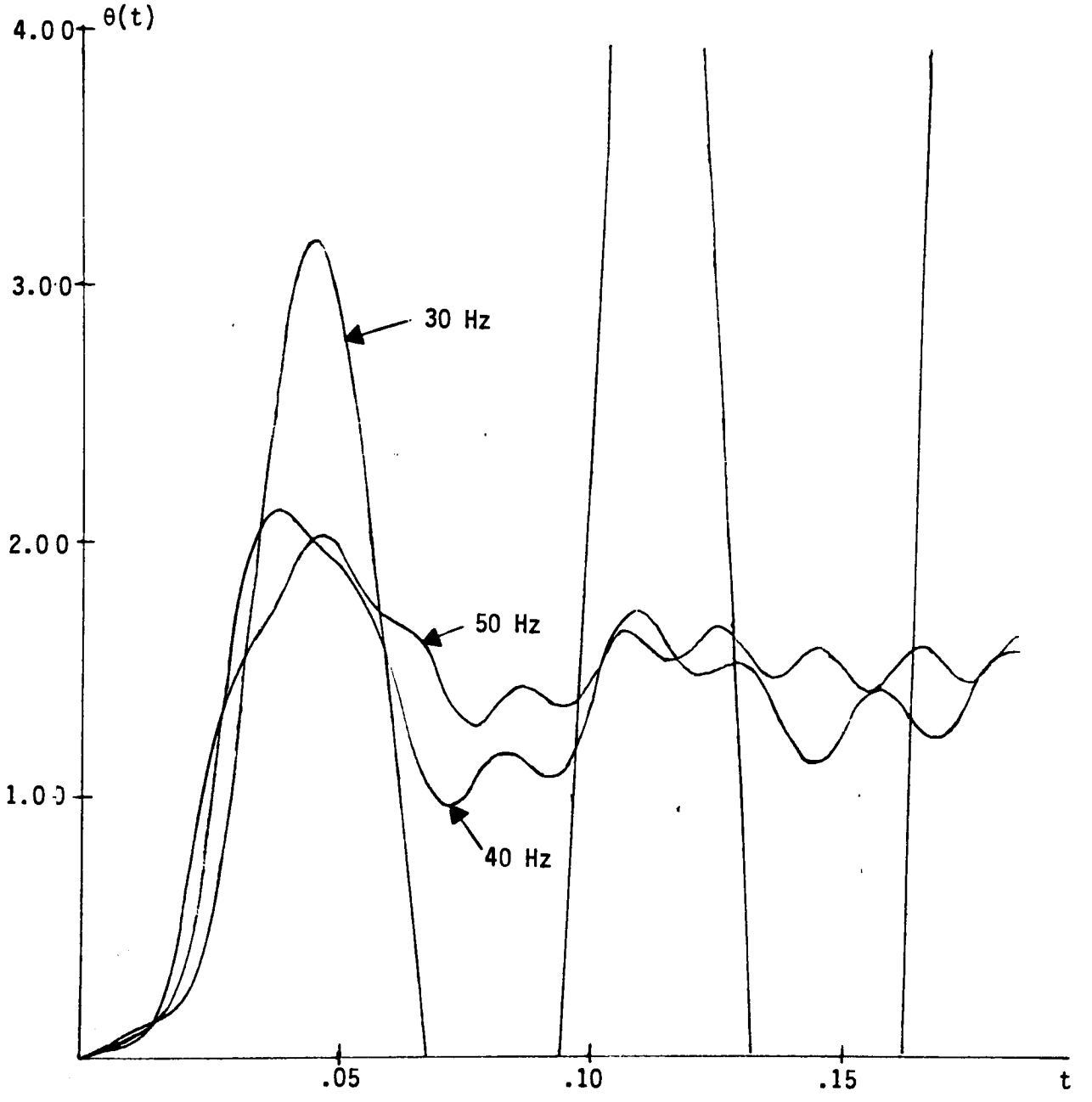

Figure 28

Uniform Sampling PWM System Response

for Switching Frequencies of 50, 40, and 30 Hertz

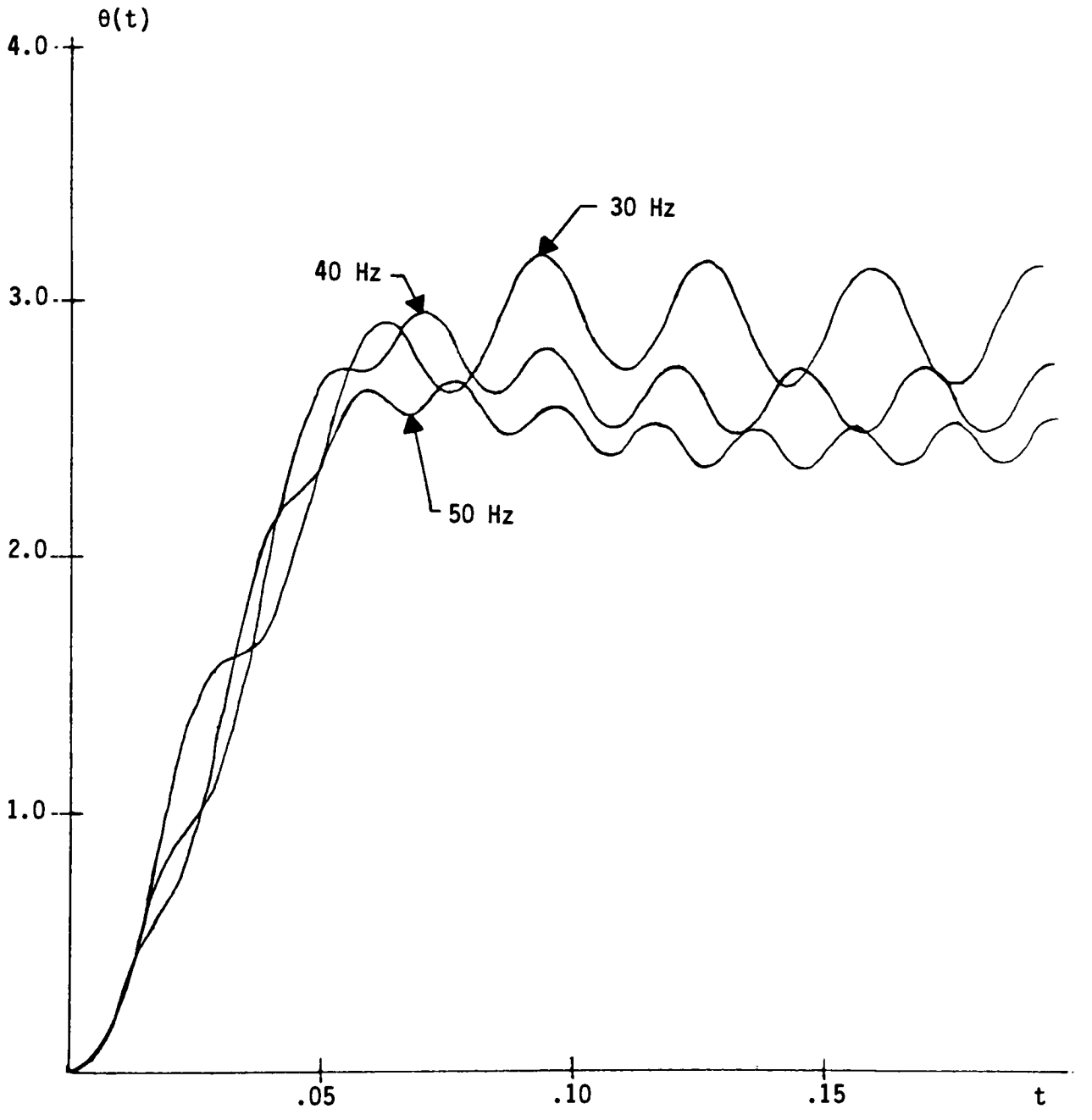

Figure 29

Natural Sampling PWM System Response

for Switching Frequencies of 50, 40, and 30 Hertz

This situation is intuitively more stable. The effect on the sample and hold analogy is to instantaneously vary the sampling frequency since the input samples which cause a change in amplifier output are not uniformly spaced. Variable sampling frequency is an added nonlinearity. Another nonlinearity seen in the computer simulation of natural sampling PWM at low switching frequencies is output chatter. The input is changing more rapidly than the dither signal when the output changes state during the first couple cycles. The result is multiple switching between positive and negative supply during a single switching period T. This phenomenon improves stability but could never be allowed in practical systems since the output transistors would have to dissipate too much power. Finite rise times and delays in practical amplifiers should prevent this phenomenon which will cause the simulations seen in Figure 29 to be more stable than a practical amplifier.

All of the PWM characteristics discussed above should be shown by the linearized PWM models for those models to be useful.

5.4 Step Response Simulation Utilizing Linearized PWM Models

If the PWM amplifier block in Figure 23 is replaced by the linearized sample and hold plus first harmonic models developed and shown in Figures 20 and 21, the output should show the same switching and stability characteristics as the nonlinear PWM signal. Figure 30 shows the unipolar PWM transient response to a two radian step command with the sampler and first harmonic running at 100 Hz corresponding to 100 Hz PWM and the first harmonic in phase with the sampler corresponding to uniform sampling.

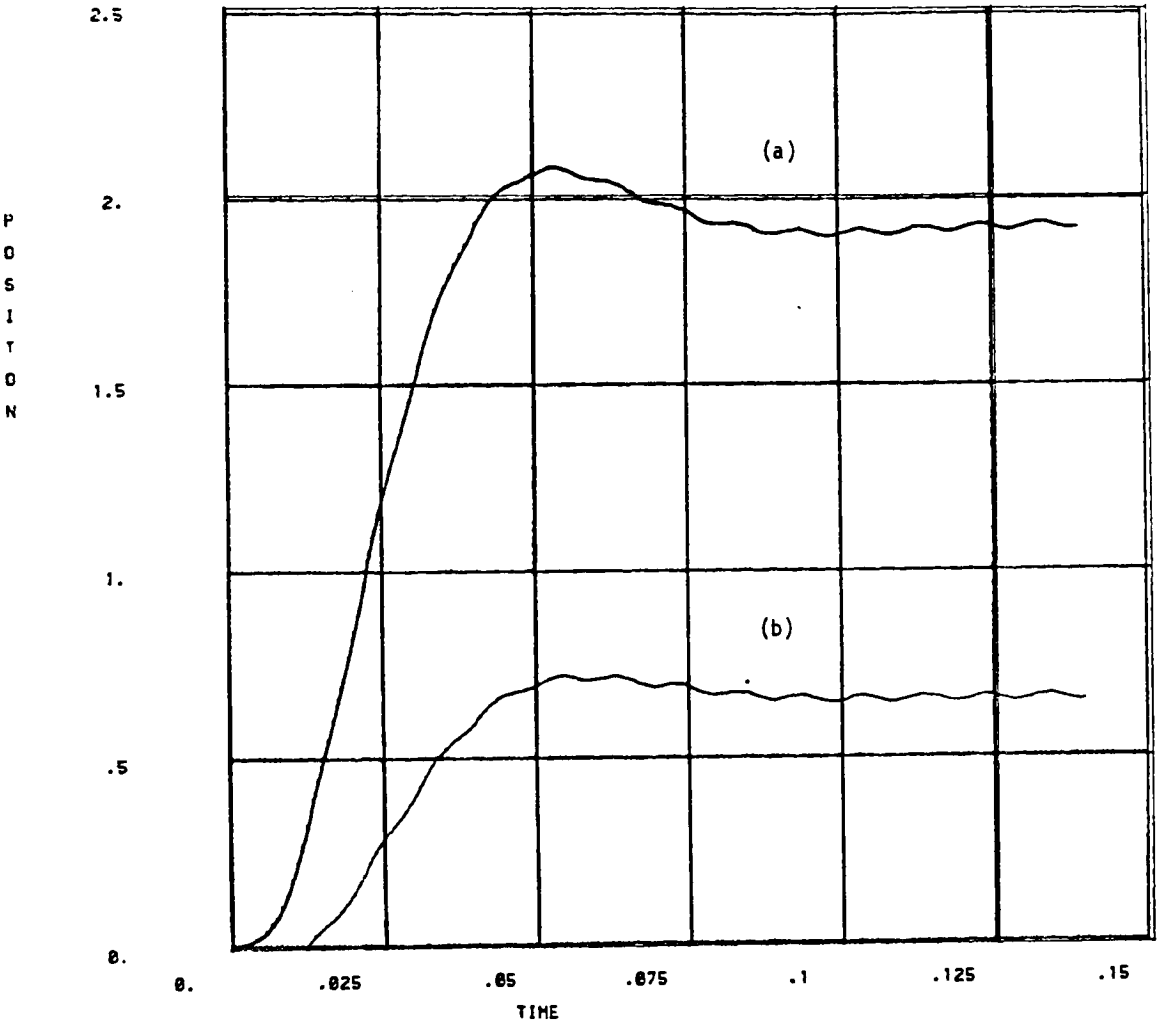

Figure 30

Unipolar PWM Transient Response to a Two Radian Step Command

(a) Double Fourier Series Model With First Harmonic Gain of $2/\pi$

(b) Taylor Series Expansion Model

Figure 30 shows the response to the double Fourier series model shown in Figure 20 with $V_s = 50$, $V_{max} = 10$, and a first harmonic gain of $2/\pi$ which asssumes a Bessel term equal to zero and agrees with the harmonic gain given by Tsai and Ukrainetz [33]. As can be seen, the response shows the rise time and overshoot characteristic of the desired system bandwidth and damping and is equivalent to the nonlinear PWM response. A closer look at the steady state shows the characteristic harmonic ripple and negative d.c. offset seen previously. The magnitude of both these effects is less than that for the nonlinear PWM response. Figure 30 also shows the response to the Taylor series model shown in Figure 20. As can be seen, the output response differs significantly from what was expected. Since the only difference between the Taylor series and double Fourier series models is the constant equilibrium current input term, the calculation of equilibrium current must be in error. This is most likely due to the assumption that the equilibrium motor velocity (ω_e) was zero. The output ripple seen in the steady state output of the nonlinear PWM amplifier in Figure 26 would seem to indicate that the equilibrium velocity was not zero. If ω_e is assumed to be $2\ V_s/K_B\pi$ in the Taylor series expansion analysis, the equilibrium current is calculated to be zero. The result would be equivalent to the double Fourier series model. Thus, only the double Fourier series model will be considered further.

Since the ripple and d.c. offset were less than expected in Figure 30, the assumption that the Bessel term in the first harmonic is zero is in question. Let the Bessel term equal its maximum value resulting in a harmonic gain of $4/\pi$. Figure 31 shows the output response of both uniform and natural sampling PWM. The rise time and overshoot for uniform sampling are essentially the same; however, the ripple and d.c. offset are now very close to that of the true uniform sampling PWM amplifier shown in Figure 26.

A closer look at the steady state in Figure 32 shows the characteristic harmonic ripple and d.c. offset seen previously. The magnitude of both these effects is very close to that for the nonlinear PWM response seen in Figure 27.

If the first harmonic phase is shifted 180° with respect to the sampler, the output response for natural sampling PWM seen in Figures 31 and 32 agrees very closely to the response of the natural sampling PWM amplifier in Figures 26 and 27. The linear model correctly predicted the change in the d.c. bias or offset from negative to positive. These results are acceptable for the servo designer interested in the switching effects on his system.

To answer the question as to whether the linear model can predict the growing instability as the switching frequency is decreased, the sampler and first harmonic frequency was run at 50, 40, and 30 Hz in Figures 33 and 34 for uniform sampling and natural sampling PWM, respectively. Although a precise point by point comparison between the nonlinear PWM response shows some differences, the overall stability characterized by rise time and overshoot magnitude and decay agrees quite well especially for the uniform sampling PWM response. Very similar waveforms were obtained down to 30 Hz which is essentially unstable. Natural sampling PWM seems to be inherently more stable than uniform sampling or the predicted linear model response. At low frequencies, the amplifier input is changing so rapidly with respect to the dither signal that the sum of input plus dither is badly skewed from a sawtooth.

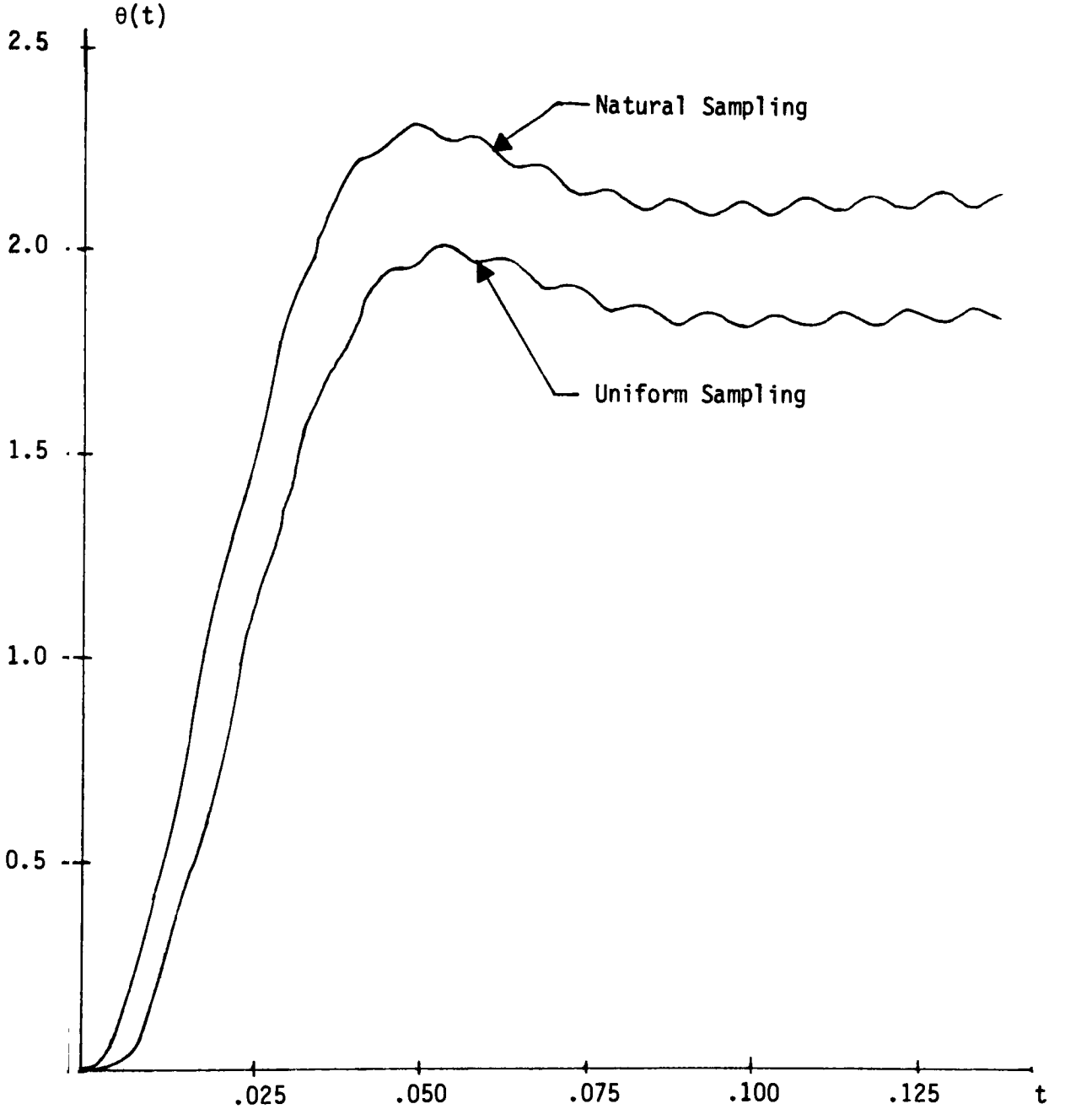

Figure 31

Transient Response of the System Utilizing a Double Fourier Series Model With First Harmonic Gain of $4/\pi$

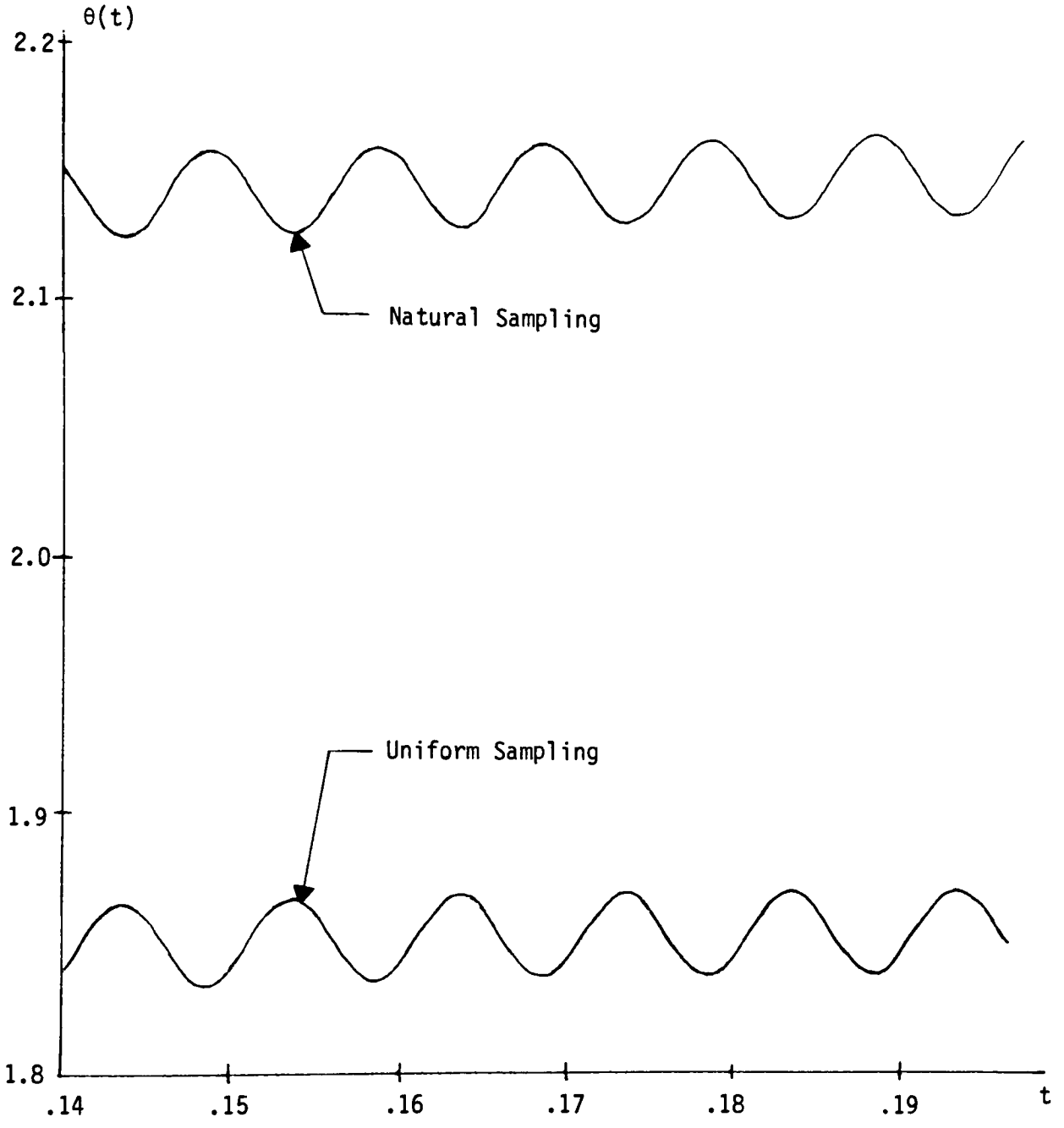

Figure 32

Steady State Response of the System Utilizing a Double Fourier Series Model With First Harmonic Gain of $4/\pi$

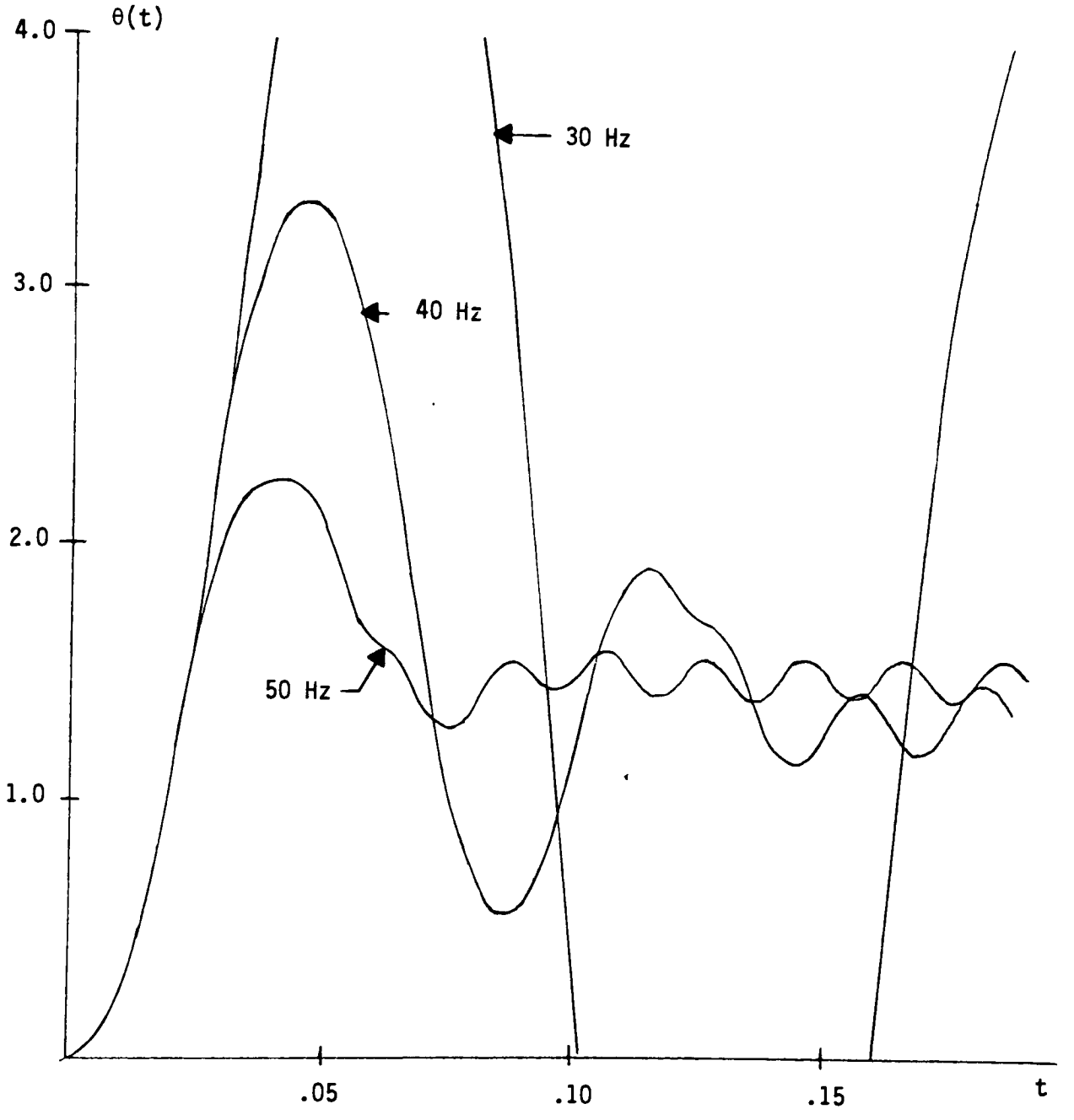

Figure 33

Linear Model Uniform Sampling PWM System Response for Switching Frequencies of 50, 40, and 30 Hz

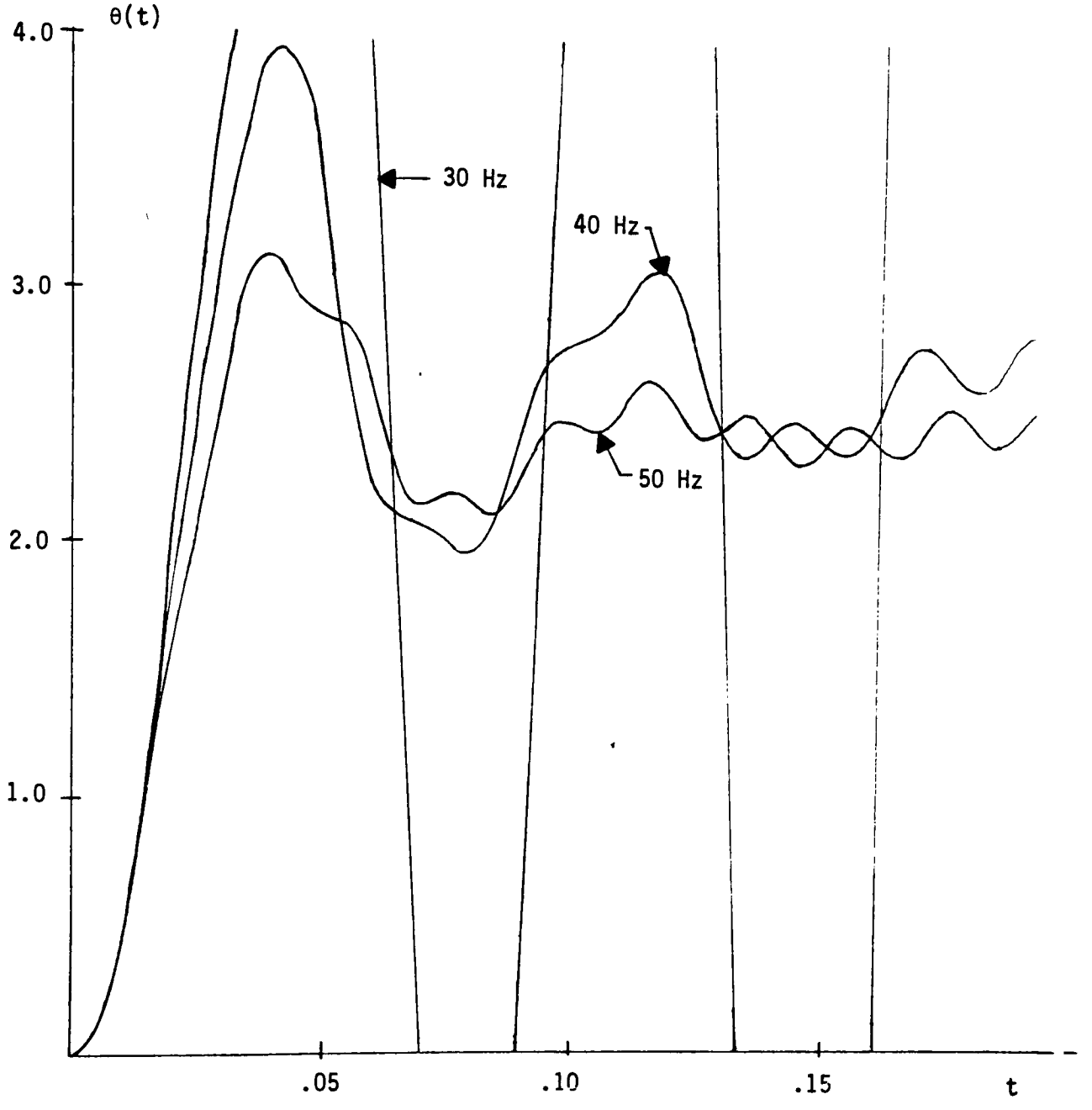

Figure 34

Linear Model Natural Sampling PWM System Response for Switching Frequencies of 50, 40, and 30 Hertz

This added nonlinearity not accounted for in the linear model development seems to be aiding system stability. Thus, the linear model is conservative with respect to stability and would be of use to the servo system designer in ensuring a stable design.

The linearized PWM models shown in Figure 35 perform adequately for the servo system designer to reasonably estimate the stability parameters of a motor control servo system for bandwidths less than 1/3 the PWM switching frequency. Further, steady state output error due to first harmonic ripple and d.c. offset can be predicted quite well using the maximum first harmonic gain of $4/\pi$. These are the terms of major interest to the designer and were the terms this analysis set out to predict.

6.0 Conclusions

This section summarizes the work presented in the previous chapters.

The PWM motor amplifier is a nonlinear device existing in a system comprised of linear components. As the system bandwidth approaches the PWM switching frequency, the PWM amplifier affects system dynamics and adds steady state offset and ripple. To allow the servo system designer to continue using standard linear analysis techniques and still observe the detrimental effects of the PWM amplifier, it is desired to develop a linearized model of the amplifier.

The type of pulse-width modulation used in motor servo control is a bipolar type where the output switches from positive to negative supply every cycle. The PWM output is generated by comparing the input to a sawtooth dither signal. If the input is sampled at the beginning of each PWM cycle, the modulation is called uniform sampling PWM. Natural sampling PWM refers to modulation where the input is allowed to change continuously during comparison with the dither signal. It was theorized that for slowly varying inputs, natural sampling PWM was equivalent to uniform sampling with the sampler delayed by 1/2 the switching period.

Through the principle of equivalent areas and the double Fourier series analysis techniques, the models shown in Figure 35 were developed. It is theoretically accurate for systems whose bandwidth are less than 1/2 the switching frequency. The first harmonic input essentially simulates the switching of the output signal while the sample and hold provides the stability simulation. The magnitude of the first harmonic contains a Bessel function term, and the harmonic magnitude can be varied between $4/\pi$ and 0.87 depending on the amplitude of the input signal.

When applied to a 10 Hz bandwidth position control servo system as shown in Figure 23, the linearized model correctly predicted the transient and steady state characteristics of a nonlinear PWM amplifier for switching frequencies approaching three times the system bandwidth. At a switching frequency ten times the system bandwidth, both the nonlinear and linearized analysis showed steady state output ripple and significant d.c. offset which may be important to a designer expecting precise final position. A first harmonic magnitude of $4/\pi$ provides results which most closely agreed with the nonlinear PWM analysis in steady state.

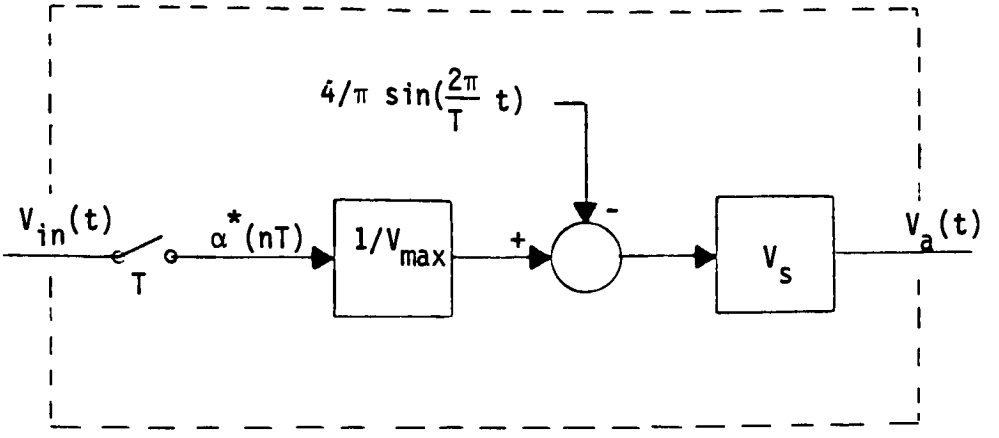

(a)

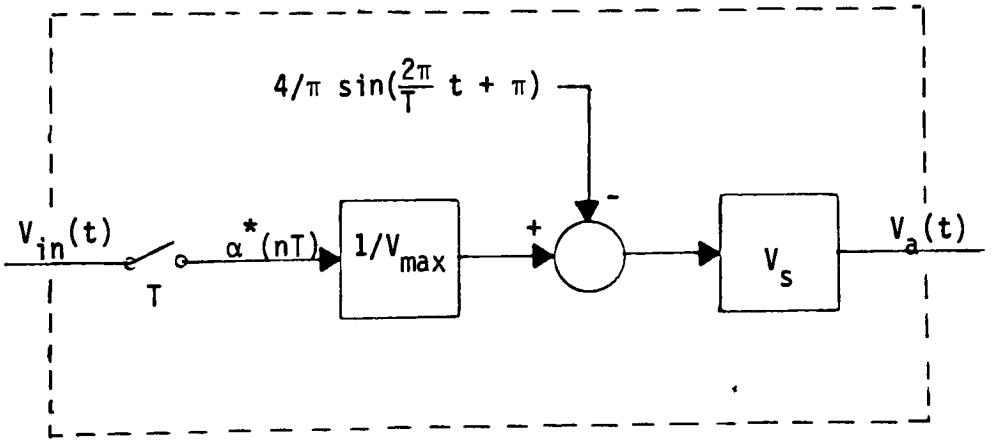

(b)

Figure 37

Final Linearized PWM Model

(a) Uniform Sampling PWM
(b) Natural Sampling PWM

The ripple is caused by the strong first harmonic of the output waveform, and the d.c. offset is caused by the interaction of the first harmonic and sampler running at the same frequency. Should the ripple and offset be excessive, the designer must utilize additional high frequency filtering to decrease the loop gain. The d.c. offset for natural sampling was correctly predicted as being of opposite polarity as uniform sampling.

At switching frequencies five, four, and three times the system bandwidth, both the nonlinear and linearized analysis showed increasingly detrimental effects on stability. These effects are due primarily to the sampling nature of the PWM amplifier. Output ripple and offsets also increase significantly and distort the system response. Since a large part of the instability is caused by the sampler, the system designer has available linear z-transform techniques to improve stability and design the proper compensator.

The natural sampling PWM amplifier was shown to be inherently more stable than predicted due to the significant variation of the input during the switching period. This results in a variable frequency sampler which is a nonlinearity beyond the scope of this analysis. Also, the simulation of low frequency natural sampling PWM showed output chatter which would never be allowed in a real

physical system. This would also add stability to the simulation. The linearized model, however, is a conservative tool in verifying system response with a PWM amplifier. For switching frequencies less than three times system bandwidth, the linearized model and its assumptions begin to break down even for uniform sampling PWM.

7.0 References:

1. Kuo, Benjamin C.; Tal, Jacob ; "Incremental Motion Control: DC Motors and Control Systems," SRL Publishing Company, 1978

2. Engineering Handbook, 5th Edition; "DC Motors, Speed Controls, Servo Systems," Electro-Craft Corporation, 1980

3. Geiger, Dana F., Chief Engineer; "Advances in Switching Servo Amplifiers," Application Note, PMI Motors, Syosset, New York

4. Tal, Jacob, "Design and Analysis of Pulsewidth-Modulated Amplifiers for DC Servo Systems," IEEE Transactions on Industrial Electronics and Control Instrumentation, Vol. IECI-23, No. 1, February 1976, pgs. 47-55

5. Damle, Prakash D., Dubey, D. K.; "Analysis of Chopper-Fed DC Series Motor," IEEE Transactions on Industrial Electronics and Control Instrumentation, Vol. IECI-23, No. 1, February 1976, pgs. 92-97

6. Honnell, M. A., "Classification and Signal Analysis of Pulse-Width Modulated Amplifiers," Amplifying Systems Laboratory Annual Report, Contract NA 38-11344, Geroge C. Marshal Spare Flight Center, NASA, September 30, 1970, pgs. 1-71

7. Ogata, Katsuhiko, "Modern Control Engineering," Prentice-Hall, Inc., 1970

8. Kreyszig, Erwin, "Advanced Engineering Mathematics," John Wiley and Sons, Inc., Second Edition, 1962

9. Kuo, Benjamin C., "Digital Control Systems," Holt, Rinehart, and Winston, Inc., 1980

10. Parrish, Edward A.; McVey, Eugene S.; "A Theoretical Model for Single-Phase Silicon-Controlled Rectifier Systems," IEEE Transactions on Automatic Control, Vol. AC-12, No. 5, October 1967, pgs. 577-579

11. Verma, Vijya Kumar, "Pulse Width Modulated Speed Control of DC Motors," Master of Engineering Thesis, Department of Electrical Engineering, Nova Scotia Technical College, Halifax, Nova Scotia, 1973

12. Dubey, G. K., "Analysis of DC Series Motor controlled by Power Pulses", Proceedings Inst. Electrical Engineering (London), Vol. 122, No. 12, December, 1975, pgs. 1397-1398

13. Georgiou, V. J., "Microprocessor Controlled Digital Pulse With Modulators", Computer Design, vol. 20. No. 1, January, 1981, pgs. 138-144

14. Andeen, R. E., "Analysis of Pulse Duration Sampled-Data Systems with Linear Elements." IRE Transactions on Automatic Control, Vol. AC-5, No. 4, September, 1960, pgs. 306-313

15. Okamoto, H., Ichida, H., Fujinami, M., Imura, S., "Precise Analysis of a Three Phase PWM Thyristor Inverter Circuit with Capacitive Load," Conf. Rec. IAS Annual Meeting 15h, cincinnati, Ohio, September 28 - October 3, 1980. Published by IEEE (Cat n 80CH 1575-0), Piscataway, N.J. 1980, pgs. 742-747

16. Eastham, J. F.; Daniels, A. R.; Lipczynski, R. T.; "A Novel Power Inverter Configuration," Conf. Rec. IAS Annual Meeting 15th, Cincinnati, Ohio, September 28 - October 3, 1980, Published by IEEE (cat n 80CH 1575-0), Piscataway, N.J., 1980, pgs. 748-751

17.. Mohanty, A. K.; Daschoudhur, R. N.; "Stability and Steady State Analysis of Non-Linear PWM System Using Multiple Input Describing Function," Inst. Engineering (India) Electron Telecommun Eng. Div., v56, pt ET 1, August, 1975. pgs. 26-27

18. The', G.; Furmage, S. G.; "Subharmonic Instability in Pulse Width Modulated Feedback System," Proceedings, Inst. Radio Electron Engineering, Australia, v 32 n 10, October, 1971, pgs. 366-372

19. Ghonaimy, M.A.R.; Aly, G. M.; "A Phase-Plane Method for the Analysis of Pulse-Width-Modulated Control Systems," Int. J. Control, Vol. 16 No. 4, October, 1972, pgs. 737-750

20. Scott, William; "Variable Pulse Width Modulator (Exploratory Development Model)," Hughes Aircraft Company, Prepared for the Army Electronics Command, February 1974

21. Karetnyi, O. Ya.; Shiryaev, V.I.; "Stability of a Second-Order Nonlinear Pulsewidth Modulated System," Autom Remote Control, V. 36 No. 2, Pt. 2, February, 1972, pgs. 346-348

22. Kravitz, Mel, Trio Laboratories, Plainview. New York, "Designing the Switching Regulator as a Closed-Loop System," Proceedings of Powercon 2, New York, New York, October 1975, pgs. 291-292

23. Kitayev, V. Ye.; Stoyanov, G. S.; "Investigation of the Stability of Pulse-Width Controlled D.C. Voltage Stabilizers," Telecommun and Ratio Eng. Pt. 2 (USA), Vol. 3. No. 8, August, 1975, pgs. 106-109

24. Bottura, C. P.; Burian, Jr., Y.; Palhares, A. G. B.; "Analysis of Two Types of Pulsewidth Modulated Electrohydraulic Control Systems," Proceedings of the 1977 IEEE Conference on Decision and Control, 1977, pgs. 980-983

25. Nikravesh, Kamaleddin Y., "Analog Computer Simulation of a Pulse Width Modulated Control System," Proceedings of the 1978 Summer Computer Simulation Conference, 1978, pgs. 228-230

26. Verma, V. K.; Baird, C. R.; Aatre, V. K.; "Pulse-Width-Modulated Speed Control of D.C. Motors," Journal of the Franklin Institute, Volume 297, Issue 2, February 1974, pgs. 89-101

27. Schwarz, Von H. C.; "Zur Bestimmung der Stabilitats Gebiete von Regelsystemen mit nichtlinearer Impulsmodulation," Regelungstechnik, Heft 10, 12 Jahrgang, 1964, pgs. 433-437

28. Taft, Charles K.; Banister, William; Slate, Edwin; "Pulse-Width Modulation Control of DC Motors," Proc. Annual Symp. Incremental Motion Control Syst. Devices 7th, Chicago, Illinois, May 24 - 27, 1978, pgs. 111-128

29. Kolk, W., "A Study of Pulse-Width Modulation in Feedback Control Systems," Doctor of Philosphy Thesis, 1972, Elec. Eng.

30. Meyer, A., "Pulse Frequency Modulation and its Effect in Feedback Systems," Doctor of Philosophy Thesis, Northwestern University, 1961, Elec. Eng.

31. Kadota, Takashi Theodore, "Analysis of Nonlinear Sampled Data Systems with Pulse-Width Modulators," Doctor of Philosophy Thesis in Electrical Engineering, University of California, 1960

32. Kadota, T. T., "Asymptotic Stability of Some Nonlinear Feedback Systems," Electronics Research Laboratory, Department of Electrical Engineering, University of California, Series No. 60, Issue No. 264, January 4. 1960

33. Tsai, S. C.; Ukrainetz, P. R.; "Response Characteristics of a Pulse-Width-Modulated Electrohydraulic Servo." Transactions of the ASME Journal of Basic Engineering, June 1970, pgs. 205-214

34. Burroughs, John D., Dr., "Easy 5 Dynamic Analysis System User's Guide," Boeing Computer Services, Co., The Boeing Company, Revision 1, July 1981

35. Black, H.S., "Modulation Theory", D. VanNostrand Company, Inc., Princeton, New Jersey, 1953, pgs. 263-280

8.0 Appendix

The following source listings for "EASY5" control analysis are included in this appendix:

1. PWMLIN -- PWM DC gain model

2. PWMNAT -- nonlinear, natural sampling PWM analysis

3. PWMUNI -- nonlinear, uniform sampling PWM analysis

4. PWML1N1 -- linearized, natural sampling PWM analysis

5. PWML1N2 -- linearized, uniform sampling PWM analysis

PWMLIN

```
PAGE 1      HEWLETT-PACKARD 32201A.7.15 EDIT/3000 WED, MAY 16, 1984

    1       GENERAL,T20,CM120000,P02.
    2       USER,EKC001,TOMSUM.SANDOR/716-722-2467/ROCHESTER,NY.
    3       GET(EASY5/UN=EKSAPP)
    4       CALL(EASY5(ONPLOTS=PLOT4,FTNLIST=0,FILIST=0,CREF=0))
    5       /*EOR
    6       *THIS MODEL IS A LINEARIZED MODEL OF A BIPOLAR PULSE WIDTH MODULATED
    7       *AMPLIFIER. OUTPUTS INCLUDE THE STEP RESPONSE WITH A CLOSE LOOK
    8       *AT STEADY STATE TO OBSERVE THE EFFECTS OF SWITCHING.
    9       *
   10       * FREQUENCY  50,40,30   HZ
   11       *
   12       *
   13       MODEL DESCRIPTION=PULSE WIDTH MODULATOR
   14       *
   15       *THE PWM WILL BE MODELED BY A ZERO ORDER SAMPLE AND HOLD (SH1 BLOCK)
   16       *WITH THE OUTPUT MULTIPLIED BY THE DC GAIN VS/E (MC5 BLOCK). THE
   17       *FIRST HARMONIC (AF1 BLOCK) IS ALSO ADDED TO THE SAMPLER OUTPUT
   18       *(MC5 BLOCK).
   19       *
   20       *
   21       *FEEDBACK AND COMPENSATION
   22       *THE GENERAL CONTROLLER (GA1 BLOCK) OUTPUTS THE ERROR BETWEEN
   23       *DESIRED AND ACTUAL POSITION AND TACHOMETER FEEDBACK IS
   24       *SUBTRACTED AS REQUIRED (MC2 BLOCK) TO CREATE THE PWM AMP
   25       *INPUT.
   26       *
   27       LOCATION = 112    GA1     INPUTS=IN2
   28       LOCATION = 114    MC2     INPUTS=GA1,LG2
   29       *
   30       *PWM AMP
   31       *THE ERROR SIGNAL IS SENT TO THE PWM AMP WHERE IT IS SAMPLED,SUMMED
   32       *WITH THE FIRST HARMONIC,AND MULTIPLIED BY THE DC AMP GAIN.
   33       *
   34       LOCATION = 64     SH1     INPUTS=MC2
   35       LOCATION = 46     AF1
   36       LOCATION = 66     MC5     INPUTS=SH1,AF1
   37       *
   38       *THE BACK EMF IS SUBTRACTED FROM THE PWM OUTPUT (MC3 BLOCK)
   39       *AND THE RESULT IS SENT TO THE PLANT.
   40       *
   41       LOCATION = 128    MC3     INPUTS=MC5,LG2
   42       *
   43       *THE PLANT CONSISTS OF THE MOTOR (LG1 BLOCK),THE MECHANICAL
   44       *LOAD (LG2 BLOCK), AND THE VELOCITY INTEGRATOR (IN1 BLOCK).
   45       *FRICTION CAN BE ADDED TO THE MOTOR TORQUE (MC4 BLOCK).
   46       *
   47       LOCATION = 140    LG1     INPUTS=MC3
   48       LOCATION = 160    MC4     INPUTS=LG1
   49       LOCATION = 180    LG2     INPUTS=MC4
   50       LOCATION = 172    IN2     INPUTS=LG2
   51       END OF MODEL
   52       PRINT
   53       /*EOR
   54       *
   55       DEFINE STATES=S2 IN2=POSITON    S2 LG2=VELOC    S2 LG1=TORQUE
   56       PARAMETER VALUES
   57       *
```

```
PAGE 2     NEWLETT-PACKARD 32201A.7.15 EDIT/3000 WED, .

   58      *PWM SECTION
   59      *SN1----S2=SAMPLED S1                    TAU IS PERIOD
   60      *AF1----S2=C1+C2*SIN(C3*T+C4)            100 HZ SIN WAVE
   61      *MC5----S2=C1*S1+C2*S3+C3*S4+C4          C1 IS DC GAIN VS/E
   62      *                                        C2 IS HARMONIC GAIN 2*VS/PI
   63      TAUSN1=.020
   64      CODAF1=1    C1 AF1=0.0    C2 AF1=1.0    C3 AF1=314.16     C4 AF1=3.1417
   65      C1 MC5=5.0    C2 MC5=-62.83    C3 MC5=0.0    C4 MC5=0.0    S4 MC5=0.0
   66      *
   67      *PLANT SECTION
   68      *GA1----S2=GKP(REF-GKF*S1)+B1A           REF IS DESIRED INPUT = STEP
   69      *                                        GKF IS POSITION FEEDBACK GAIN
   70      *                                        GKP IS PLANT GAIN
   71      *                                        B1A IS BIAS OR OFFSET = 0
   72      *MC2----S2=C1*S1+C2*S3+C3*S4+C5           S1 IS AMPLIFIED POS. ERROR,C1=1
   73      *                                        C2 IS TACH FEEDBACK GAIN (SIGN)
   74      *MC3----S2=C1*S1+C2*S3+C3*S4+C4           S1 IS PWM OUTPUT,C1=1.0
   75      *                                        C3 IS THE BACK EMF GAIN (SIGN)
   76      *LG1----S2=(Z0/(S+P0))                   Z0 IS MOTOR GAIN
   77      *                                        P0 IS MOTOR POLE
   78      *MC4----S2=C1*S1+C2*S3+C3*S4+C4           S1 IS MOTOR TORQUE, C1=1.0
   79      *LG2----S2=(Z0/(S+P0))                   Z0 IS 1/INERTIA
   80      *                                        P0 IS MECH. POLE
   81      *IN2----S2=GKI/S                         GKI IS LINEAR PITCH
   82      *
   83      REFGA1=2.0    GKFGA1=1.0    GKPGA1=5.01     BIAGA1=0.0
   84      C1 MC2=1.0    C2 MC2=-.1040    C3 MC2=0.0    C4 MC2=0.0    S4 MC2=0.0
   85      C1 MC3=1.0    C2 MC3=-.0862    C3 MC3=0.0    C4 MC3=0.0    S4 MC3=0.0
   86      Z0 LG1=10170.    P0 LG1=666.0
   87      C1 MC4=1.0    C2 MC4=0.0    C3 MC4=0.0    C4 MC4=0.0
   88      Z0 LG2=9.01    P0 LG2=.090
   89      GKI IN2=1.0
   90      INITIAL CONDITIONS
   91      *
   92      *START ALL STATES AT ZERO FOR STEP RESPONSE
   93      *
   94      TORQUE=0.0     VELOC=0.0    POSITON=0.0
   95      *
   96      *RUN WAVEFORMS
   97      *
   98      PRINTER PLOTS
   99      ONLINE PLOTS
  100      SI MANUAL SCALES
  101      OUTRATE=10
  102      PRATE=100
  103      DISPLAY1
  104      POSITON,VS,TIME,YRANGE=0.0,4.0
  105      TINC=.00010
  106      TMAX=.20
  107      INT MODE=3
  108      SIMULATE
  109      PARAMETER VALUES
  110      TAUSN1=.025    C3 AF1=251.33
  111      SIMULATE
  112      PARAMETER VALUES
  113      TAUSN1=.033333     C3 AF1=188.496
  114      SIMULATE
```

```
PAGE 3      HEWLETT-PACKARD 32201A.7.15 EDIT/3000 WED,

  115       /*EOF
  116       //GENERAL   JOB
```

PWNNAT

```
PAGE 1      HEWLETT-PACKARD 32201A.7.15 EDIT/3000 FRI, MAY  4, 1984,  9:10 AM (C) HI

    1       GENERAL,T20,CM120000,P02.
    2       USER,EKC001,TOMSUM,SANDOR/716-722-2467/ROCHESTER,NY-
    3       GET(EASY5/UN=EKSAPP)
    4       CALL(EASY5)
    5       /*EOR
    6       *NATURAL SAMPLING PWM      100,50,40 HZ
    7       *.
    8       *THIS MODEL IS FOR A BIPOLAR PULSE WIDTH MODULATED AMPLIFIER.
    9       *MODULATION IS ACHIEVED BY SUMMING THE INPUT WITH A SAWTOOTH
   10       *WAVE OF PERIOD T AND SENDING THE SUM THROUGH A HIGH VOLTAGE
   11       *COMPARATOR. THE COMPARATOR OUTPUTS POSITIVE OR NEGATIVE SUPPLY
   12       *DEPENDING ON THE SIGN OF THE INPUT.
   13       *
   14       MODEL DESCRIPTION=PULSE WIDTH MODULATOR
   15       *
   16       *THE SAWTOOTH IS GENERATED IN A FORTRAN BLOCK BY RAMPING
   17       *FROM -10 TO 10 AND RESETTING THE RAMP BACK TO -10 WHENEVER
   18       *THE OUTPUT EXCEEDS 10
   19       *
   20       LOCATION = 25    FORT
   21       ADD VARIABLES=STOOTH
   22       ADD PARAMETERS=CORREC,RAMP
   23       FORTRAN STATEMENTS
   24             STOOTH=RAMP*TIME-CORREC
   25             IF(STOOTH.GE.10.0000)CORREC=CORREC+20.0
   26             STOOTH=RAMP*TIME-CORREC
   27       *
   28       *THE PWM IS GENERATED BY SUMMING THE INPUT WITH THE SAWTOOTH
   29       *(MC BLOCK) AND OUTPUTTING POSITIVE OR NEGATIVE SUPPLY
   30       *VOLTAGE DEPENDING ON THE SIGN OF THE SUM (FORTRAN BLOCK)
   31       *
   32       LOCATION = 46    MC1     INPUTS=MC2,FORT(STOOTH=S)
   33       LOCATION = 66    FORT    INPUTS=S2 MC1
   34       ADD VARIABLES=PWM
   35       FORTRAN STATEMENTS
   36             IF(S2 MC1.GE.0.00000)PWM=50.0
   37             IF(S2 MC1.LT.0.00000)PWM=-50.0
   38       *
   39       *FEEDBACK AND COMPENSATION
   40       *THE GENERAL CONTROLLER (GA1 BLOCK) OUTPUTS THE ERROR BETWEEN
   41       *DESIRED AND ACTUAL POSITION AND TACHOMETER FEEDBACK IS
   42       *SUBTRACTED AS REQUIRED (MC2 BLOCK) TO CREATE THE PWM AMP
   43       *INPUT.
   44       *
   45       LOCATION = 112   GA1     INPUTS=IN2
   46       LOCATION = 114   MC2     INPUTS=GA1,LG2
   47       *
   48       *THE BACK EMF IS SUBTRACTED FROM THE PWM OUTPUT (MC3 BLOCK)
   49       *AND THE RESULT IS SENT TO THE PLANT
   50       *
   51       LOCATION = 128   MC3     INPUTS=LG2,FORT(PWM=S)
   52       *
   53       *THE PLANT CONSISTS OF THE MOTOR (LG1 BLOCK),THE MECHANICAL
   54       *LOAD (LG2 BLOCK), AND THE VELOCITY INTEGRATOR (IN1 BLOCK).
   55       *FRICTION CAN BE ADDED TO THE MOTOR TORQUE (MC4 BLOCK).
   56       *
   57       LOCATION = 140   LG1     INPUTS=MC3
```

```
PAGE 2     HEWLETT-PACKARD 32201A.7.15 EDIT/3000 FRI, MAY  4, 1984,

   58      LOCATION = 160    MC4     INPUTS=LG1
   59      LOCATION = 180    LG2     INPUTS=MC4
   60      LOCATION = 172    IN2     INPUTS=LG2
   61      END OF MODEL
   62      PRINT
   63      /*EOR
   64      *
   65      DEFINE STATES=S2 IN2=POSITON   S2 LG2=VELOC   S2 LG1=TORQUE
   66      PARAMETER VALUES
   67      *
   68      *PWM SECTION
   69      *MC1----S2=C1*S1+C2*S3+C3*S4+C4       C1 IS INPUT GAIN
   70      *                                     C2 IS SAWTOOTH GAIN
   71      *
   72      CORREC=0.00     RAMP=2000.0
   73      C1 MC1=1.0    C2 MC1=1.0    C3 MC1=0.0    C4 MC1=0.0    S4 MC1=0.0
   74      *
   75      *PLANT SECTION
   76      *GA1----S2=GKP(REF-GKF*S1)+B1A        REF IS DESIRED INPUT = STEP
   77      *                                     GKF IS POSITION FEEDBACK GAIN
   78      *                                     GKP IS PLANT GAIN
   79      *                                     B1A IS BIAS OR OFFSET = 0
   80      *MC2----S2=C1*S1+C2*S3+C3*S4+C5       S1 IS AMPLIFIED POS. ERROR,C1=1
   81      *                                     C2 IS TACH FEEDBACK GAIN (SIGN)
   82      *MC3----S2=C1*S1+C2*S3+C3*S4+C4       C1 IS BACK EMF GAIN (SIGN)
   83      *                                     S3 IS PWM, C2=1.0
   84      *LG1----S2=(Z0/(S+P0))                Z0 IS MOTOR GAIN
   85      *                                     P0 IS MOTOR POLE
   86      *MC4----S2=C1*S1+C2*S3+C3*S4+C4       S1 IS MOTOR TORQUE, C1=1.0
   87      *LG2----S2=(Z0/(S+P0))                Z0 IS 1/INERTIA
   88      *                                     P0 IS MECH. POLE
   89      *IN2----S2=GKI/S                      GKI IS LINEAR PITCH
   90      *
   91      REFGA1=2.0    GKFGA1=1.0    GKPGA1=5.01     BIAGA1=0.0
   92      C1 MC2=1.0    C2 MC2=-.1040    C3 MC2=0.0    C4 MC2=0.0    S4 MC2=0.0
   93      C1 MC3=-.0862    C2 MC3=1.0    C3 MC3=0.0    C4 MC3=0.0    S4 MC3=0.0
   94      Z0 LG1=10170.    P0 LG1=666.0
   95      C1 MC4=1.0    C2 MC4=0.0    C3 MC4=0.0    C4 MC4=0.0
   96      Z0 LG2=9.01    P0 LG2=.090
   97      GKIIN2=1.0
   98      INITIAL CONDITIONS
   99      *
  100      *START THE PWM INTEGRATOR AT -10 FOR SYMMETRY,ALL OTHERS ZERO
  101      *
  102         TORQUE=0.0    VELOC=0.0    POSITON=0.0
  103      *
  104      *RUN WAVEFORMS
  105      *
  106      PRINTER PLOTS
  107      ONLINE PLOTS
  108      SI MANUAL SCALES
  109      OUTRATE=10
  110      PRATE=50
  111      DISPLAY1
  112      POSITON,VS,TIME,YRANGE=0.0,2.5
  113      TINC=.00001
  114      TMAX=.14
```

```
115     INT MODE=3
116     SIMULATE
117     XIC=X
118     INITIAL TIME=.14
119     PRINTER PLOTS
120     ONLINE PLOTS
121     SI MANUAL SCALES
122     OUTRATE=20
123     PRATE=50
124     DISPLAY1
125     POSITON,VS,TIME,YRANGE=1.80,2.20
126     TINC=.00001
127     TMAX=0.20
128     INT MODE=3
129     SIMULATE
130     /*EOF
131     //GENERAL  JOB
```

PWMUNI

```
PAGE 1      HEWLETT-PACKARD 32201A.7.15 EDIT/3000 FRI, MAY  4, 1984,  9:11 AM (C) HEWLE

    1       GENERAL,T20,CM120000,P02.
    2       USER,EKC001,TOMSUM.SANDOR/716-722-2467/ROCHESTER,NY.
    3       GET(EASY5/UN=EKSAPP)
    4       CALL(EASY5(ONPLOTS=PLOT8,FTNLIST=0,FILIST=0,CREF=0))
    5       /*EOR
    6       *LEADING EDGE PWM     100HZ      CLOSE LOOK AT RIPPLE
    7       *
    8       *THIS MODEL IS FOR A BIPOLAR PULSE WIDTH MODULATED AMPLIFIER.
    9       *MODULATION IS ACHIEVED BY SUMMING THE INPUT WITH A SAWTOOTH
   10       *WAVE OF PERIOD T AND SENDING THE SUM THROUGH A HIGH VOLTAGE
   11       *COMPARATOR. THE COMPARATOR OUTPUTS POSITIVE OR NEGATIVE SUPPLY
   12       *DEPENDING ON THE SIGN OF THE INPUT.
   13       *
   14       MODEL DESCRIPTION=PULSE WIDTH MODULATOR
   15       *
   16       *THE SAWTOOTH IS GENERATED IN A FORTRAN BLOCK BY RAMPING
   17       *FROM -10 TO 10 AND RESETTING THE RAMP BACK TO -10 WHENEVER
   18       *THE OUTPUT EXCEEDS 10
   19       *
   20       LOCATION = 25    FORT
   21       ADD VARIABLES=STOOTH
   22       ADD PARAMETERS=CORREC,RAMP
   23       FORTRAN STATEMENTS
   24             STOOTH=RAMP*TIME-CORREC
   25             IF(STOOTH.GE.10.0000)CORREC=CORREC+20.0
   26             STOOTH=RAMP*TIME-CORREC
   27       *
   28       *THE PWM IS GENERATED BY SUMMING THE INPUT WITH THE SAWTOOTH
   29       *(MC BLOCK) AND OUTPUTTING POSITIVE OR NEGATIVE SUPPLY
   30       *VOLTAGE DEPENDING ON THE SIGN OF THE SUM (FORTRAN BLOCK)
   31       *
   32       LOCATION = 44    SM1      INPUTS=MC2
   33       LOCATION = 46    MC1      INPUTS=SM1,FORT(STOOTH=S)
   34       LOCATION = 66    FORT     INPUTS=S2 MC1
   35       ADD VARIABLES=PWM
   36       FORTRAN STATEMENTS
   37             IF(S2 MC1.GE.0.00000)PWM=50.0
   38             IF(S2 MC1.LT.0.00000)PWM=-50.0
   39       *
   40       *FEEDBACK AND COMPENSATION
   41       *THE GENERAL CONTROLLER (GA1 BLOCK) OUTPUTS THE ERROR BETWEEN
   42       *DESIRED AND ACTUAL POSITION AND TACHOMETER FEEDBACK IS
   43       *SUBTRACTED AS REQUIRED (MC2 BLOCK) TO CREATE THE PWM AMP
   44       *INPUT.
   45       *
   46       LOCATION = 112   GA1      INPUTS=IN2
   47       LOCATION = 114   MC2      INPUTS=GA1,LG2
   48       *
   49       *THE BACK EMF IS SUBTRACTED FROM THE PWM OUTPUT (MC3 BLOCK)
   50       *AND THE RESULT IS SENT TO THE PLANT
   51       *
   52       LOCATION = 128   MC3      INPUTS=LG2,FORT(PWM=S)
   53       *
   54       *THE PLANT CONSISTS OF THE MOTOR (LG1 BLOCK),THE MECHANICAL
   55       *LOAD (LG2 BLOCK), AND THE VELOCITY INTEGRATOR (IN1 BLOCK).
   56       *FRICTION CAN BE ADDED TO THE MOTOR TORQUE (MC4 BLOCK).
   57       *
```

```
PAGE 2     HEWLETT-PACKARD 32201A.7.15 EDIT/3000 FRI, MAY  4, 1984,  9:11 AM (C) HEWLETT-PA

    LOCATION = 140    LG1     INPUTS=MC3
    LOCATION = 160    MC4     INPUTS=LG1
    LOCATION = 180    LG2     INPUTS=MC4
    LOCATION = 172    IN2     INPUTS=LG2
    END OF MODEL
    PRINT
    /*EOR
    *
    DEFINE STATES=S2 IN2=POSITON
    *
    PARAMETER VALUES
    *
    *PWM SECTION
    *MC1----S2=C1*S1+C2*S3+C3*S4+C4        C1 IS INPUT GAIN
    *                                      C2 IS SAWTOOTH GAIN
    *
    TAUSH1=.01000
    CORREC=10.0     RAMP=2000.0
    C1 MC1=1.0    C2 MC1=1.0    C3 MC1=0.0    C4 MC1=0.0    S4 MC1=0.0
    *
    *PLANT SECTION
    *GA1----S2=GKP(REF-GKF*S1)+B1A        REF IS DESIRED INPUT = STEP
    *                                     GKF IS POSITION FEEDBACK GAIN
    *                                     GKP IS PLANT GAIN
    *                                     B1A IS BIAS OR OFFSET = 0
    *MC2----S2=C1*S1+C2*S3+C3*S4+C5       S1 IS AMPLIFIED POS. ERROR,C1=1
    *                                     C2 IS TACH FEEDBACK GAIN (SIGN)
    *MC3----S2=C1*S1+C2*S3+C3*S4+C4       C1 IS BACK EMF GAIN (SIGN)
    *                                     S3 IS PWM, C2=1.0
    *LG1----S2=(Z0/(S+P0))                Z0 IS MOTOR GAIN
    *                                     P0 IS MOTOR POLE
    *MC4----S2=C1*S1+C2*S3+C3*S4+C4       S1 IS MOTOR TORQUE, C1=1.0
    *LG2----S2=(Z0/(S+P0))                Z0 IS 1/INERTIA
    *                                     P0 IS MECH. POLE
    *IN2----S2=GKI/S                      GKI IS LINEAR PITCH
    *
    REFGA1=2.0    GKFGA1=1.0    GKPGA1=5.01     B1AGA1=0.0
    C1 MC2=1.0    C2 MC2=-.1040    C3 MC2=0.0    C4 MC2=0.0    S4 MC2=0.0
    C1 MC3=-.0862    C2 MC3=1.0    C3 MC3=0.0    C4 MC3=0.0    S4 MC3=0.0
    Z0 LG1=10170.    P0 LG1=666.0
    C1 MC4=1.0    C2 MC4=0.0    C3 MC4=0.0    C4 MC4=0.0
    Z0 LG2=9.01    P0 LG2=.090
    GKIIN2=1.0
    INITIAL CONDITIONS
    *
    *START THE PWM INTEGRATOR AT -10 FOR SYMMETRY,ALL OTHERS ZERO
    *
       S2 LG1=0.0    S2 LG2=0.0    POSITON=0.0
    *
    *RUN WAVEFORMS
    *
    PRINTER PLOTS
    ONLINE PLOTS
    SI MANUAL SCALES
    OUTRATE=20
    PRATE=50
    DISPLAY1
```

```
115     POSITON,VS,TIME,YRANGE=0.0,2.5
116     TINC=.00001
117     TMAX=.14
118     INT MODE=3
119     SIMULATE
120     XIC=X
121     PRINTER PLOTS
122     ONLINE PLOTS
123     INITIAL TIME=.140
124     TMAX=.20
125     TINC=.00001
126     OUTRATE=20
127     PRATE=50
128     SI MANUAL SCALES
129     DISPLAY1
130     POSITON,VS,TIME,YRANGE=1.80,2.20
131     INT MODE=3
132     SIMULATE
133     /*EOF
134     //GENERAL  JOB
```

PWMLIN1

```
PAGE 1     HEWLETT-PACKARD 32201A.7.15 EDIT/3000 FRI, MAY  4, 1984,

    1      GENERAL,T20,CM120000,P02.
    2      USER,EKC001,TOMSUM.SANDOR/716-722-2467/ROCHESTER,NY.
    3      GET(EASY5/UN=EKSAPP)
    4      CALL(EASY5(ONPLOTS=PLOT1,FTNLIST=0,FILIST=0,CREF=0))
    5      /*EOR
    6      *THIS MODEL IS A LINEARIZED MODEL OF A BIPOLAR PULSE WIDTH MODULATED
    7      *AMPLIFIER. OUTPUTS INCLUDE THE STEP RESPONSE WITH A CLOSE LOOK
    8      *AT STEADY STATE TO OBSERVE THE EFFECTS OF SWITCHING.
    9      *
   10      MODEL DESCRIPTION=PULSE WIDTH MODULATOR
   11      *
   12      *THE PWM WILL BE MODELED BY A ZERO ORDER SAMPLE AND HOLD (SH1 BLOCK)
   13      *WITH THE OUTPUT MULTIPLIED BY THE DC GAIN VS/E (MC5 BLOCK). THE
   14      *FIRST HARMONIC (AF1 BLOCK) IS ALSO ADDED TO THE SAMPLER OUTPUT
   15      *(MC5 BLOCK).
   16      *
   17      *
   18      *FEEDBACK AND COMPENSATION
   19      *THE GENERAL CONTROLLER (GA1 BLOCK) OUTPUTS THE ERROR BETWEEN
   20      *DESIRED AND ACTUAL POSITION AND TACHOMETER FEEDBACK IS
   21      *SUBTRACTED AS REQUIRED (MC2 BLOCK) TO CREATE THE PWM AMP
   22      *INPUT.
   23      *
   24      LOCATION = 112    GA1     INPUTS=IN2
   25      LOCATION = 114    MC2     INPUTS=GA1,LG2
   26      *
   27      *PWM AMP
   28      *THE ERROR SIGNAL IS SENT TO THE PWM AMP WHERE IT IS SAMPLED,SUMMED
   29      *WITH THE FIRST HARMONIC,AND MULTIPLIED BY THE DC AMP GAIN.
   30      *
   31      LOCATION = 64     SH1     INPUTS=MC2
   32      LOCATION = 46     AF1
   33      LOCATION = 66     MC5     INPUTS=SH1,AF1
   34      *
   35      *THE BACK EMF IS SUBTRACTED FROM THE PWM OUTPUT (MC3 BLOCK)
   36      *AND THE RESULT IS SENT TO THE PLANT.
   37      *
   38      LOCATION = 128    MC3     INPUTS=MC5,LG2
   39      *
   40      *THE PLANT CONSISTS OF THE MOTOR (LG1 BLOCK),THE MECHANICAL
   41      *LOAD (LG2 BLOCK), AND THE VELOCITY INTEGRATOR (IN1 BLOCK).
   42      *FRICTION CAN BE ADDED TO THE MOTOR TORQUE (MC4 BLOCK).
   43      *
   44      LOCATION = 140    LG1     INPUTS=MC3
   45      LOCATION = 160    MC4     INPUTS=LG1
   46      LOCATION = 180    LG2     INPUTS=MC4
   47      LOCATION = 172    IN2     INPUTS=LG2
   48      END OF MODEL
   49      PRINT
   50      /*EOR
   51      *
   52      DEFINE STATES=S2 IN2=POSITON    S2 LG2=VELOC    S2 LG1=TORQUE
   53      PARAMETER VALUES
   54      *
   55      *PWM SECTION
   56      *SH1----S2=SAMPLED S1                  TAU IS PERIOD
   57      *AF1----S2=C1+C2*SIN(C3*T+C4)          100 HZ SIN WAVE
```

```
PAGE 2     HEWLETT-PACKARD 32201A.7.15 EDIT/3000 FRI, MAY  4, 1984,

   58      *MC5----S2=C1*S1+C2*S3+C3*S4+C4      C1 IS DC GAIN VS/E
   59      *                                    C2 IS HARMONIC GAIN 2*VS/PI
   60      *THESE VALUES ARE FOR A HIGH FREQ PWM AND LESS RIPPLE
   61      TAUSH1=.010
   62      CODAF1=1    C1 AF1=0.0    C2 AF1=1.0    C3 AF1=628.32     C4 AF1=0.0
   63      C1 MC5=5.0    C2 MC5=-31.53    C3 MC5=0.0    C4 MC5=0.0    S4 MC5=0.0
   64      *
   65      *PLANT SECTION
   66      *GA1----S2=GKP(REF-GKF*S1)+BIA       REF IS DESIRED INPUT = STEP
   67      *                                    GKF IS POSITION FEEDBACK GAIN
   68      *                                    GKP IS PLANT GAIN
   69      *                                    BIA IS BIAS OR OFFSET = 0
   70      *MC2----S2=C1*S1+C2*S3+C3*S4+C5      S1 IS AMPLIFIED POS. ERROR,C1=1
   71      *                                    C2 IS TACH FEEDBACK GAIN (SIGN)
   72      *MC3----S2=C1*S1+C2*S3+C3*S4+C4      S1 IS PWM OUTPUT,C1=1.0
   73      *                                    C3 IS THE BACK EMF GAIN (SIGN)
   74      *LG1----S2=(Z0/(S+P0))               Z0 IS MOTOR GAIN
   75      *                                    P0 IS MOTOR POLE
   76      *MC4----S2=C1*S1+C2*S3+C3*S4+C4      S1 IS MOTOR TORQUE, C1=1.0
   77      *LG2----S2=(Z0/(S+P0))               Z0 IS 1/INERTIA
   78      *                                    P0 IS MECH. POLE
   79      *IN2----S2=GKI/S                     GKI IS LINEAR PITCH
   80      *
   81      REFGA1=2.0    GKFGA1=1.0    GKPGA1=5.01     BIAGA1=0.0
   82      C1 MC2=1.0    C2 MC2=-.1040    C3 MC2=0.0    C4 MC2=0.0    S4 MC2=0.0
   83      C1 MC3=1.0    C2 MC3=-.0862    C3 MC3=0.0    C4 MC3=0.0    S4 MC3=0.0
   84      Z0 LG1=10170.    P0 LG1=666.0
   85      C1 MC4=1.0    C2 MC4=0.0    C3 MC4=0.0    C4 MC4=0.0
   86      Z0 LG2=9.01    P0 LG2=.090
   87      GKIIN2=1.0
   88      INITIAL CONDITIONS
   89      *
   90      *START ALL STATES AT ZERO FOR STEP RESPONSE
   91      *
   92      TORQUE=0.0     VELOC=0.0    POSITON=0.0
   93      *
   94      *RUN WAVEFORMS
   95      *
   96      PRINTER PLOTS
   97      ONLINE PLOTS
   98      SI MANUAL SCALES
   99      OUTRATE=10
  100      PRATE=100
  101      DISPLAY1
  102      POSITON,VS,TIME,YRANGE=0.0,2.5
  103      TINC=.00010
  104      TMAX=.14
  105      INT MODE=3
  106      SIMULATE
  107      XIC-X
  108      IHITIAL TIME=.14
  109      PRINTER PLOTS
  110      ONLINE PLOTS
  111      SI MANUAL SCALES
  112      OUTRATE=2
  113      PRATE=100
  114      DISPLAY1
```

```
PAGE 3     HEWLETT-PACKARD 32201A.7.15 EDIT/3000 FRI, MAY  4, 1984,

  115      POSITON,VS,TIME,YRANGE=1.80,2.20
  116      TINC=.0001
  117      TMAX=0.20
  118      INT MODE=3
  119      SIMULATE
  120      /*EOF
  121      //GENERAL   JOB
```

PWMLIN2

```
PAGE 1      HEWLETT-PACKARD 32201A.7.15 EDIT/3000 WED, MAY 16, 1984

    1       GENERAL,T20,CM120000,P02.
    2       USER,EKC001,TOMSUM.SANDOR/716-722-2467/ROCHESTER,NY.
    3       GET(EASY5/UN=E<SAPP)
    4       CALL(EASY5)
    5       EXIT,U.
    6       DAYFILE,DAY1.
    7       REPLACE,DAY1
    8       /*EOR
    9       *THIS MODEL IS FOR A BIPOLAR PULSE WIDTH MODULATED AMPLIFIER.
   10       *MODULATION IS ACHIEVED BY SUMMING THE INPUT WITH A SAWTOOTH
   11       *WAVE OF PERIOD T AND SENDING THE SUM THROUGH A HIGH VOLTAGE
   12       *COMPARATOR. THE COMPARATOR OUTPUTS POSITIVE OR NEGATIVE SUPPLY
   13       *DEPENDING ON THE SIGN OF THE INPUT.
   14       *
   15       MODEL DESCRIPTION=PULSE WIDTH MODULATOR
   16       *
   17       *THE PWM IS MODELED BY A DC GAIN BLOCK (MC3 BLOCK)
   18       *
   19       *
   20       *FEEDBACK AND COMPENSATION
   21       *THE GENERAL CONTROLLER (GA1 BLOCK) OUTPUTS THE ERROR BETWEEN
   22       *DESIRED AND ACTUAL POSITION AND TACHOMETER FEEDBACK IS
   23       *SUBTRACTED AS REQUIRED (MC2 BLOCK) TO CREATE THE PWM AMP
   24       *INPUT.
   25       *
   26       LOCATION = 112    GA1     INPUTS=IN2
   27       LOCATION = 114    MC2     INPUTS=GA1,LG2
   28       *
   29       *THE ERROR SIGNAL IS MULTIPLIED BY THE PWM DC GAIN (C1 MC3 BLOCK) AND
   30       *THE BACK EMF IS SUBTRACTED FROM THE PRODUCT (MC3 BLOCK)
   31       *
   32       LOCATION = 128    MC3     INPUTS=MC2,LG2
   33       *
   34       *THE PLANT CONSISTS OF THE MOTOR (LG1 BLOCK),THE MECHANICAL
   35       *LOAD (LG2 BLOCK), AND THE VELOCITY INTEGRATOR (IN1 BLOCK).
   36       *FRICTION CAN BE ADDED TO THE MOTOR TORQUE (MC4 BLOCK).
   37       *
   38       LOCATION = 140    LG1     INPUTS=MC3
   39       LOCATION = 160    MC4     INPUTS=LG1
   40       LOCATION = 180    LG2     INPUTS=MC4
   41       LOCATION = 172    IN2     INPUTS=LG2
   42       END OF MODEL
   43       PRINT
   44       /*EOR
   45       *
   46       DEFINE STATES=S2 IN2=POSITON
   47       PARAMETER VALUES
   48       *
   49       *PLANT SECTION
   50       *GA1----S2=GKP(REF-GKF*S1)+B1A        REF IS DESIRED INPUT = STEP
   51       *                                     GKF IS POSITION FEEDBACK GAIN
   52       *                                     GKP IS PLANT GAIN
   53       *                                     B1A IS BIAS OR OFFSET = 0
   54       *MC2----S2=C1*S1+C2*S3+C3*S4+C5       S1 IS AMPLIFIED POS. ERROR,C1=1
   55       *                                     C2 IS TACH FEEDBACK GAIN (SIGN)
   56       *MC3----S2=C1*S1+C2*S3+C3*S4+C4       C1 IS THE PWM DC GAIN
   57       *                                     C3 IS THE BACK EMF GAIN (SIGN)
```

```
PAGE 2     HEWLETT-PACKARD 32201A.7.15 EDIT/3000 WED,

   58      *LG1----S2=(Z0/(S+P0))                  Z0 IS MOTOR GAIN
   59      *                                       P0 IS MOTOR POLE
   60      *MC4----S2=C1*S1+C2*S3+C3*S4+C4         S1 IS MOTOR TORQUE, C1=1.0
   61      *LG2----S2=(Z0/(S+P0))                  Z0 IS 1/INERTIA
   62      *                                       P0 IS MECH. POLE
   63      *IN2----S2=GKI/S                        GKI IS LINEAR PITCH
   64      *
   65      REFGA1=2.0    GKFGA1=1.0    GKPGA1=5.01     BIAGA1=0.0
   66      C1 MC2=1.0    C2 MC2=-.1040    C3 MC2=0.0    C4 MC2=0.0    S4 MC2=0.0
   67      C1 MC3=5.0    C2 MC3=-.0862    C3 MC3=0.0    C4 MC3=0.0    S4 MC3=0.0
   68      Z0 LG1=10170.    P0 LG1=666.0
   69      C1 MC4=1.0    C2 MC4=0.0    C3 MC4=0.0    C4 MC4=0.0
   70      Z0 LG2=9.01    P0 LG2=.090
   71      GKIIN2=1.0
   72      INITIAL CONDITIONS
   73      *
   74      *START ALL STATES AT ZERO FOR STEP RESPONSE
   75      *
   76      S2 LG1=0.0    S2 LG2=0.0    POSITON=0.0
   77      *
   78      *RUN WAVEFORMS
   79      *
   80      PRINTER PLOTS
   81      ONLINE PLOTS
   82      SI MANUAL SCALES
   83      OUTRATE=10
   84      PRATE=50
   85      DISPLAY1
   86      POSITON,VS,TIME,YRANGE=0.0,2.5
   87      TINC=.00025
   88      TMAX=.14
   89      INT MODE=2
   90      SIMULATE
   91      XIC-X
   92      INITIAL TIME=.14
   93      PRINTER PLOTS
   94      ONLINE PLOTS
   95      SI MANUAL SCALES
   96      OUTRATE=2
   97      PRATE=50
   98      DISPLAY1
   99      POSITON,VS,TIME,YRANGE=1.8,2.2
  100      TINC=.00010
  101      TMAX=0.20
  102      INT MODE=2
  103      SIMULATE
  104      /*EOF
  105      //GENERAL  JOB
```